



SOCIEDAD ESPAÑOLA DE MECÁNICA DE ROCAS

XVIII Jornada Técnica Anual

Mecánica de Rocas y Geología Estructural

RELACIÓN DE PONENCIAS

The geological evolution of fracture networks in rocks

Prof. John Cosgrove (Imperial College London, Reino Unido)

The help of structural geology in tunneling activities

Dr. Philippe Vaskou (Geostock, Francia)

Estructura interna y propiedades mecánicas de la falla de Alhama (Murcia)

Dr. Juan Miguel Insúa Arévalo (Universidad Complutense de Madrid, España)

Mecanismo de inicio de la rotura en materiales de comportamiento frágil bajo condiciones traccionales

Dra. Carmen C. García Covadonga (Universidad de Oviedo, España)

13 de mayo de 2021

Jornada «en línea»

Índice

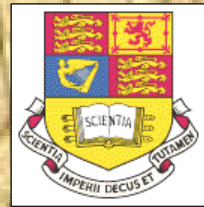
The geological evolution of fracture networks in rocks (Prof. John Cosgrove - Imperial College London, Reino Unido	1
The help of structural geology in tunneling activities (Dr. Philippe Vaskou - Geostock, Francia)	18
Estructura interna y propiedades mecánicas de la falla de Alhama (Murcia) (Dr. Juan Miguel Insúa Arévalo - Universidad Complutense de Madrid, España)	50
Mecanismo de inicio de la rotura en materiales de comportamiento frágil bajo condiciones traccionales (Dra. Carmen C. García Covadonga - Universidad de Oviedo, España)	72

The Geological Evolution of Fracture Networks in Rocks

XVIII JORNADA TÉCNICA 2021
SOCIEDAD ESPAÑOLA DE MECANICA DE ROCAS

Mecanica de Rocas Y Geología Estructural
13 de Mayo de 2021

John Cosgrove
Department of Earth Science & Engineering
Imperial College
London



Lecture outline

- Determine what controls the geometry of a fracture set in a rock (brief discussion of **stress and brittle failure**)
- What controls the geometry of a fracture network (made up of several fracture sets) (Concept of **fracture analysis**)
- Then attempt to apply these ideas to a **Field study to determine the geometry of the fracture network** in a fractured rock mass

Intensely fractured granite - Jersey, Channel Islands UK



Consider **links** between **Rock Mechanics and Structural Geology**

- The links exists because **both groups of earth scientists use the same mechanical principles** to resolve problems
- But applied under **different Boundary conditions**
- **Structural Geologists** look at rock deformation (the response of the rock mass to stress) under conditions of;
High pressure, high temperature, Long time intervals & slow strain rates
- **The Rock Engineer** considers deformation under conditions of;
low Temperature, low pressure, over relatively short time intervals (10s to 100s ys) & fast strain rates

Structural Geologist is interesting in determining;

- How the fracture network in a rock developed and
- What it can tell us about the evolution of the regional stress regimes through geological time. i.e. **how the rock mass deformed in the past**

The Rock Engineer is interested in;

- The impact of the fracture network within a rock mass on the likely **future deformation history** i.e.
- How the fractured rock mass **will** respond to an imposed change in boundary conditions.

Structural geologists use 'Fracture Analysis' to analyse the brittle tectonic history of a region & this yields';

- Detailed information about the **3D geometry of the network** and
- Its **properties** (Connectivity permeability strength etc.).

Information of 1st order importance to the Rock Engineer.

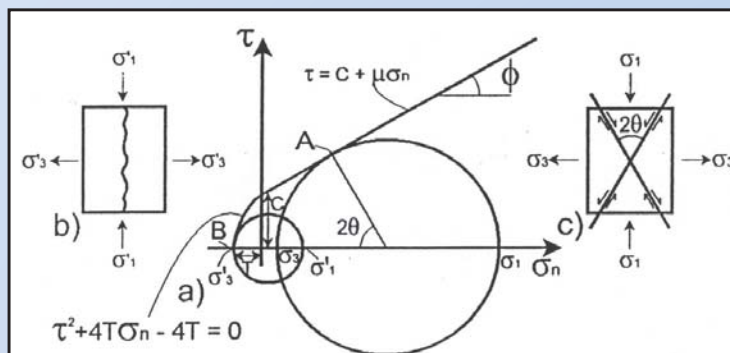
- A MAJOR CHALLENGE FOR A ROCK ENGINEER WHEN ATTEMPTING TO CONSTRUCT EITHER IN OR ON A **FRACTURED ROCK MASS** IS THAT OF DETERMINING ITS **GEOMECHANICAL PROPERTIES**.
- THESE ARE KNOWN TO DEPEND ON BOTH THE **INTRINSIC PROPERTIES OF THE ROCK** AND ON THE **GEOMETRY OF THE FRACTURE NETWORK** WHICH CONTROLS ITS BULK MECHANICAL PROPERTIES –
- AN UNDERSTANDING OF THE STRUCTURAL GEOLOGY OF THE STUDY AREA AND OF ITS TECTONIC EVOLUTION CAN BE USED TO START TO **QUANTIFY THESE PROPERTIES** AND TO INFORM
 - I) THE SITING AND ORIENTATION OF ENGINEERING STRUCTURES AND
 - II) ANY NUMERICAL MODEL.

Consider what controls the **GEOMETRY OF A FRACTURE SET** in a rock

The FORMATION OF A FRACTURE SET in the crust in response to a GEOLOGICAL STRESS FIELD.

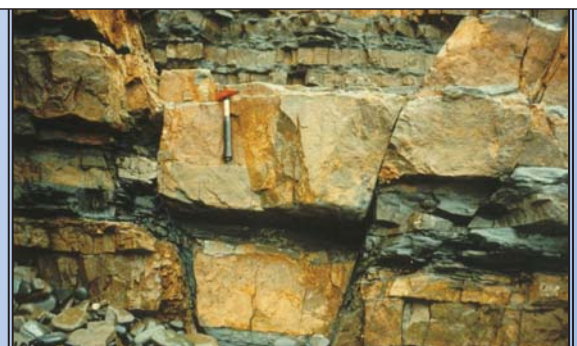
From the theory of **BRITTLE FAILURE** we know

Fracture ORIENTATION – is controlled by the **stress orientation**
Fracture TYPE- is controlled by the **differential stress** ($\sigma_1 - \sigma_3$)



Extensional fractures – Liassic limestone beds

Conjugate normal faults – cutting turbidites



THE PRINCIPAL CAUSES OF STRESS IN THE CRUST ARE:

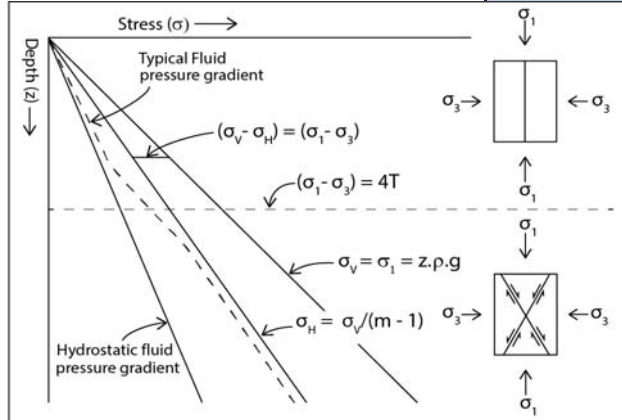
- **GRAVITY** (the overburden stress) generates large **vertical stresses**
- **PLATE TECTONICS** generates large **horizontal stresses**

OVERBURDEN STRESS. In a tectonically relaxed region of the crust the state of stress is determined dominantly by the overburden;

$$\sigma_v = \sigma_1 = z \cdot \rho \cdot g$$

This σ_v will induce a **horizontal stress** whose magnitude will be determined by the **boundary conditions** & the **Poisson's ratio** of the rock.

$$\sigma_h = \sigma_v / (m - 1)$$



Other factors influence the state of stress in the crust – e.g., GEOTHERMAL GRADIENT

Effect of Geothermal gradient on the STRESS STATE

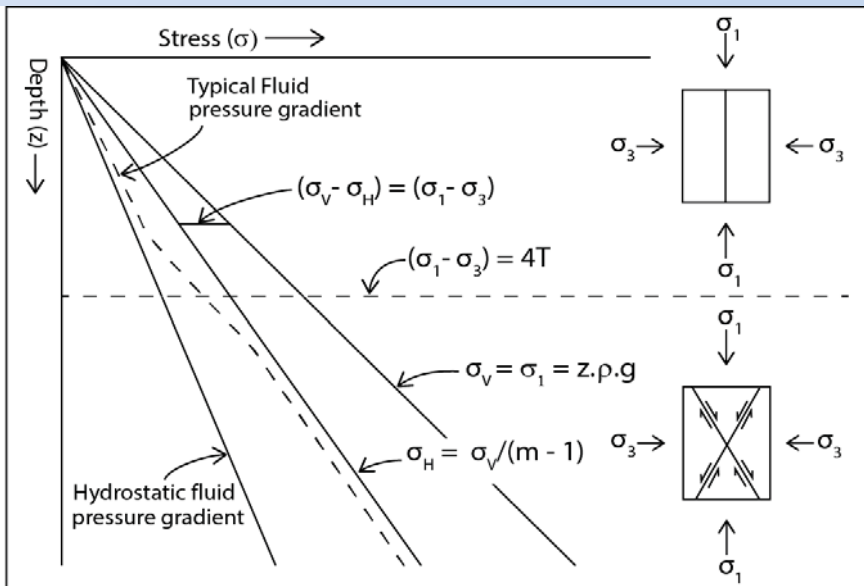
Coefficient of thermal Expansion = α

Temperature change = ΔT

Expansion (strain = e)
 $e = \alpha \cdot \Delta T$

$\sigma = E \cdot e = E \cdot \alpha \cdot \Delta T$

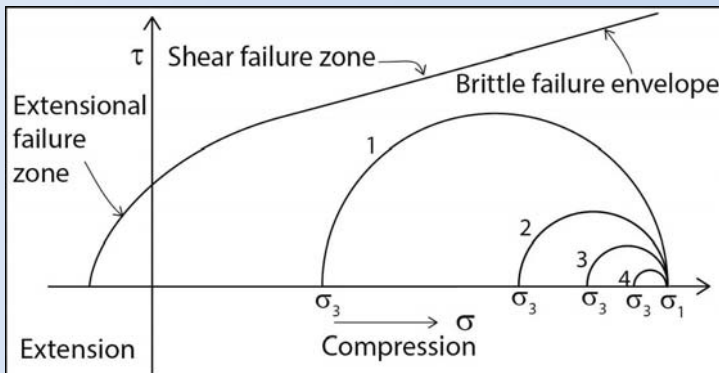
$$\begin{aligned}\sigma_z &= \rho \cdot g \cdot z \\ \sigma_x &= [\sigma_z / (m - 1)] + E \cdot \alpha \cdot \Delta T \\ \sigma_y &= [\sigma_z / (m - 1)] + E \cdot \alpha \cdot \Delta T\end{aligned}$$



Stress values are determined by Young's modulus, E, Poisson's number, m , Coef. thermal Expansion, α, Fluid pressure, etc.

IMPLICATION OF THESE EQUATIONS

Stress state in adjacent layers at the same depth can be **very different** depending on the **intrinsic properties** of the layers.



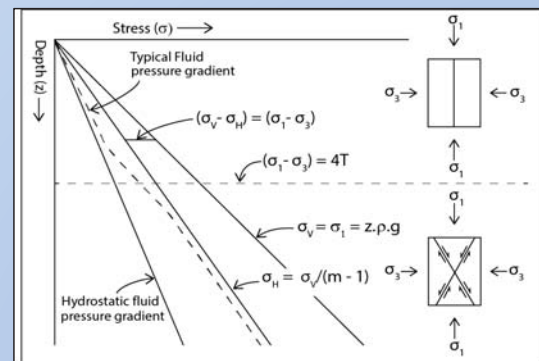
At any particular depth in the crust, adjacent layers will experience, **Same vertical stress**

$$\sigma_v = \rho.g.z$$

Different horizontal stresses

$$\sigma_x = [\sigma_z / (m - 1)] + E.\alpha.dT$$

$$\sigma_y = [\sigma_z / (m - 1)] + E.\alpha.dT$$



Note – Stresses are compressive - The stress states are **STABLE** – won't cause failure

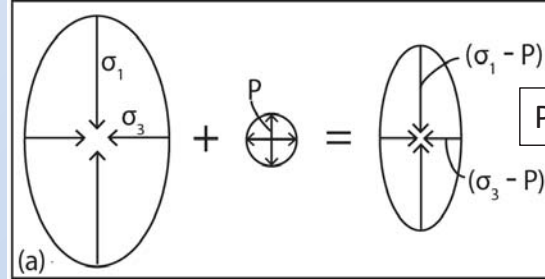
PROBLEM

Upper crust generally contains many Joints

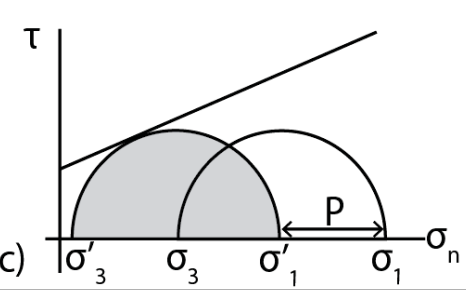
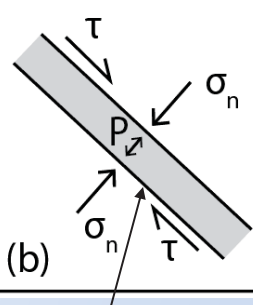
- extensional (tensile) failure – which needs an extensional stress
- BUT the min. principal stress σ_3 generally compressive



Role of Fluid Pressure on Rock Failure



P = Fluid pressure



Effective stress: $\sigma'_n = (\sigma_n - P_f)$

Fracture

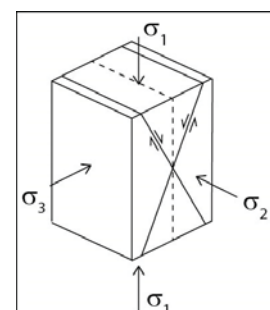
DRY

WET

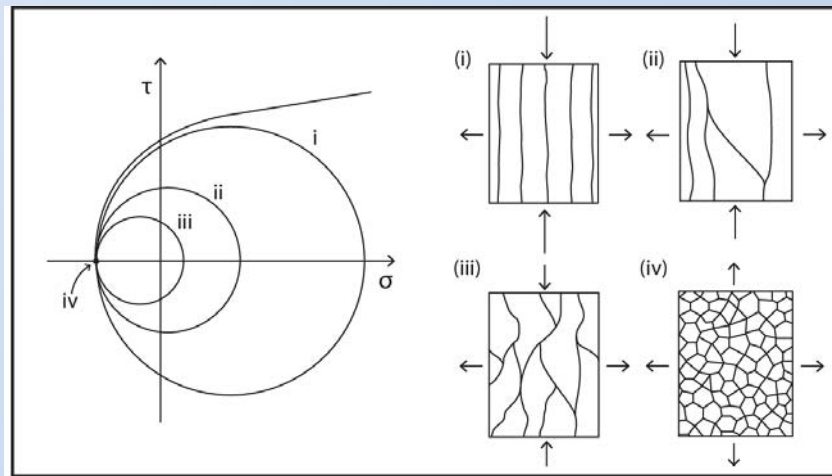
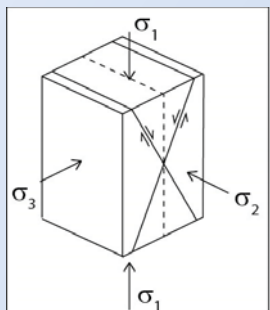
Tensile Failure: $\sigma_3 < -T$ $(\sigma_3 - P_f) < -T$

Shear Failure: $\tau > C_o + \mu \sigma_n$ $\tau > C_o + \mu (\sigma_n - P_f)$

- The **REGULARITY** of the fractures can vary from set to set – in both the vertical plane (σ_1, σ_3 plane) and horizontal plane (σ_2, σ_3 plane)
- In addition, within a fracture set the fractures may be **EVENLY DISTRIBUTED** (regularly spaced) or may tend to **CLUSTER**
- We need to understand **what controls fracture clustering & regularity**



Stress states (i) to (iv) all will produce **extensional** failure



Veins infilling extensional fractures.

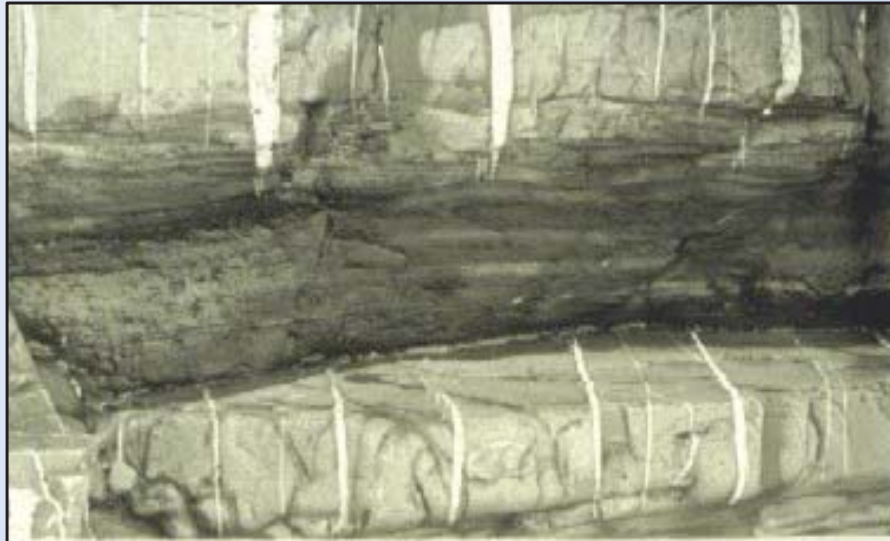
Note the difference in the regularity of the structures

It reflects the different values of differential stress ($\sigma_v - \sigma_h$)

in the **vertical** section ($\sigma_1 - \sigma_3$)



Decreasing differential stress – ($\sigma_1 - \sigma_3$) **decreasing regularity**



Veins infilling extensional fractures.

Note the difference in the regularity of the structures

It reflects the different values of differential stress

$$(\sigma_v - \sigma_h) = (\sigma_1 - \sigma_3)$$

in the **vertical** section

$(\sigma_2 - \sigma_3)$ controls **REGULARITY** in the **horizontal** section - bedding

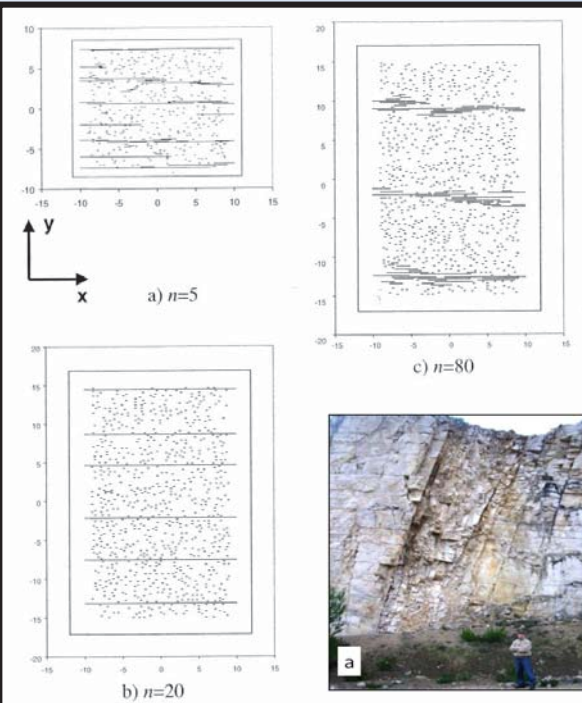
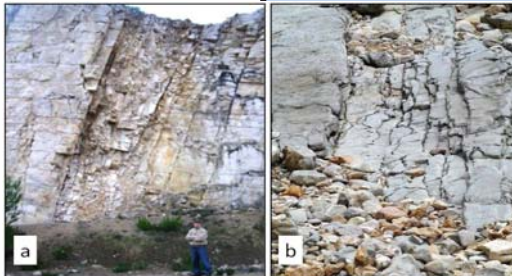


Fig. 40. Examples of sub-critical fracture growth for sub-critical indices (n^*)
a) $n = 5$, b) $n = 20$ and c) $n = 80$. All simulations start with the same randomly located parallel flaws and an extensional strain was applied in the y direction at a constant strain rate. n is determined by rock type and environmental conditions and, as can be seen from the experimental results, has a dramatic influence of fracture spacing

*It can be demonstrated empirically that $v = A(K_I/K_{Ic})^n$ where K_I is the stress intensity factor at the crack tip, K_{Ic} is the critical fracture toughness v is the sub-critical crack propagation velocity, A is a proportionality constant and the power n the sub-critical index. (From Olson 2004.)

FRACTURE CLUSTERING

Related to fracture mechanics properties
(**Stress intensity factor** at the crack tip)



Fracture network made up of 2 fracture sets – with different regularities

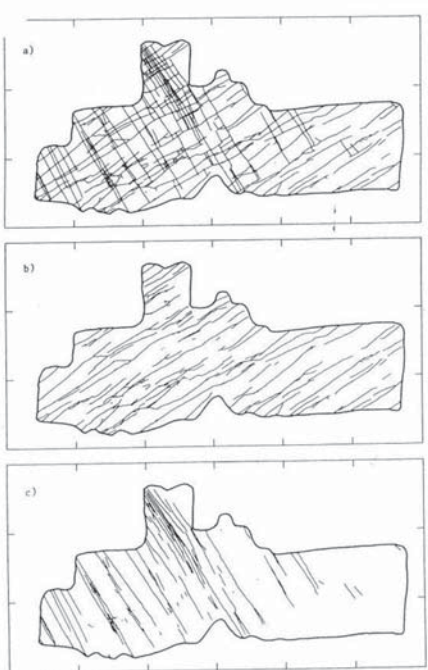
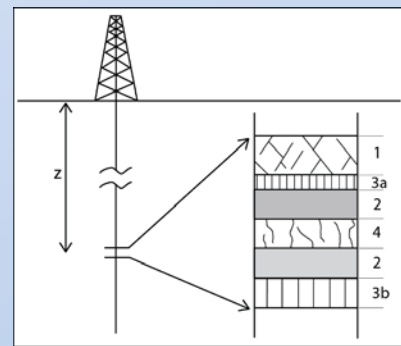
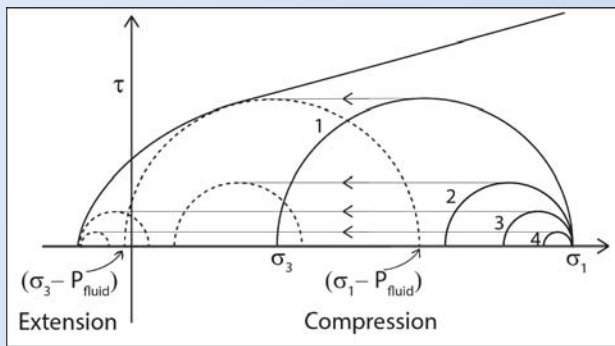


Fig. 14. (a) Map of joint traces exposed on a bedding plane surface. b) The older joint set formed under near isotropic remote stress. c) The younger set formed under strongly deviatoric remote stress. (The distance between map ticks is 1m.) (From Olson & Pollard. 1988.)

- Note the older **joint set (b)** is irregular and was formed in a stress field with a **low differential stress**
- In contrast the later **joint set (c)** is **more regular** reflecting the **high differential stress** operating during its formation

In addition, the second set is **clustered** whereas the earlier set is not. This indicates the **changes in properties of the rock through time** as a result of compaction, cementation and diagenesis

We can **use the fractures to track the changes** in both the **stress regime** and the **rock properties** over geological time.



- Simplest possible stress field (an overburden stress)
- One deformation
- Complex assemblage of fracture sets at any particular depth in the crust.
- Rocks generally subjected to multiple stress fields and therefore form multiple fracture sets resulting in fracture networks
- Anticipate that fracture networks will be complex

Summary

- Simplest possible stress field (overburden load)
- Simplest deformation history (1 event)

Results in:

- Complex assemblage of fracture sets at any particular depth in the crust.

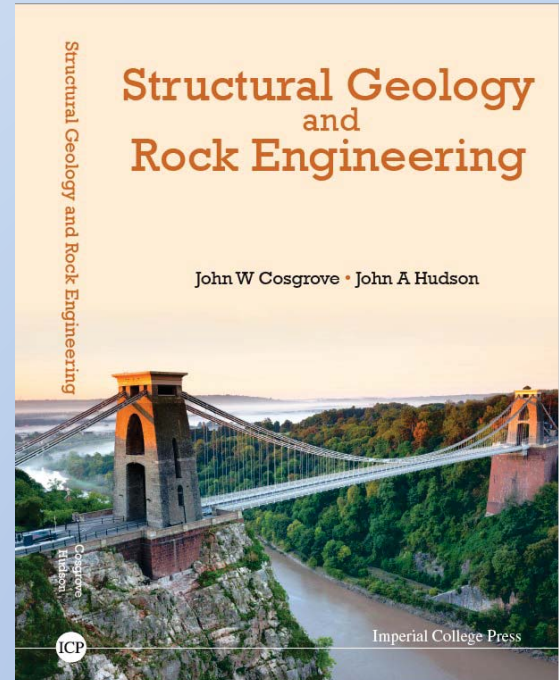
Note that:

- Rocks generally subjected to multiple stress fields and therefore form multiple fracture sets resulting in fracture networks
- Anticipate fracture networks with complex geometries

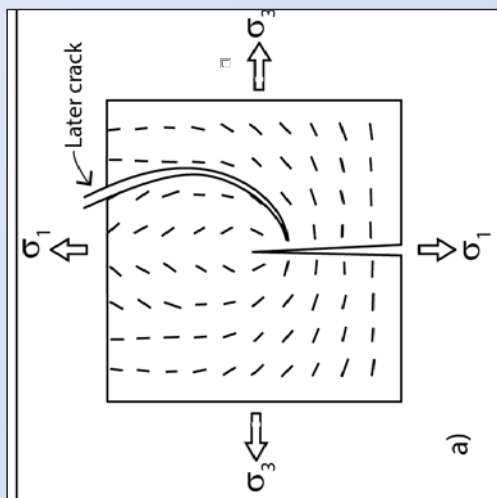
What influences the detailed geometry of fracture networks?

the answer to this question forms the basis of
FRACTURE ANALYSIS
Described in detail in Cosgrove and Hudson

Because the **type, orientation & regularity** of fractures are intimately **controlled by their causative stress fields**, to understand what controls the geometry of fracture networks it is necessary to understand what controls the orientation of stress in the crust during the formation of each fracture set.



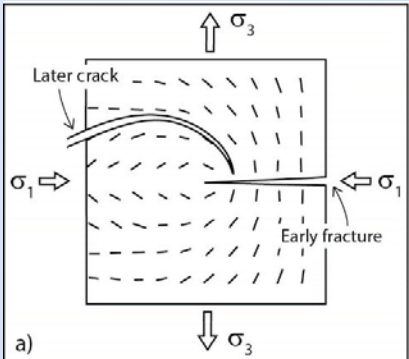
Pre existing fracture impact on the **REGULARITY** of later fractures



The free surface represented by the open fracture **can't sustain a shear stress**.

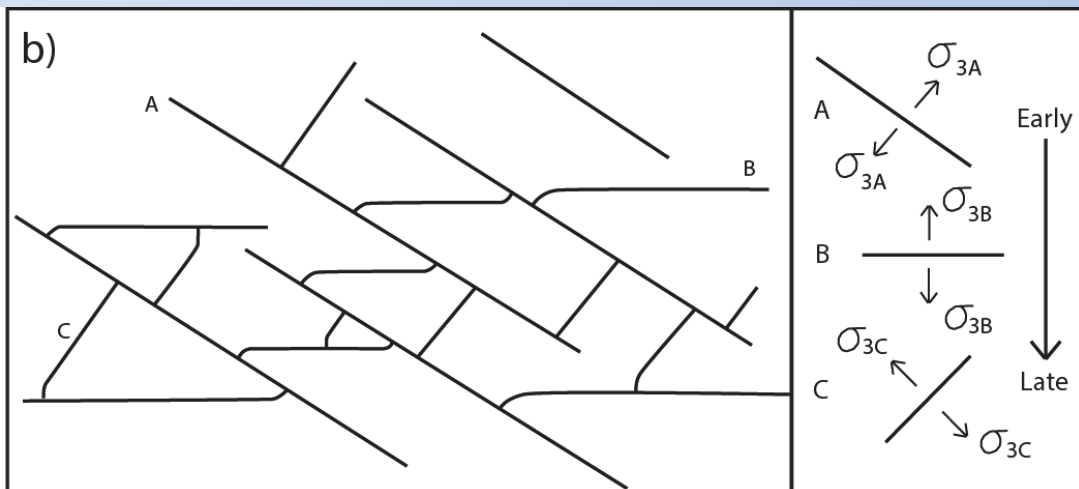
The stress trajectories must Therefore rotate into orientations Either **PARALLEL** or **NORMAL** To the fracture wall





Using the curving and abutting relationships between the different fracture sets their relative age can be established

Set A is older than set B which is older than set C



The **interaction** between early fractures and later stress fields provides the **mechanical basis for Fracture analysis**

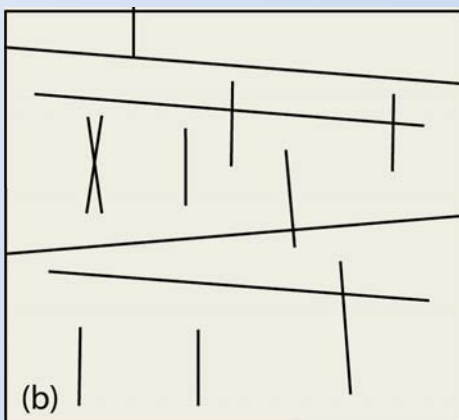
young fractures tend to curve towards and **abut against** older fractures.

Know that fractures in a particular fracture set are usually **regularly spaced**.

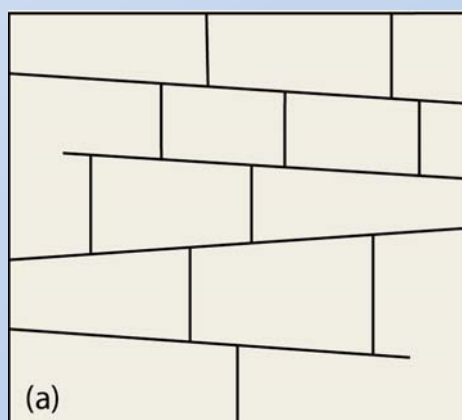
Given the number, length and orientation of fractures in **two** fracture sets 'X' & 'Y' and their abutting relationships we can **REALISTICALLY** reproduce the **geometry of the fracture network** with these data

Is it important to get the network topology right?

A – a stochastic model



B – a natural fracture network

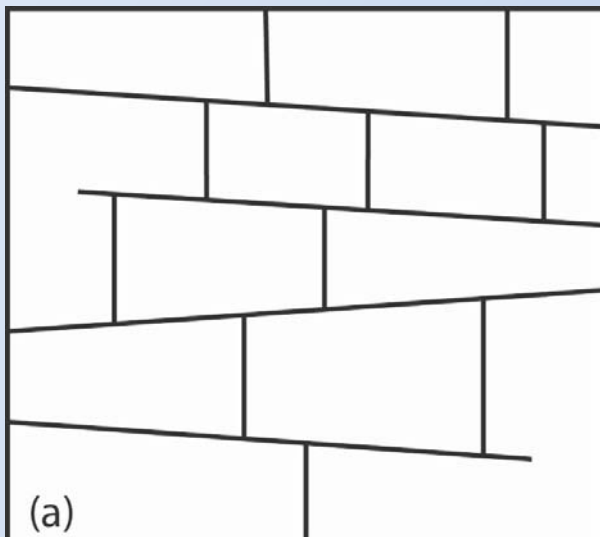


Sets	$A = B$
Number	$A = B$
Density	$A = B$
Mean lengths	$A = B$

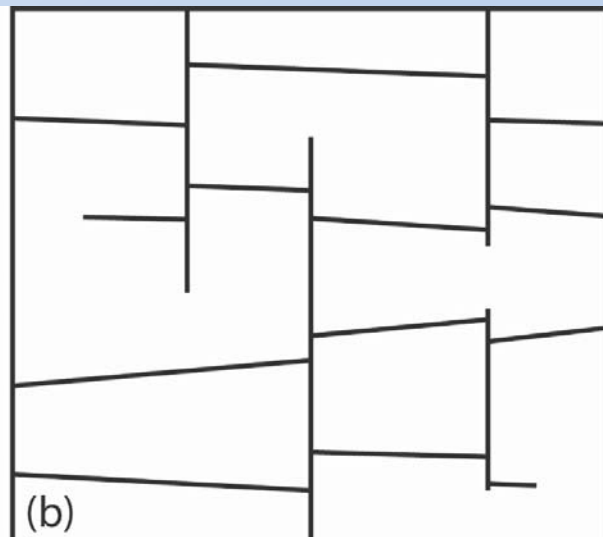
Connectivity	$A > B$
Backbone	$a > B$
Flow	$A > B$

See that the fundamental properties of the fracture network, particularly those related to **fluid flow & bulk strength**, are very sensitive to the fracture organisation within the Networks. **TO CONSTRUCT THE CORRECT GEOMETRY** one needs an **understanding** of the **MECHANICS OF FRACTURE FORMATION AND FRACTURE INTERACTION**.

See the network geometry is also sensitive to the **chronology** of fracture sets



Horizontal 1st Vertical 2nd



Vertical 1st Horizontal 2nd

TO DETERMINE THE GEOMETRY OF A FRACTURE NETWORK AT AN ENGINEERING SITE

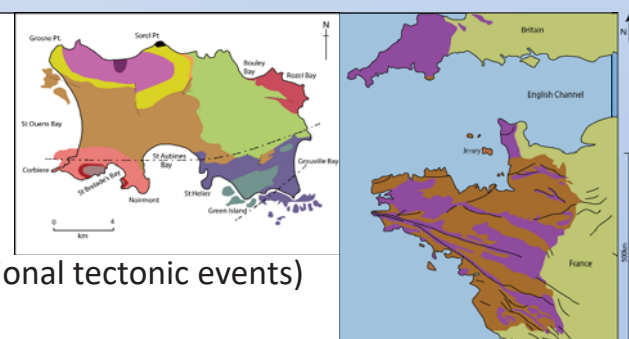
- 1) A ROCK ENGINEER NEEDS TO UNDERSTAND THE BULK MECHANICAL PROPERTIES OF A FRACTURED ROCK MASS IN ORDER TO CONSTRUCT WITHIN IT AND UPON IT
- 2) THESE PROPERTIES ARE DETERMINED BY THE GEOMETRY OF THE FRACTURE NETWORK WITHIN THE ROCK
- 3) THE CHALLENGE IS TO DETERMINE THIS GEOMETRY FOR ANY ENGINEERING SITE
- 4) THERE ARE TWO WAYS THIS CAN BE ACHIEVED
 - (i) A THEORETICAL STUDY
 - (ii) A DETAILED FIELD-BASED STUDY
- 5) IDEALLY BOTH APPROACHES SHOULD BE USED.

Study area - Late Precambrian GRANITE on Jersey – Channel Islands

Theoretical analysis of the fracture network in the granite

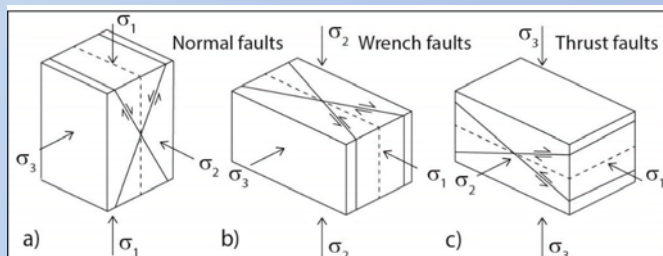
There are three major geological processes that are likely to cause the development of fractures in the rock;

- BURIAL,
- TECTONISM, (there are often several regional tectonic events)
- EXHUMATION,



Study area affected by 4 important tectonic events and all have generated fracture sets.

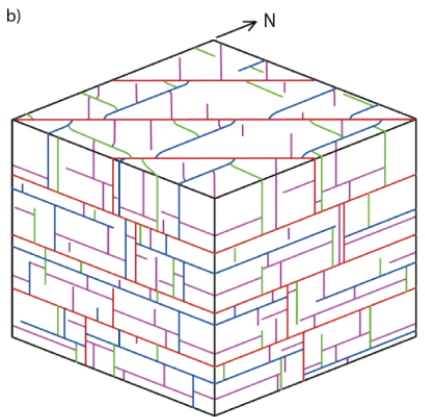
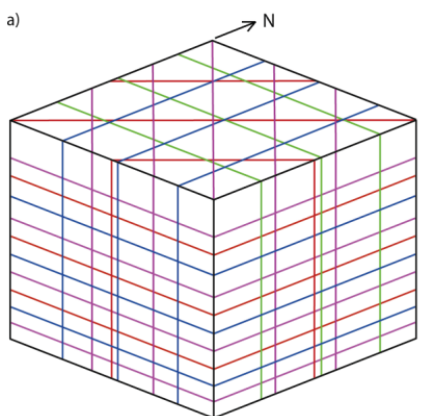
- The Cadomian Orogeny
- The Variscan Orogeny
- The Mesozoic extension and
- The Alpine Orogeny



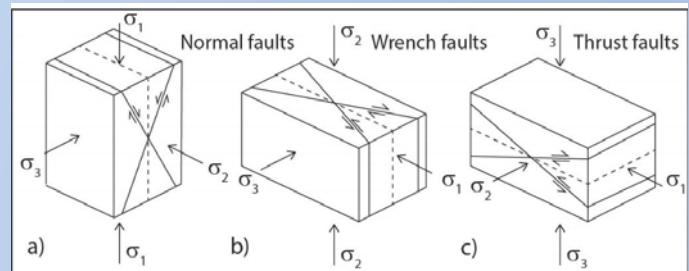
The granite is dominated by EXTENSIONAL FRACTURES therefore ignore predicted faults

EXTENSIONAL FRACTURES linked to tectonism

a) Chronology ignored b) Chronology considered

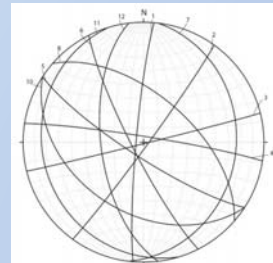
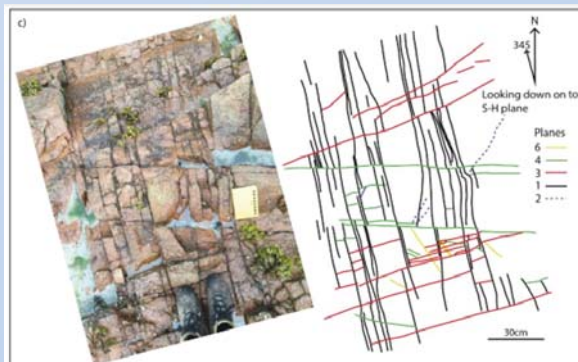
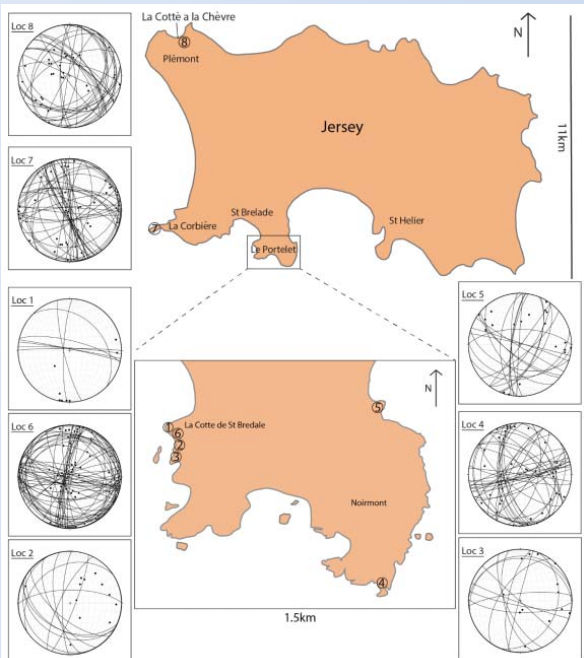


Alpine Orogeny	NW - SE or NNW-SSE Compression	Vertical extensional fractures associated with a strike-slip regime Horizontal extensional fractures associated with a thrust regime
Mesozoic Extension	E-W Extension	Vertical extensional fractures associated with an extensional regime
Hercynian Orogeny	N-S Compression	Vertical extensional fractures associate with a strike-slip regime horizontal extensional fractures associated with a thrust regime
Cadomian Orogeny	NE - SW Compression	Vertical extensional fractures associated with a strike-slip regime horizontal extensional fractures associated with a thrust regime



DETAILED FIELD-BASED STUDY OF THE EXTENSIONAL FRACTURES IN THE GRANITE.

Outcrops show the RELATIVE AGES of the sets

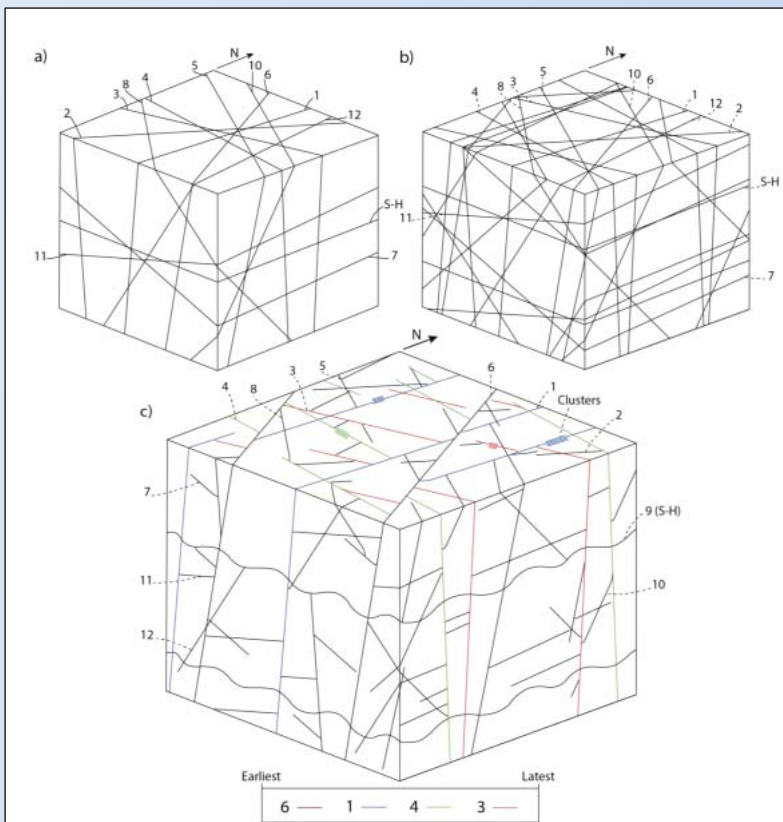


Set number	Dip	Dip Direction	Strike	Number of planes	Variance
1	85	275	185	38	0.56
2	87	126	036	17	0.73
3	89	166	076	26	0.78
4	86	009	279	34	0.71
5	80	213	123	10	0.40
6	82	243	153	19	0.32
7	24	097	007	10	0.02
8	58	041	311	18	0.03
9 (S-H)	04	266	176	49	0.10
10	41	213	123	8	0.01
11	17	253	163	7	0.00
12	61	263	173	10	0.01

12 main sets identified

Field work reveals the ORIENTATION of the various sets of extensional fractures

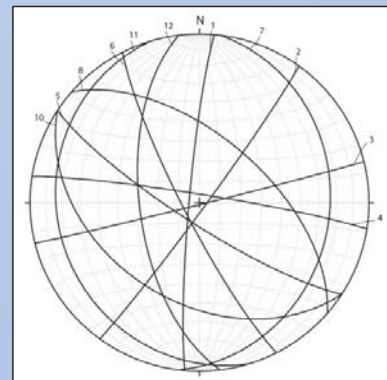
THE CONSTRUCTION OF THE FRACTURE NETWORK



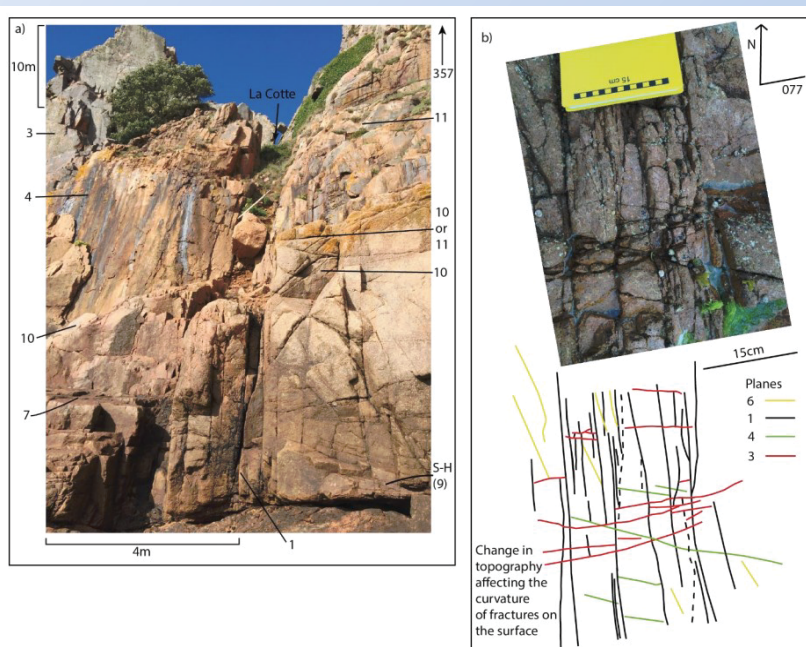
a) 1 Fracture from each set all passing through the centre of the model

b) 2 fractures from each set, not constrained to pass through the centre of the model – NO CHRONOLOGY

c) As b) but with the chronology observed

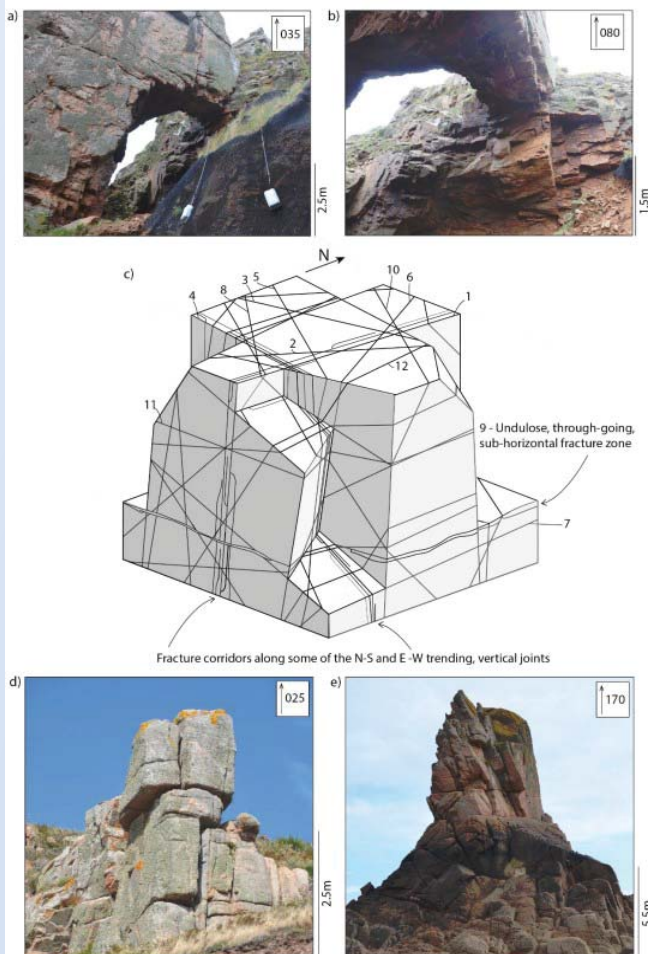
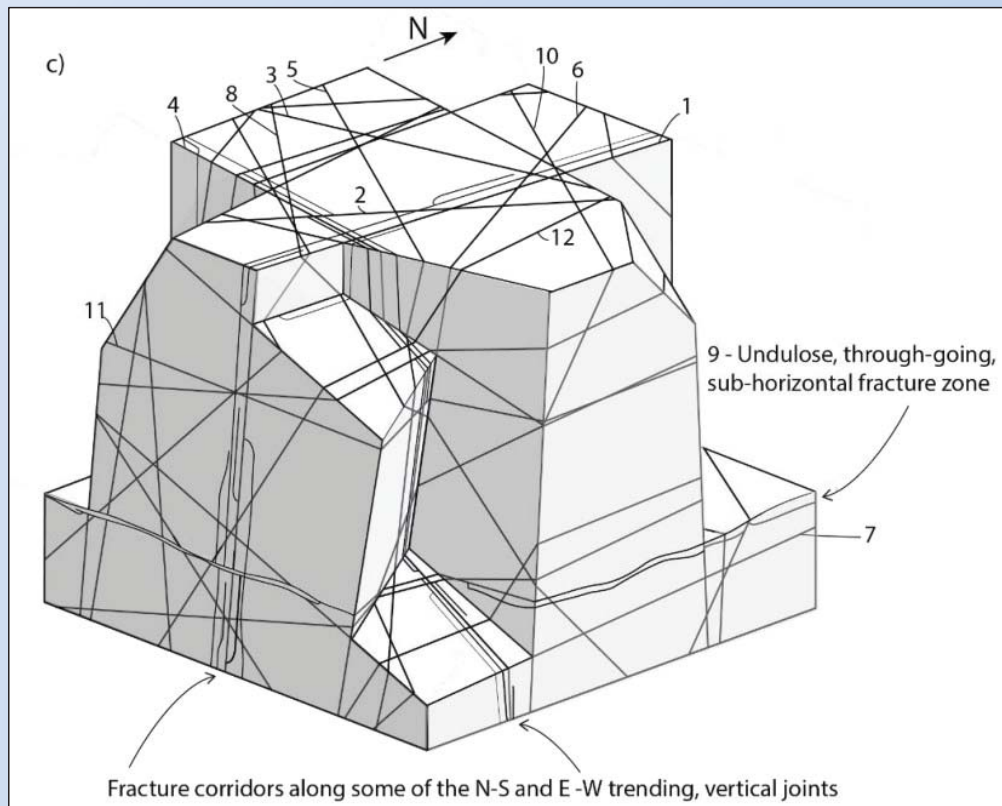


- **REFINEMENT OF THE MODEL** Details – some irregularities
- Field work will highlight any features of the different fracture sets that need integrating into the model.
- E.g., A tendency to form **FRACTURE CORRIDORS** where the fractures are clustered together rather than being uniformly spaced, was noted.



FINAL MODEL – Based on

- (i) field observations,
- (ii) a sound understanding of the mechanics of fracture formation and interaction
- (iii) the tectonic history of the study area



Conclusions

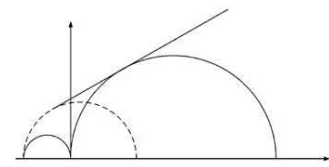
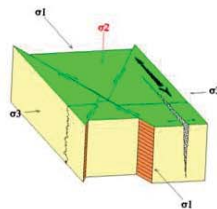
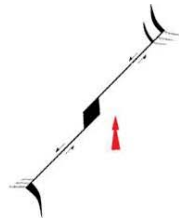
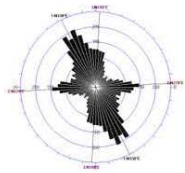
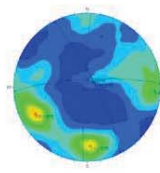
The structural geologist understands

- i) the **brittle failure of rocks** and the control of stress on fracture orientation, type and regularity, and
- ii) The **mechanical interaction between different fracture sets** during the build up of a fracture network

This enables a realistic model of the geometry of a fracture network in a rock mass to be determined when this is combined with a

- iii) Detailed **field study** of the engineering site, and when ideally there exists
- iv) a knowledge of the **geological history** of the study area.

THANK YOU



THE HELP OF STRUCTURAL GEOLOGY

WHEN USING ROCK MASS CLASSIFICATIONS
& MAPPING DURING TUNNELLING ACTIVITIES

Philippe VASKOU

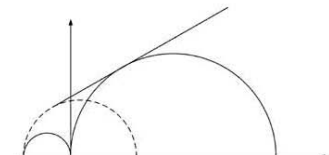
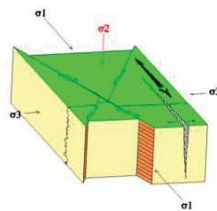
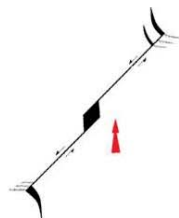
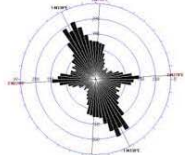
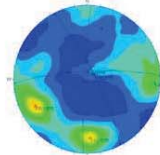
Independent Expert in Underground Engineering / University of Cergy-Paris



XVIII JORNADA TÉCNICA ANUAL

MECÁNICA DE ROCAS Y GEOLÓGIA ESTRUCTURAL

13 DE MAYO 2021



OBJECTIVES OF THIS LECTURE

- to present a few structural aspects & principles about fractures
- to apply these principles in underground works, on a practical point of view, with examples related to:
 - tunnel mapping
 - Rock Mass Classification assessment
 - permeability of fractures vs. in situ stresses

RESTRICTIONS & LIMITATIONS

- limited to underground works (tunnels, shafts, caverns, mines)
- limited to brittle deformations

CONTENT

1 Difficulties & Issues in Tunnels

2 Help of structural geology in Tunnels

for RMC assessment & face/wall mapping, based on

2a - the length of fractures

2b - the termination of fractures

3 *In situ* stress regime and fracture permeability

4 Conclusion

1 – DIFFICULTIES & ISSUES IN TUNNELS

**The subject & the concepts are similar but in practice,
above ground and underground works can be very different**

ABOVE GROUND WORKS

outcrops
quarries
etc.



UNDERGROUND WORKS

tunnels
caverns
shafts

1 – DIFFICULTIES & ISSUES IN TUNNELS

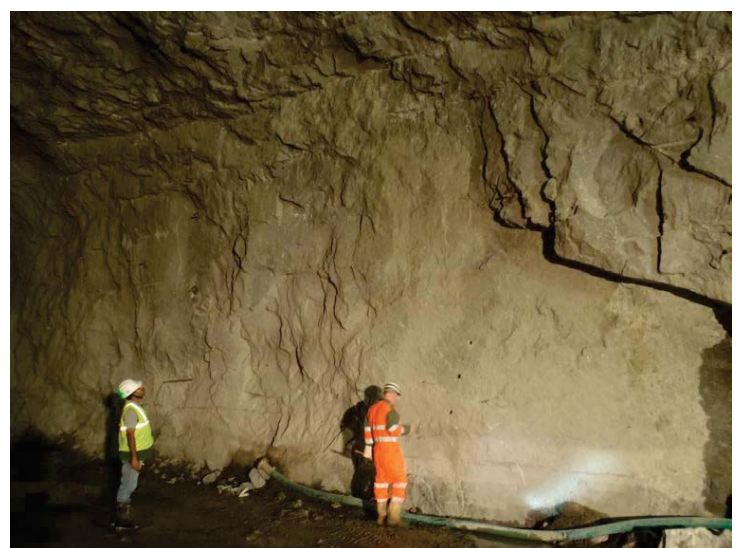
- Low lighting
- Limited ventilation
- Air dust

} reduce visibility



1 – DIFFICULTIES & ISSUES IN TUNNELS

- Water dripping → making measurements & taking notes are uneasy
- Height → out of reach zones



1 – DIFFICULTIES & ISSUES IN TUNNELS

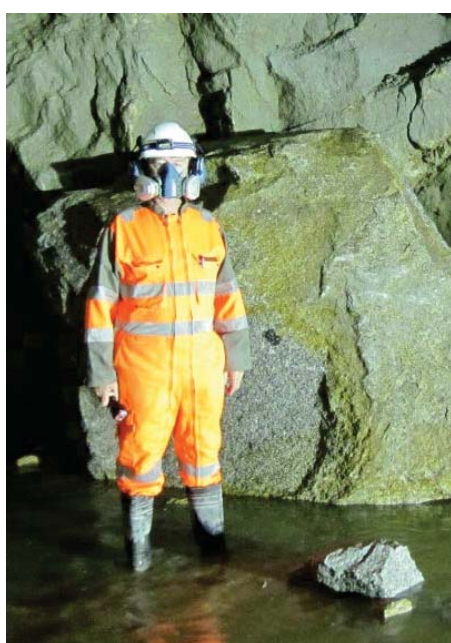
In Shafts:

- **Limited space**
 - **Access mean**
- impossibility to make close observations
→ difficulties to make accurate measurements



1 – DIFFICULTIES & ISSUES IN TUNNELS

- **Wearing of PPEs**
- reduces the field of vision



1 – DIFFICULTIES & ISSUES IN TUNNELS

- and too often most important:

Limited allocated time window !

Except in research tunnels (e.g. for nuclear waste repositories) where mapping is the objective, in industrial projects, observations, measurements & mapping are done too quickly:

- **work is incompletely done,**
- **quality & accuracy of maps can be relatively poor...**

1 – DIFFICULTIES & ISSUES IN TUNNELS

Considering and taking into account all these constraints,

HOW TO CARRY OUT MAPPING CORRECTLY?

IN A MINIMUM TIME FRAME?

WHILE KEEPING THE 2 MAIN OBJECTIVES OF MAPPING

- **Stability** → analysis of wedges in 3D
- **Water issues** → identification of previous fractures & need for grouting

2 – HELP OF STRUCTURAL GEOLOGY IN TUNNELS

Mapping and Rock Mass assessment are often associated;
 Classical RMC used: **RMR** (Bieniawski) and **Q-system** (Barton)

RMR (Bieniawski)	Q-system (Barton)
Matrix Strength	Number of Joint Sets (N, N+random)
RQD	RQD
Spacing of discontinuities	Joint Alteration
Conditions of discontinuities: - Length (persistence) - Separation (aperture) - Roughness - Infilling - Weathering	Joint Roughness: - Discontinuous - Rough, irregular - Smooth - Slickensided
Ground Water - Inflow per 10m - Water P / major principal σ	Joint Water Reduction - Inflow or water P
	Stress Reduction Factor

2 – HELP OF STRUCTURAL GEOLOGY IN TUNNELS

Easy to observe/measure vs. more subjective parameters

RMR (Bieniawski)	Q-system (Barton)
Matrix Strength	Number of Joint Sets (N, N+random)
RQD	RQD
Spacing of discontinuities	Joint Alteration
Conditions of discontinuities: - Length (persistence) - Separation (aperture) - Roughness - Infilling - Weathering	Joint Roughness: - Discontinuous - Rough, irregular - Smooth - Slickensided
Ground Water - Inflow per 10m - Water P / major principal σ	Joint Water Reduction - Inflow or water P
	Stress Reduction Factor

2 – HELP OF STRUCTURAL GEOLOGY IN TUNNELS

In tunnels, structural **observations** may help assessing:

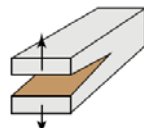
- the length of fractures (RMR persistence)
- the roughness of fractures (RMR & Q):
quick discrimination of rough / smooth / slickensided

In addition,

- a visual control/validation of fracture "permeability"
(pervious set vs. impervious sets)
- using to the *in situ* stress regime (virgin stress)

2a – THE LENGTH OF FRACTURES

CONCEPT OF FRACTURE LENGTH



For joints (Mode 1 prevailing fractures)

Principle: Extensional fractures cannot propagate though a free surfaces: free surface of existing fractures cannot sustain shear stress → rotation of stress trajectory

Result: **The earlier initial set is the longest one,** and later sets (2nd, 3rd, etc.) stop again the *pre-existing* ones

*Concept of Fracture Chronology
(John Cosgrove, SinoRock)*



2a – THE LENGTH OF FRACTURES

Relative chronology:

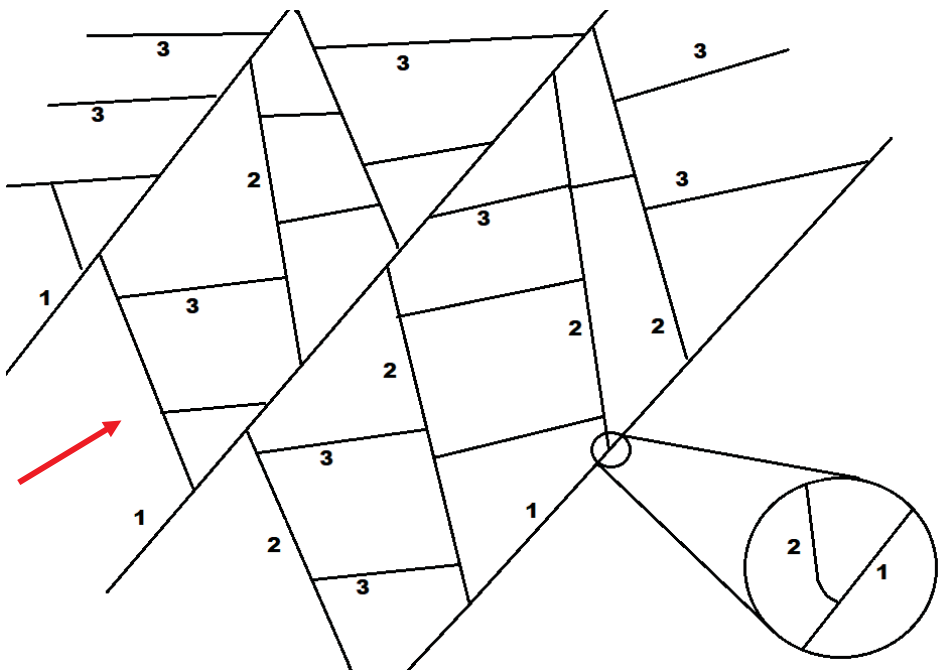
J1 earlier than J2

J2 earlier than J3

Using this principle,
in terms of length:

$J1 > J2 > J3$

example on quarry



2a – THE LENGTH OF FRACTURES

Applying this principle in tunnels:

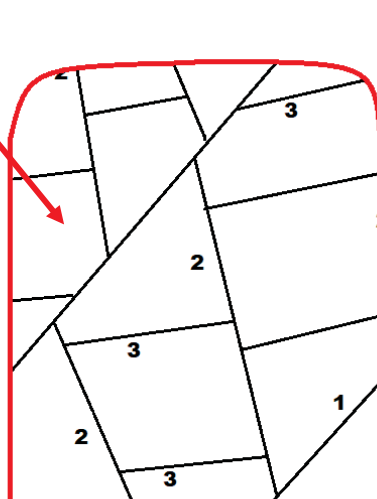
same example but limited to a tunnel face

here, distinguishing
the longest set
may be more difficult...
J1 or J2?

Since J3 stops on J2
& J2 stops on J1

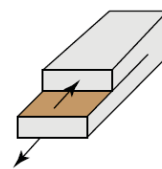
in terms of chronology & length

$J1 > J2 > J3$



2a – THE LENGTH OF FRACTURES

For faults (Mode 2 prevailing fractures):



Principle: Faults grow by coalescence of individual shear fractures

Result: The longest faults are the most recent ones

2a – THE LENGTH OF FRACTURES

Applying these principles in tunnels:

- Quicker assessment of joint length, when limited observation zones (*set stopping on another*)
 - Thin shear fractures are less persistent than thicker ones (*coalescence*)
- } Extensional fractures (Joints)
- } Shear fractures (Faults)

Direct use in RMR (persistence)

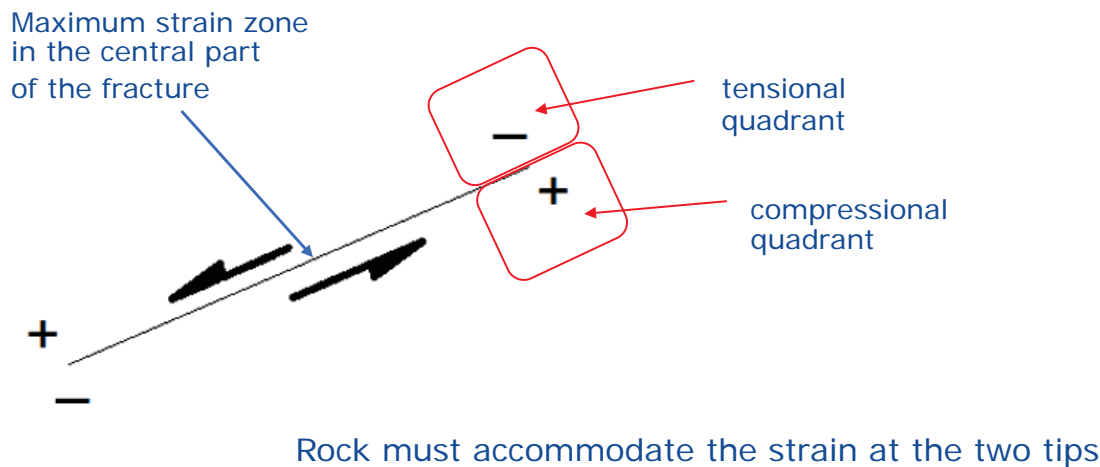
However, the visual identification of faults can be difficult in homogeneous rock masses (gneiss, granite, fine-grained limestone) when no marker is available

This can be done using fracture termination...

2b – THE TERMINATION OF FRACTURES

Most fractures show shear movement, even if not the original mode of failure

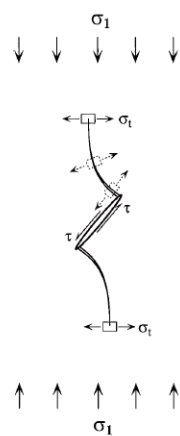
Shearing creates **tension** and **compression** at the **tips** of the fracture



2b – THE TERMINATION OF FRACTURES

Fracture arrest:

Rock mechanicians know about wing cracks from laboratory testing



...but in the brittle crust, many other possibilities do exist

2b – THE TERMINATION OF FRACTURES

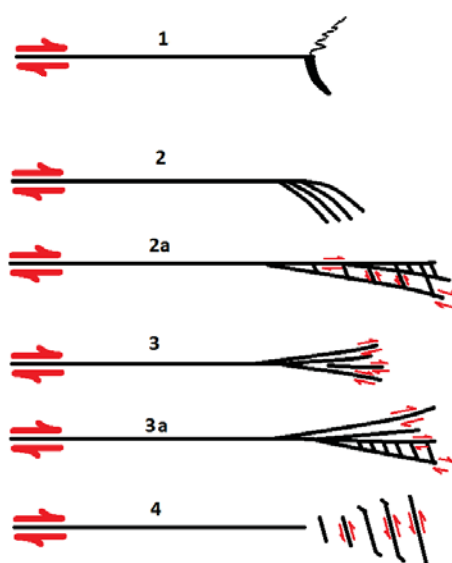
Basically, in hard rocks, the total strain of a single movement along a shear fracture can be accommodated at the fracture tips either by:

- tension joint(s) → wing crack(s) $\sigma_t \approx 1/10 \sigma_c$
- strain distribution into several small shear fractures
- deformation...

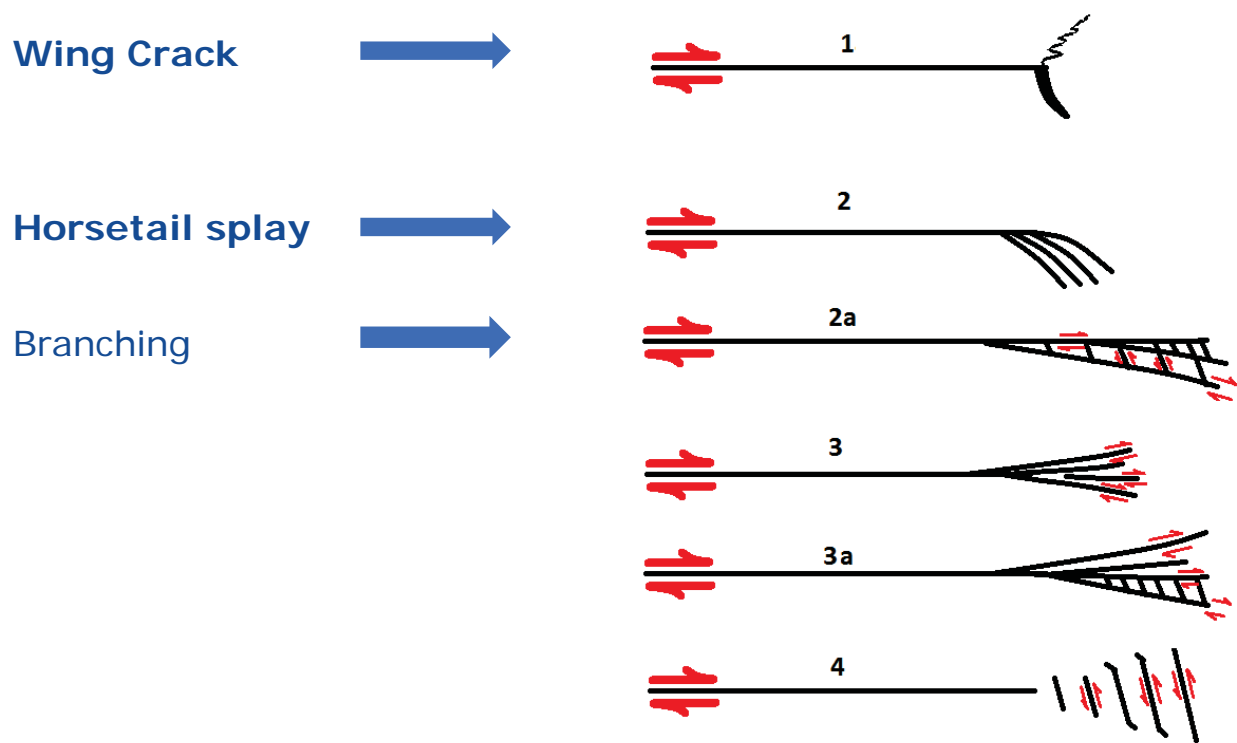
2b – THE TERMINATION OF FRACTURES

Basically, in hard rocks, the total strain of a single movement along a shear fracture can be accommodated at the fracture tips either by:

- tension joint(s) → wing crack(s)
- strain distribution into several small shear fractures
- deformation



2b – THE TERMINATION OF FRACTURES



2b – THE TERMINATION OF FRACTURES

Most Common strain adaptations:

- in tensional quadrant
 - local tensional opening of joints in Mode 1 ($\sigma_T \approx 1/10 \sigma_c$)
 - distribution of total strain into several cracks

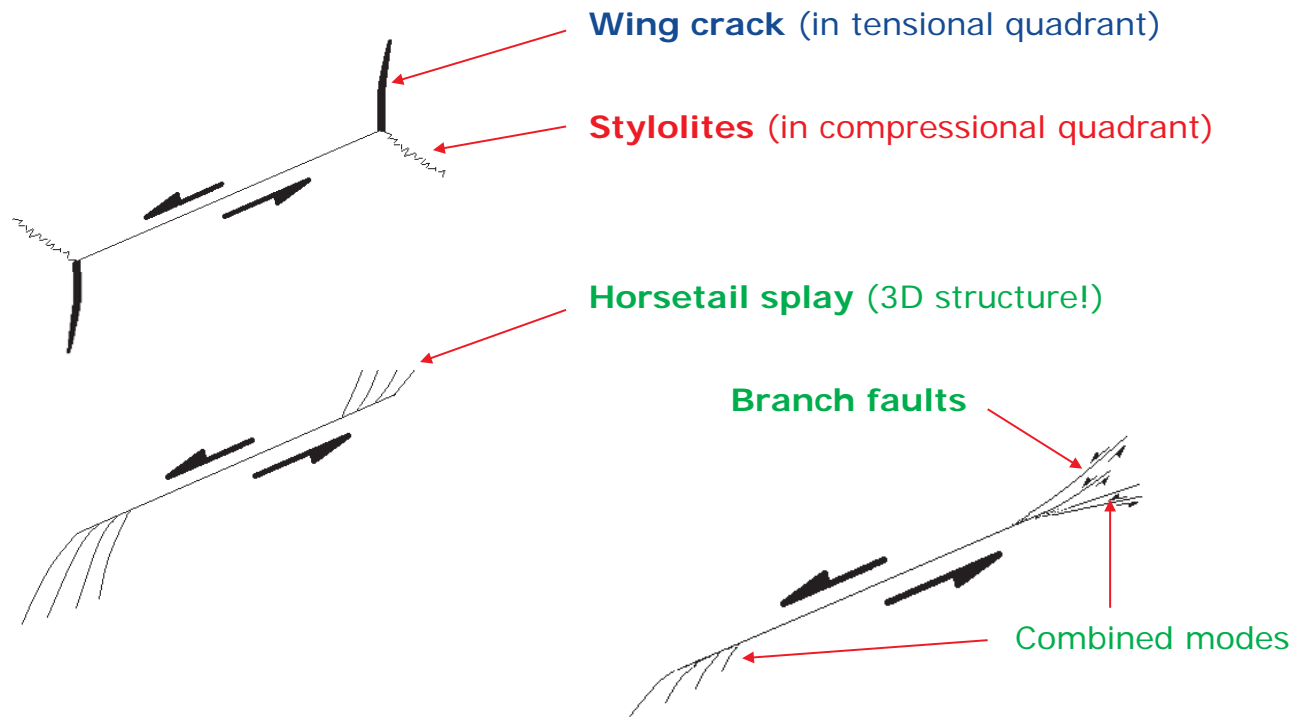
- in compressional quadrant
 - distribution of total strain into several cracks

- pressure solution

ALL ROCK TYPES

LIMITED ROCK TYPES
e.g. limestone, salt

2b – THE TERMINATION OF FRACTURES



2b – THE TERMINATION OF FRACTURES

Fracture terminations have very similar shapes **whatever the scale**

➤ **Small scale**



2b – THE TERMINATION OF FRACTURES

Fracture terminations have very similar shapes **whatever the scale**

➤ Small scale

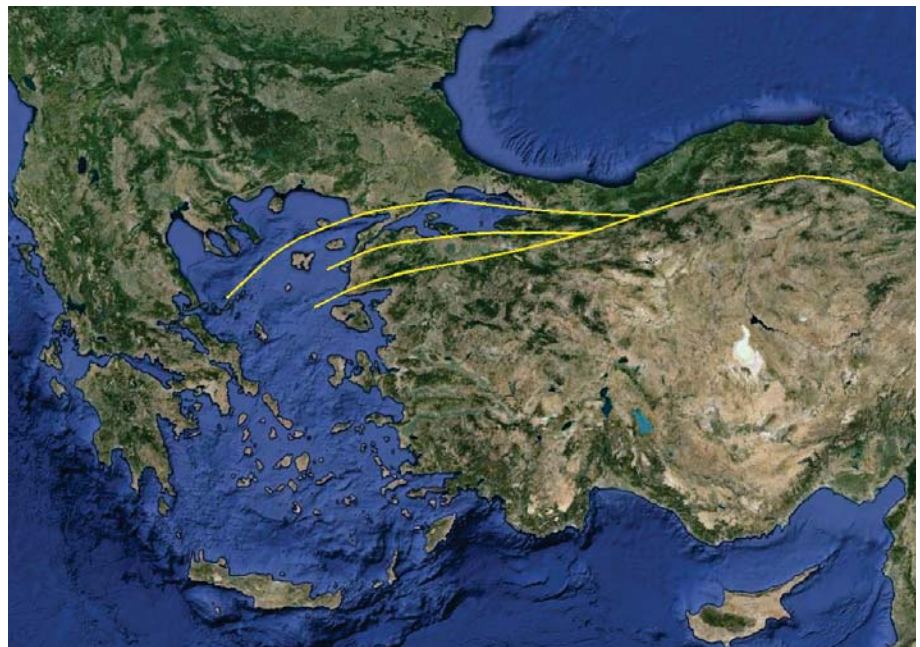


➤ Medium scale

2b – THE TERMINATION OF FRACTURES

Fracture terminations have very similar shapes **whatever the scale**

➤ Small scale



➤ Medium scale

➤ Large to
very large scale

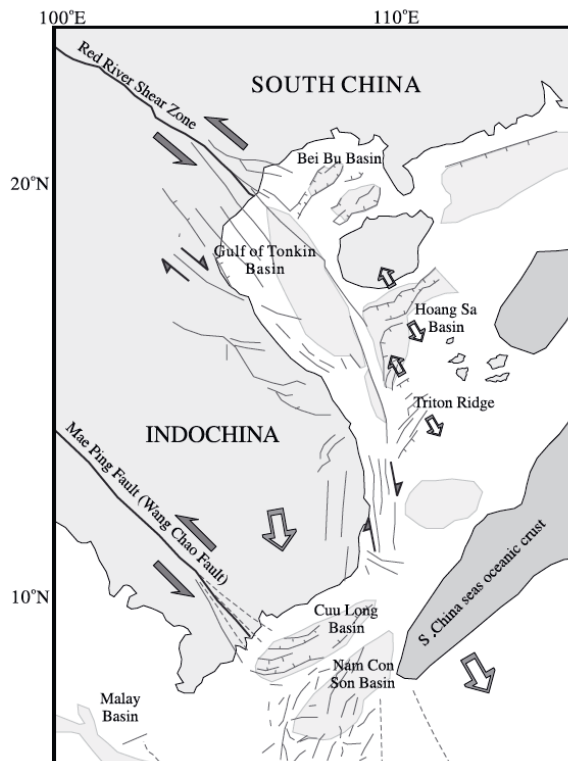
2b – THE TERMINATION OF FRACTURES

Fracture terminations have very similar shapes whatever the scale

➤ Small scale

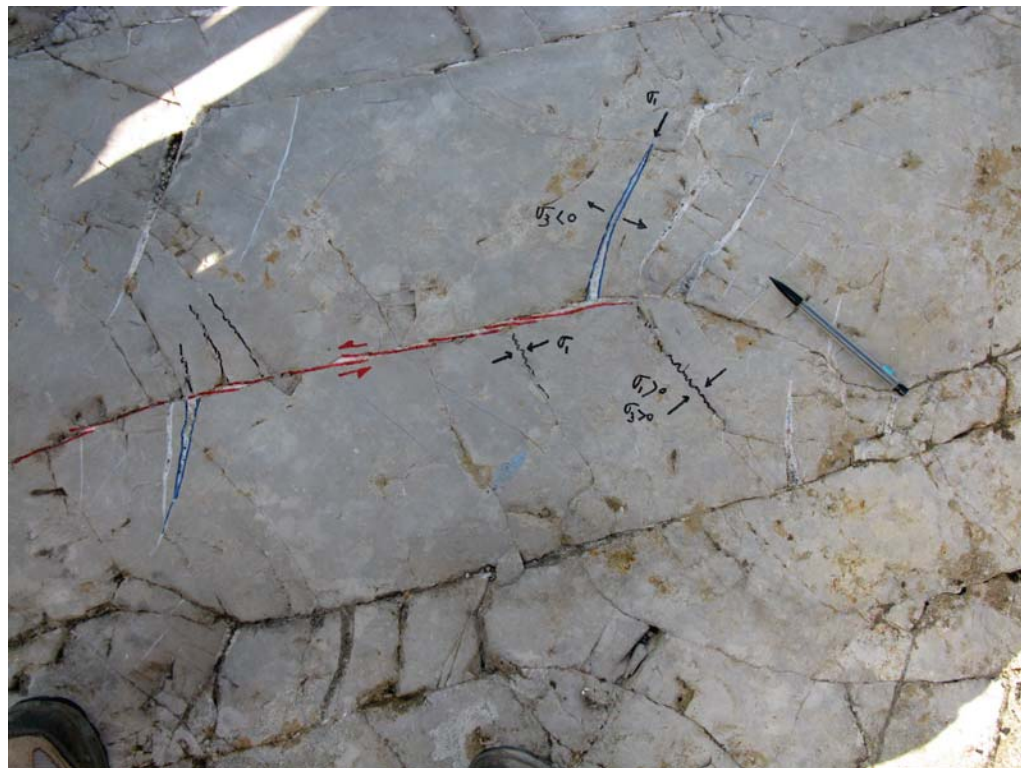
➤ Medium scale

➤ Large to
very large scale



2b – THE TERMINATION OF FRACTURES

Example in a limestone (France)



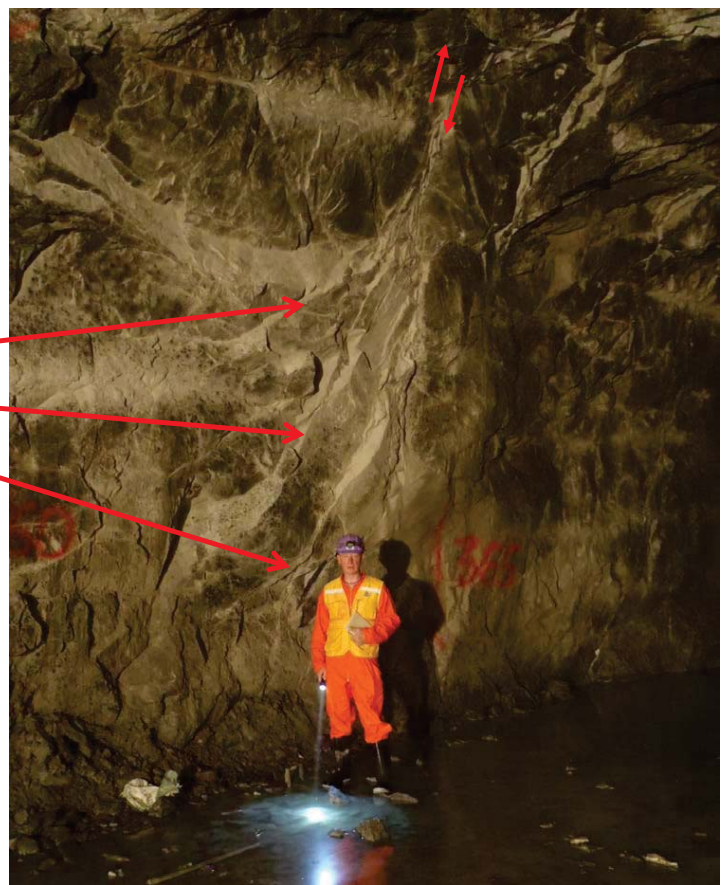
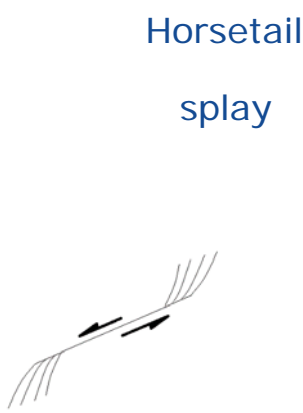
Wing cracks

+

Stylolites

2b – THE TERMINATION OF FRACTURES

Example in a Gneiss (India)



2b – THE TERMINATION OF FRACTURES

Example in a Granite (Japan)



2b – THE TERMINATION OF FRACTURES

Example in a volcano-sedimentary rock (Singapore)



Combined modes:

- Brittle fractures (horsetail type)
- En échelon tension gashes
- Main fracture (fault)

2b – THE TERMINATION OF FRACTURES

In tunnels, these observations allow assessing descriptive parameters:

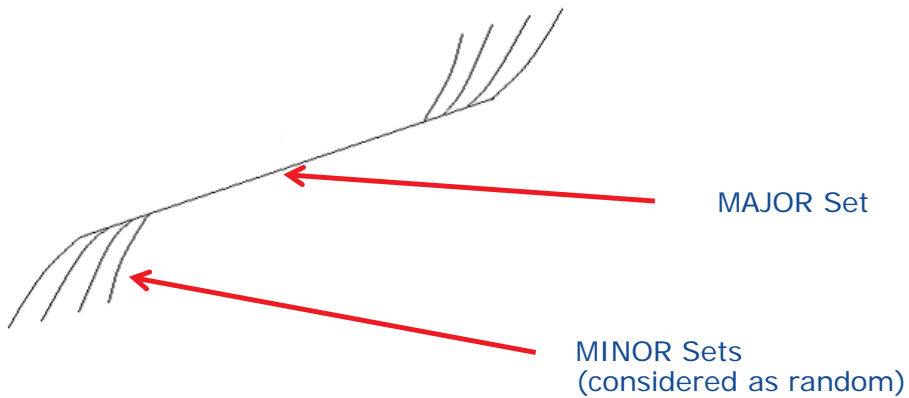
- origin of fractures (tension vs. shear; Mode 1 vs. Mode 2)
- rough estimation of fracture offset (without marker)
- assessment of movement (strike-slip, dip-slip)
- ranking of fractures (main vs. minor)

➔ Direct use in Rock Mass Classifications: Jn, persistence, Jr

2b – THE TERMINATION OF FRACTURES

Example of application in tunnel & RMC

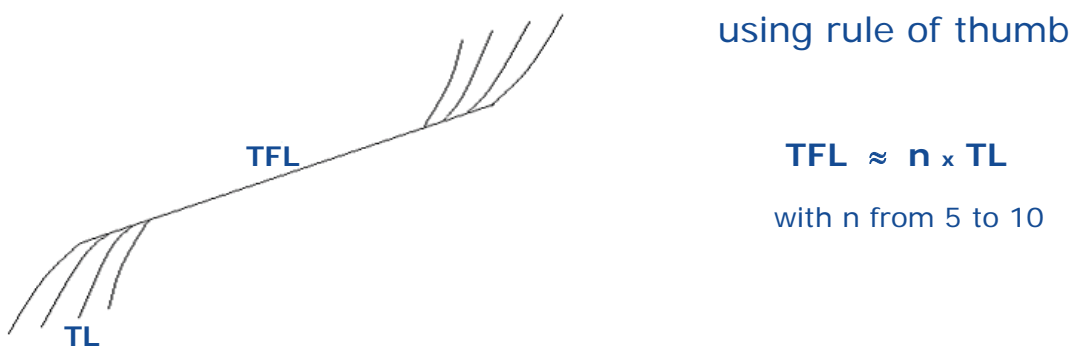
- Number of joint sets (**Jn** in Q-system)



2b – THE TERMINATION OF FRACTURES

Example of application in tunnel & RMC

- Rating of Discontinuity Length (RMR Persistence)

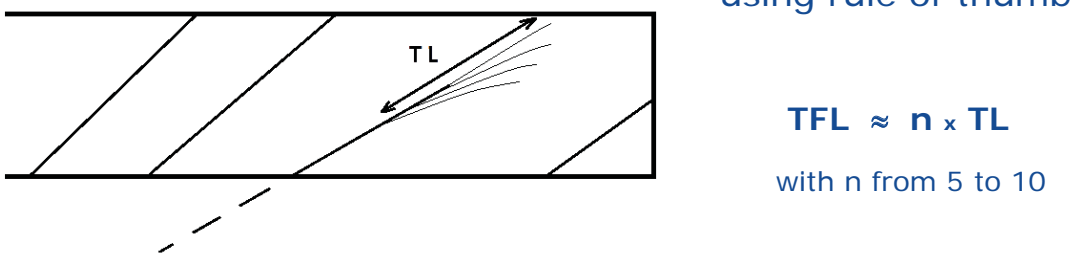


This works whatever the scale (small fracture to large fault!)

2b – THE TERMINATION OF FRACTURES

Example of application in tunnel & RMC

- Rating of Discontinuity Length (RMR Persistence)

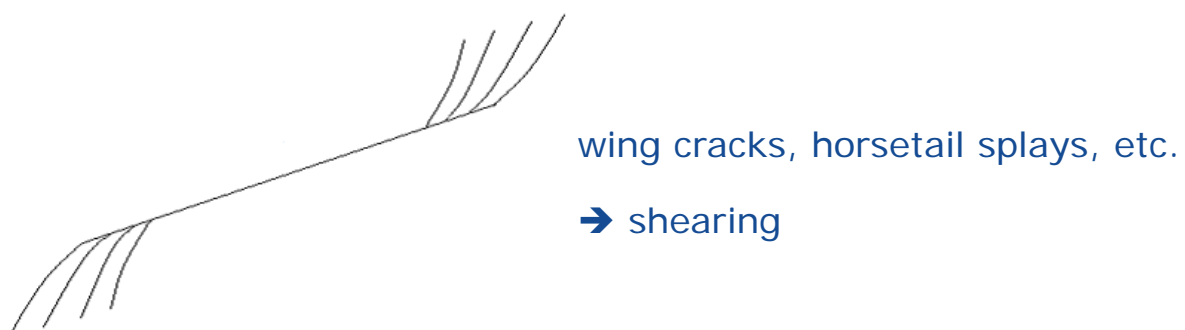


This works whatever the scale (small fracture to large fault!)

2b – THE TERMINATION OF FRACTURES

Example of application in tunnel & RMC

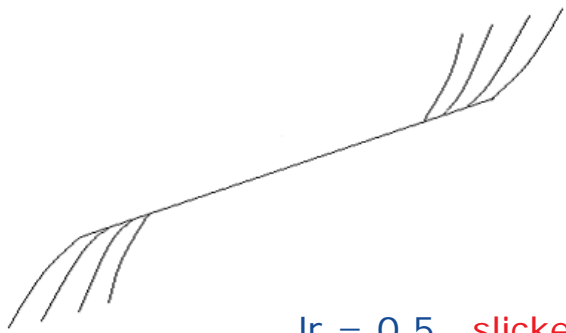
- Evidence of shear displacement (Mode 2 vs. Mode 1)



2b – THE TERMINATION OF FRACTURES

Example of application in tunnel & RMC

➤ Assessment of Roughness:



when impossibility to observe
fracture walls, presence of
wing cracks, horsetail splays, etc.
→ slickensided shall be considered
(to be on the safe side)

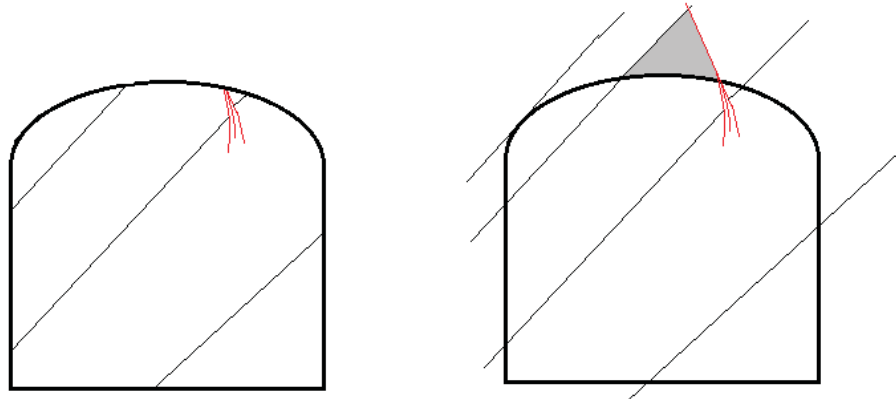
or $J_r = 0,5$ slickensided planar
 $J_r = 1,5$ slickensided undulating

2b – THE TERMINATION OF FRACTURES

Example of application in tunnel mapping

➤ Stability of wedges:

even truncated observations can be used for understanding the
structure and therefore the stability



2b – THE TERMINATION OF FRACTURES

Summary of applications in tunnels

Fracture observation	may gives clues on	RMC
History (setting)	Length (by chronology, S1 > S2 > S3)	RMR (persistence)
In presence of terminations	Length (rough estimate)	RMR (persistence)
	Fracture type joint vs.fault; Mode 1 vs. Mode 2	RMR roughness Jr (random)
	Assessment of shear displacement (even without marker)	Jr (slickensided)
	Type of movement (dip-dip; strike-slip; dextral...)	Jr (slickensided)
	Ranking of fractures (main vs. minor fractures)	Jn (random)

3 – IN SITU STRESS REGIME & FRACTURE PERMEABILITY

When assessing water flow in fractures for RMR or Q-system, structural observations may allow a validation (site or tunnel scale) between permeability and *in situ* stress regime

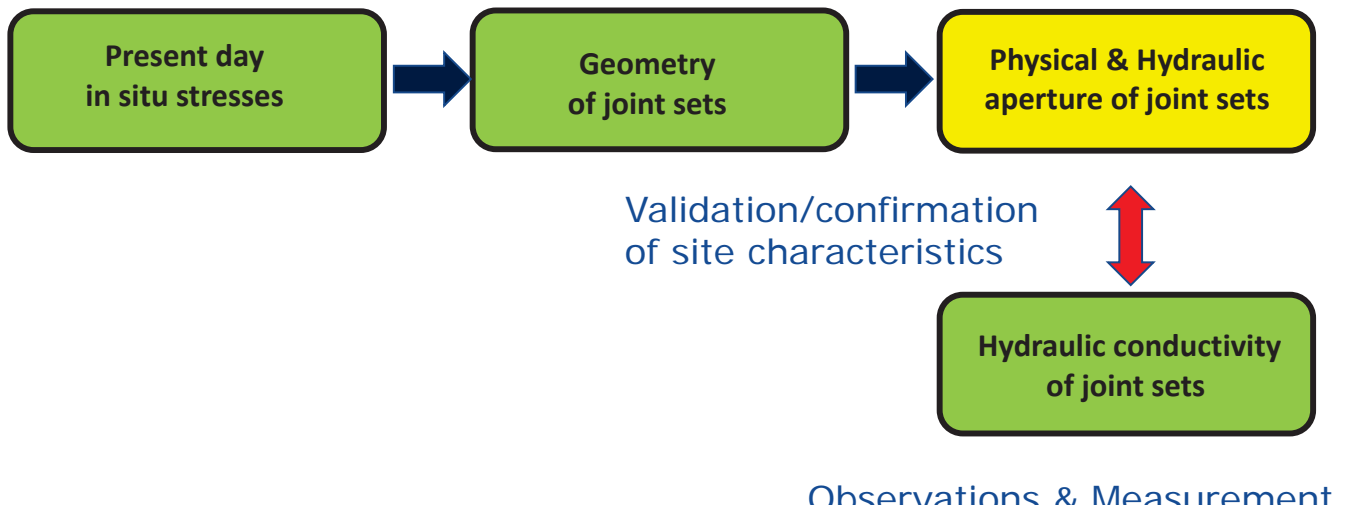
Theory:

The most pervious fractures are those having planes normal to the minimum stress component (σ_3)

The least pervious fractures are those having plane normal to the maximum stress component (σ_1)

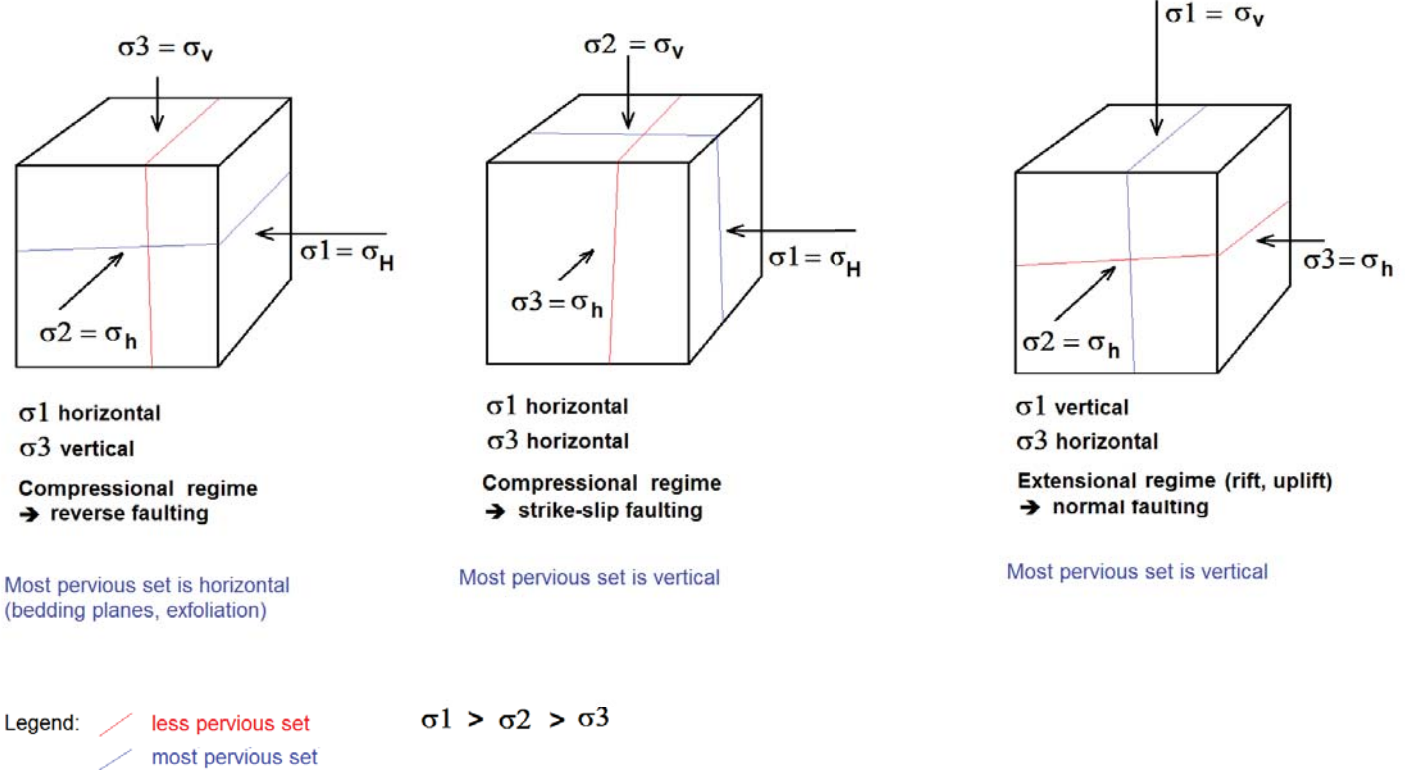
3 – IN SITU STRESS REGIME & FRACTURE PERMEABILITY

Theory (on pre-existing fractures!)



This approach can be used at site scale (SI) but also in tunnels

3 – IN SITU STRESS REGIME & FRACTURE PERMEABILITY



3 – IN SITU STRESS REGIME & FRACTURE PERMEABILITY

This approach can be done semi-qualitatively during excavation of tunnels, caverns, with a visual assessment

But a more accurate assessment can be done earlier during a Site Investigation using the 3 required parameters:

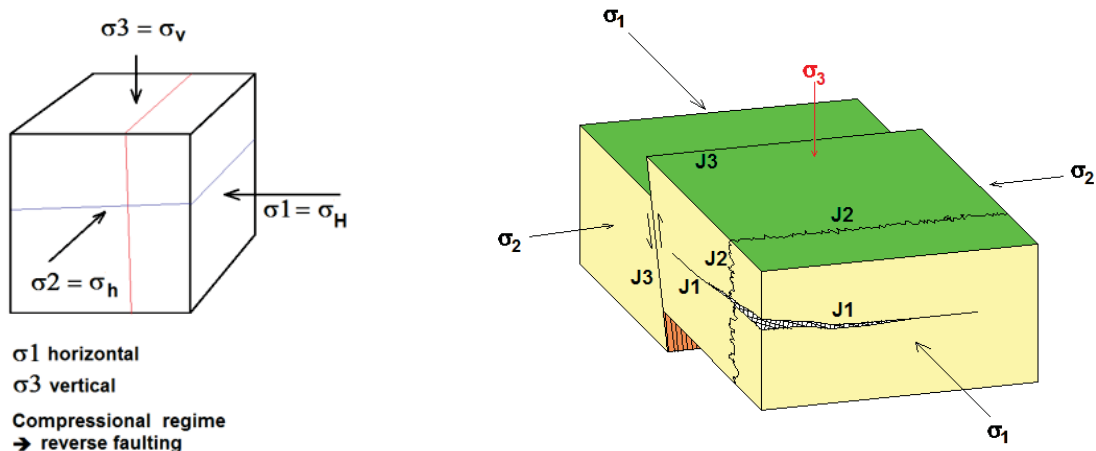
- the geometry of fractures (BHTV)
- the orientation and magnitude of stress components
 - e.g. using Hydrofracturing, overcoring
- permeability measurements
 - e.g. long duration Packer tests, interference tests, etc.

Excel spreadsheet

- ➔ normal stress σ_n acting on each fracture set
- ➔ most and least pervious set

3 – IN SITU STRESS REGIME & FRACTURE PERMEABILITY

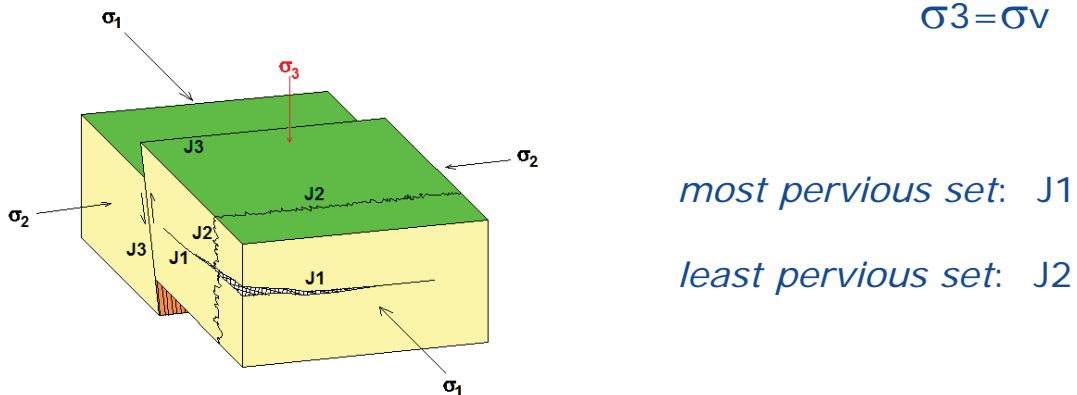
But the reality is always more complicated than the theory ...



3 – IN SITU STRESS REGIME & FRACTURE PERMEABILITY

... and fractures are not always horizontal and vertical.

Example in the most common sub-surface situation $\sigma_1 = \sigma_H$

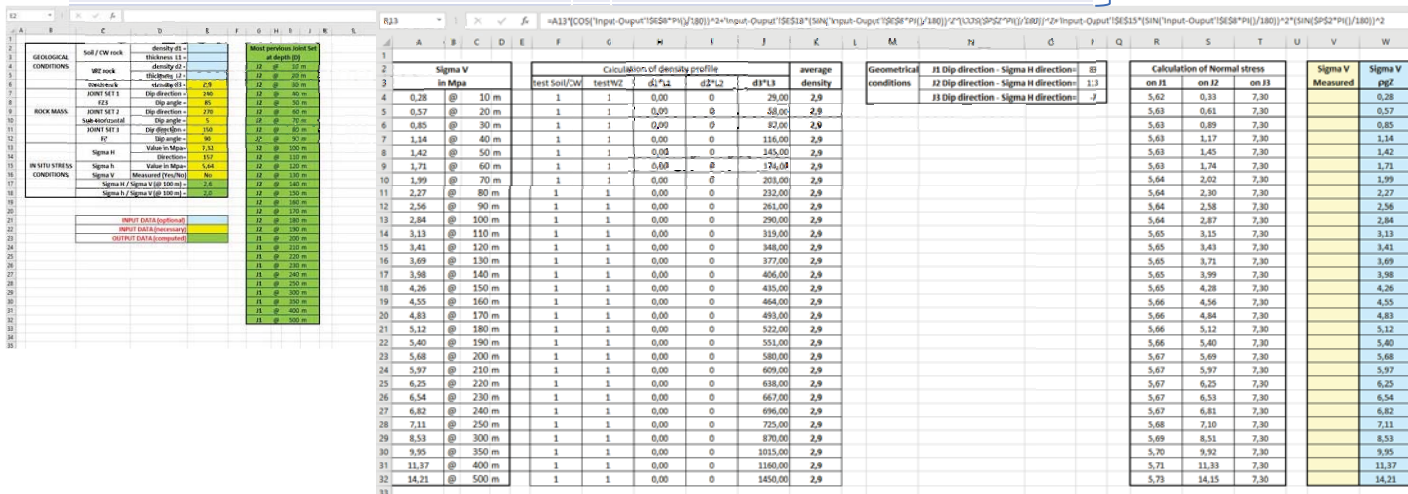


Easy to “visualise” but natural fractures have various geometries, (strike, dip angle) making more difficult to anticipate the hydraulic conductivity. Some computing become necessary...

3 – IN SITU STRESS REGIME & FRACTURE PERMEABILITY

Input Data		Output Data	
Geometry of main joint sets: Dip direction & Dip		σ_n & τ on each set	
Results of in situ stress measurements: σ_H , σ_h , σ_v and σ_H direction		Estimation of most and least pervious set (mechanical and hydraulic joint apertures*)	

using Excel
spreadsheets



3 – IN SITU STRESS REGIME & FRACTURE PERMEABILITY

Input Data	Output Data	
Geometry of main joint sets: Dip direction & Dip	σ_n & τ on each set	Excel
Results of in situ stress measurements: σ_H , σ_h , σ_v and σ_H direction	Estimation of most and least pervious set (mechanical and hydraulic joint apertures*)	Excel
Mohr-Coulomb and Barton-Bandis joint parameters: C , ϕ and JRC, JCS, ϕ_r	Joint set stability with regard to shearing Plot of the Mohr circles and polar graph	Java

3 – IN SITU STRESS REGIME & FRACTURE PERMEABILITY

To assess the potential fracture permeability of fractures, whatever their orientation (azimuth and dip angle), a simple Excel spreadsheet can be used

Global validation at a Site Scale:

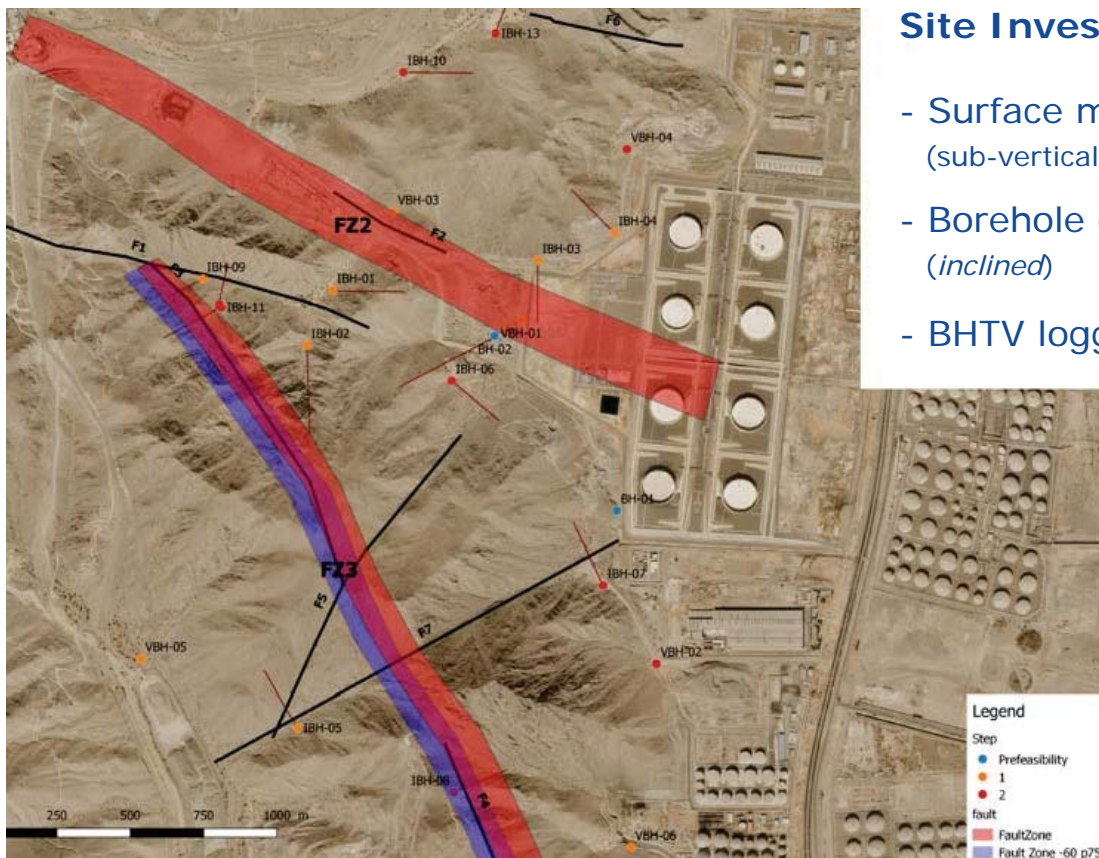
Comprehensive validation of a site at the End of a Site Investigation:

- surface mapping
- geometrical attitude of fractures (via BHTV logging)
- hydrogeological testing
- in situ stress measurements

Validation during the early phases of tunnel excavation:

- geometrical attitude of fractures (actual vs. anticipated)
- visual assessment of pervious fracture sets

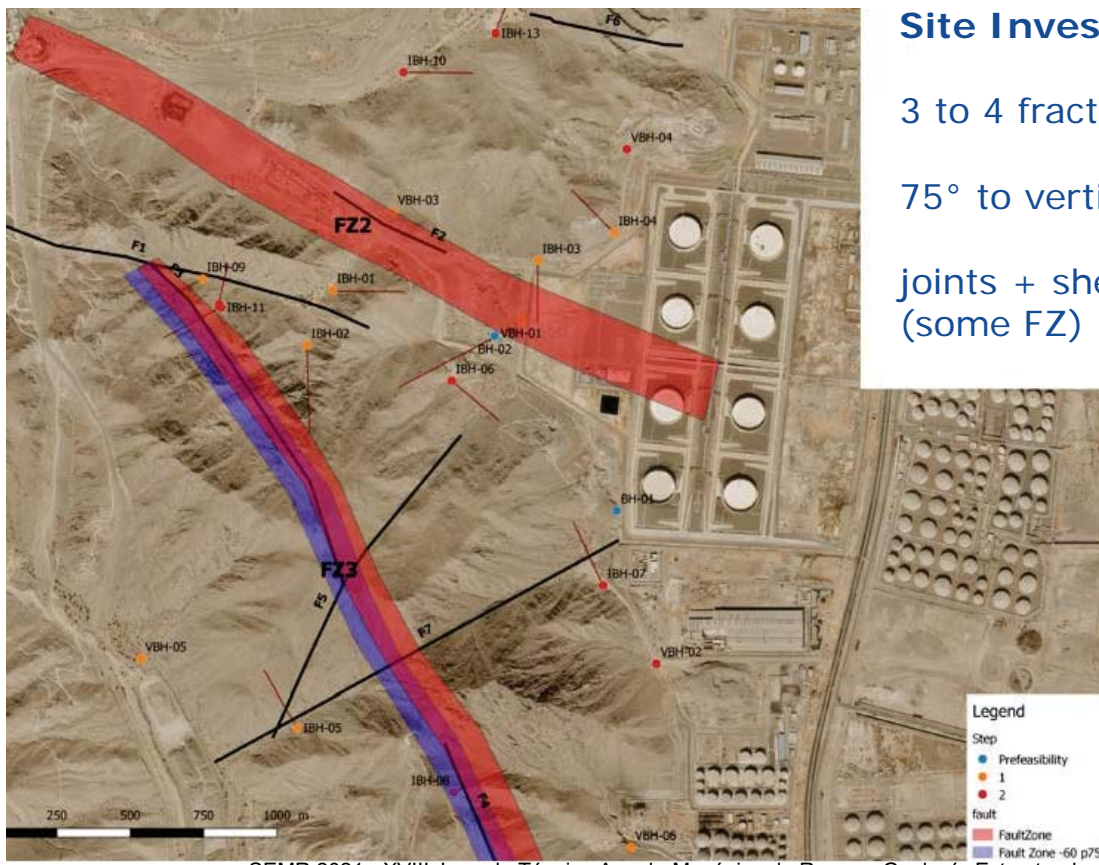
3 – IN SITU STRESS REGIME & FRACTURE PERMEABILITY



Site Investigation:

- Surface mapping (sub-vertical structures)
- Borehole drilling (*inclined*)
- BHTV logging

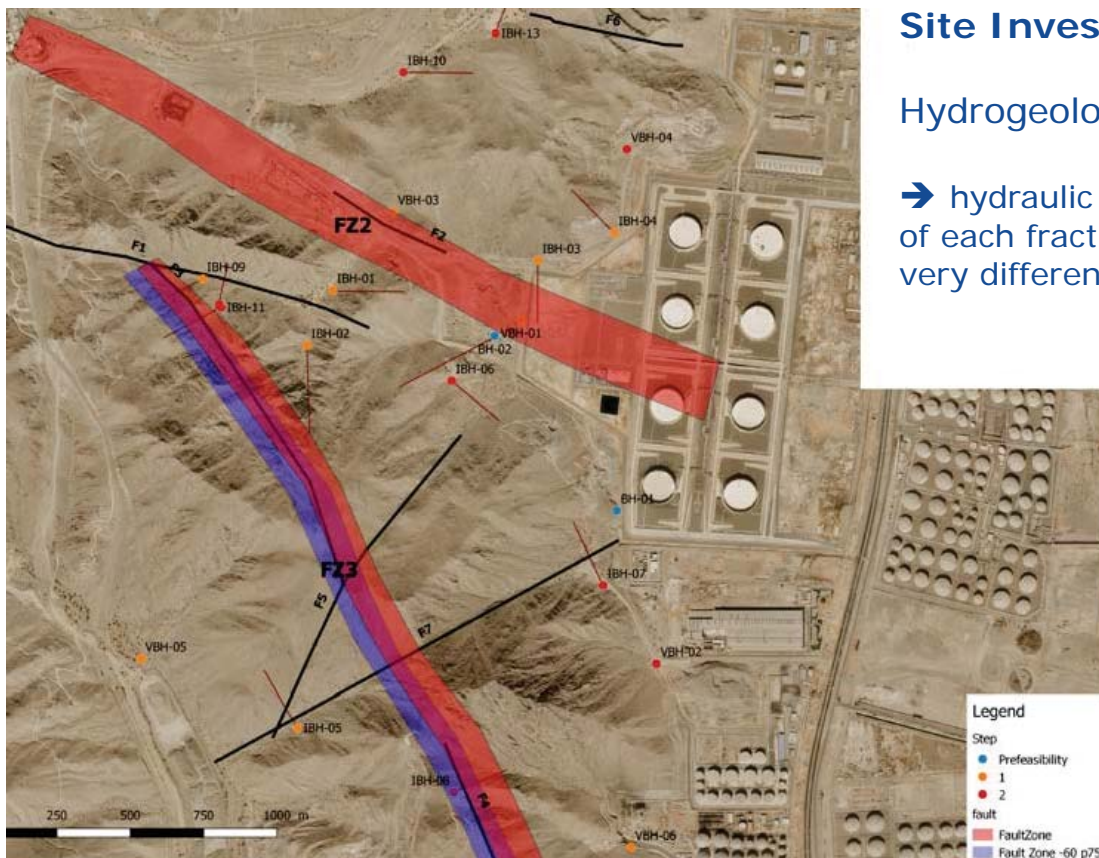
3 – IN SITU STRESS REGIME & FRACTURE PERMEABILITY



Site Investigation:

- 3 to 4 fracture sets
- 75° to vertical
- joints + shear fractures (some FZ)

3 – IN SITU STRESS REGIME & FRACTURE PERMEABILITY

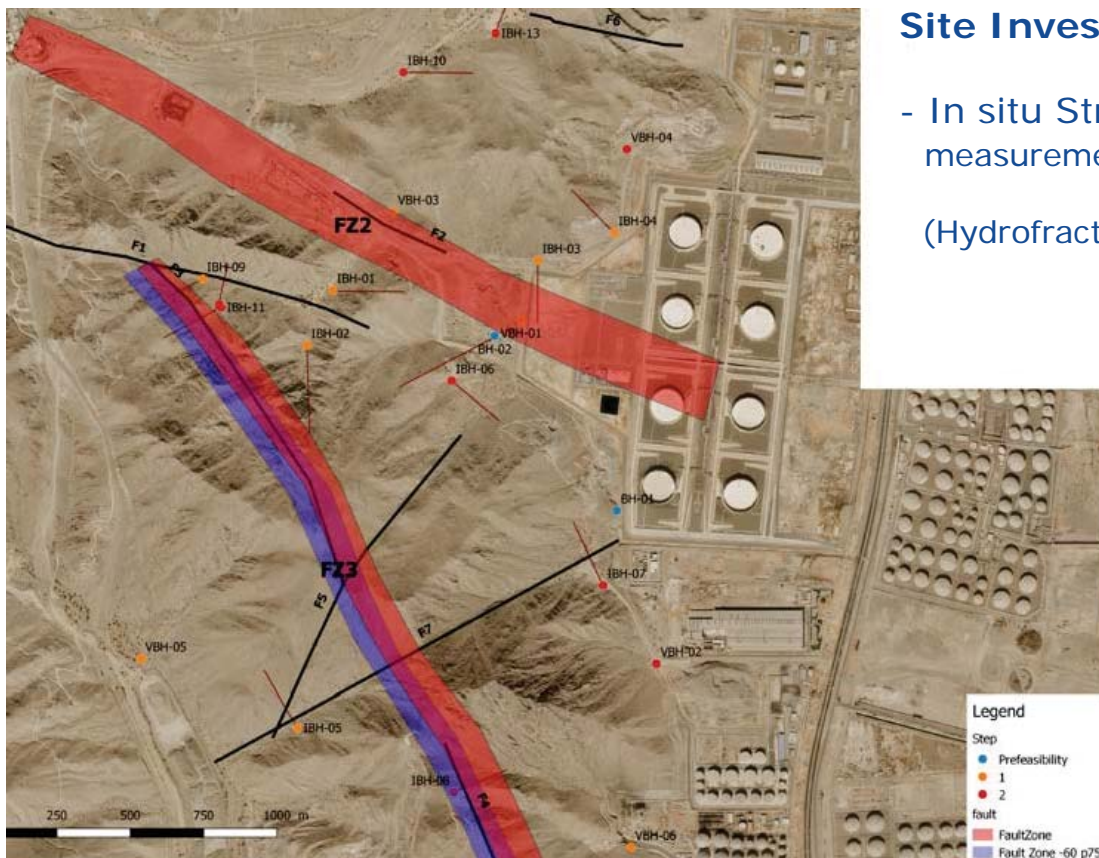


Site Investigation:

Hydrogeological testing

→ hydraulic conductivity of each fracture set can be very different

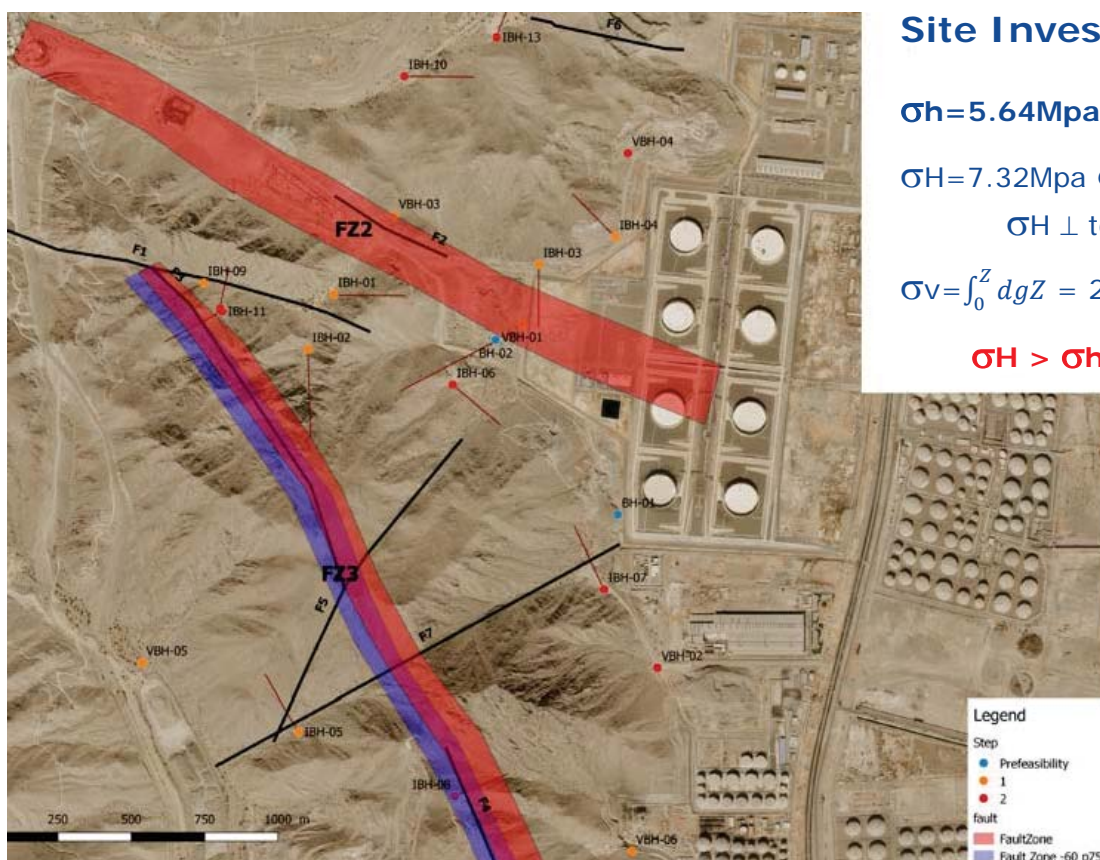
3 – IN SITU STRESS REGIME & FRACTURE PERMEABILITY



Site Investigation:

- In situ Stress measurements in BH (Hydrofracturing tests)

3 – IN SITU STRESS REGIME & FRACTURE PERMEABILITY



Site Investigation:

$\sigma_h = 5.64 \text{ MPa} @ 100\text{m}; N67^\circ E$

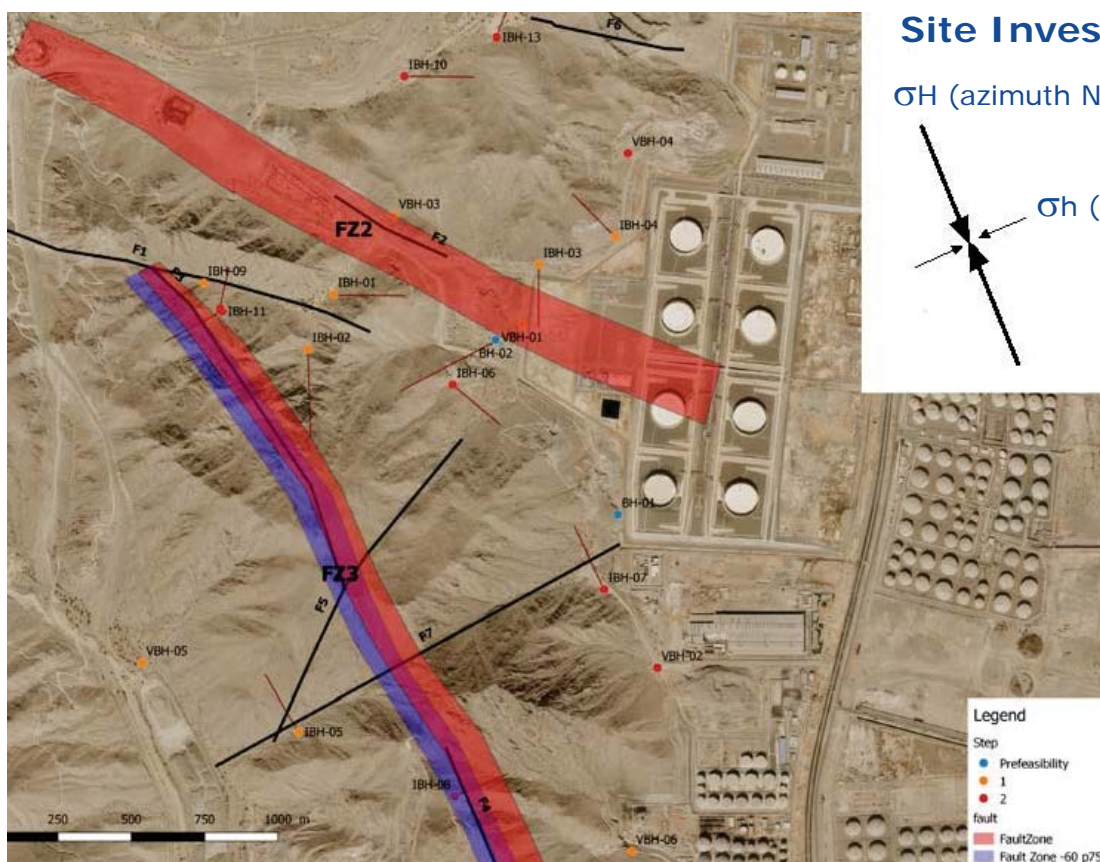
$\sigma_H = 7.32 \text{ MPa} @ 100\text{m}$

$\sigma_H \perp \text{to } \sigma_h \rightarrow N157^\circ E$

$$\sigma_v = \int_0^Z dgZ = 2.84 \text{ MPa} @ 100\text{m}$$

$$\sigma_H > \sigma_h > \sigma_v$$

3 – IN SITU STRESS REGIME & FRACTURE PERMEABILITY

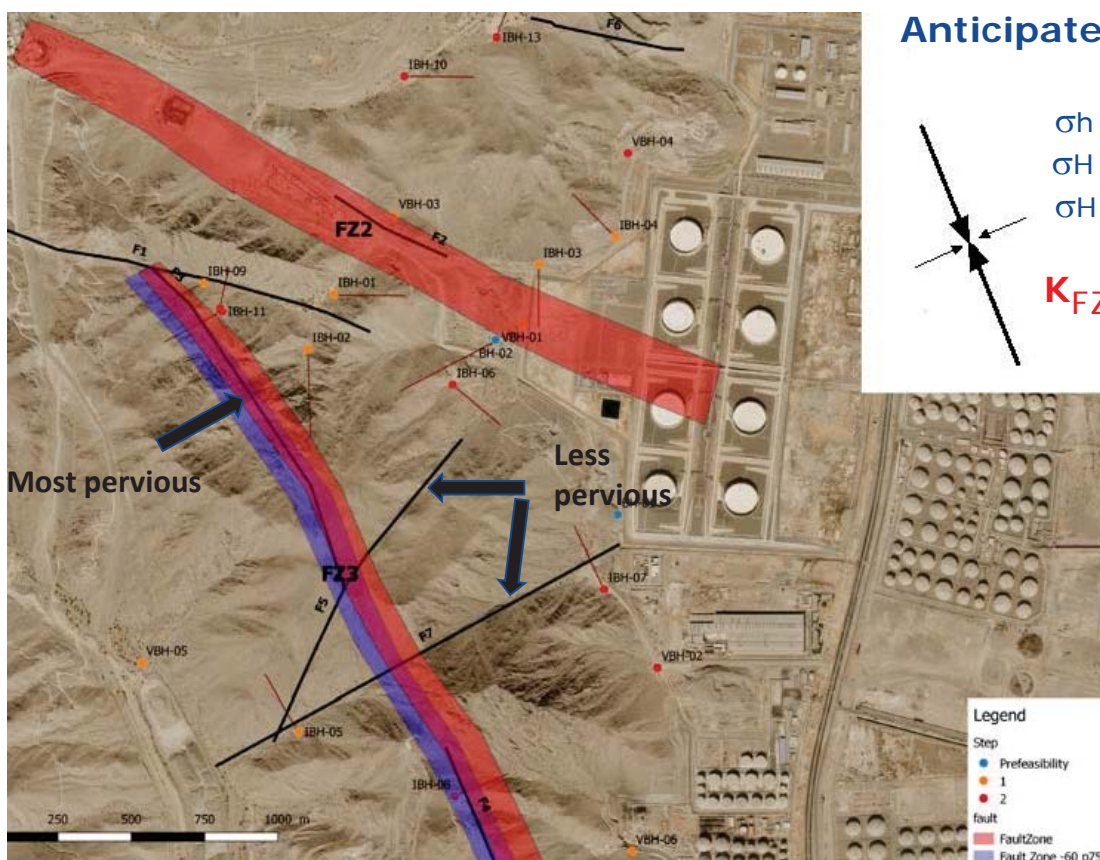


Site Investigation:

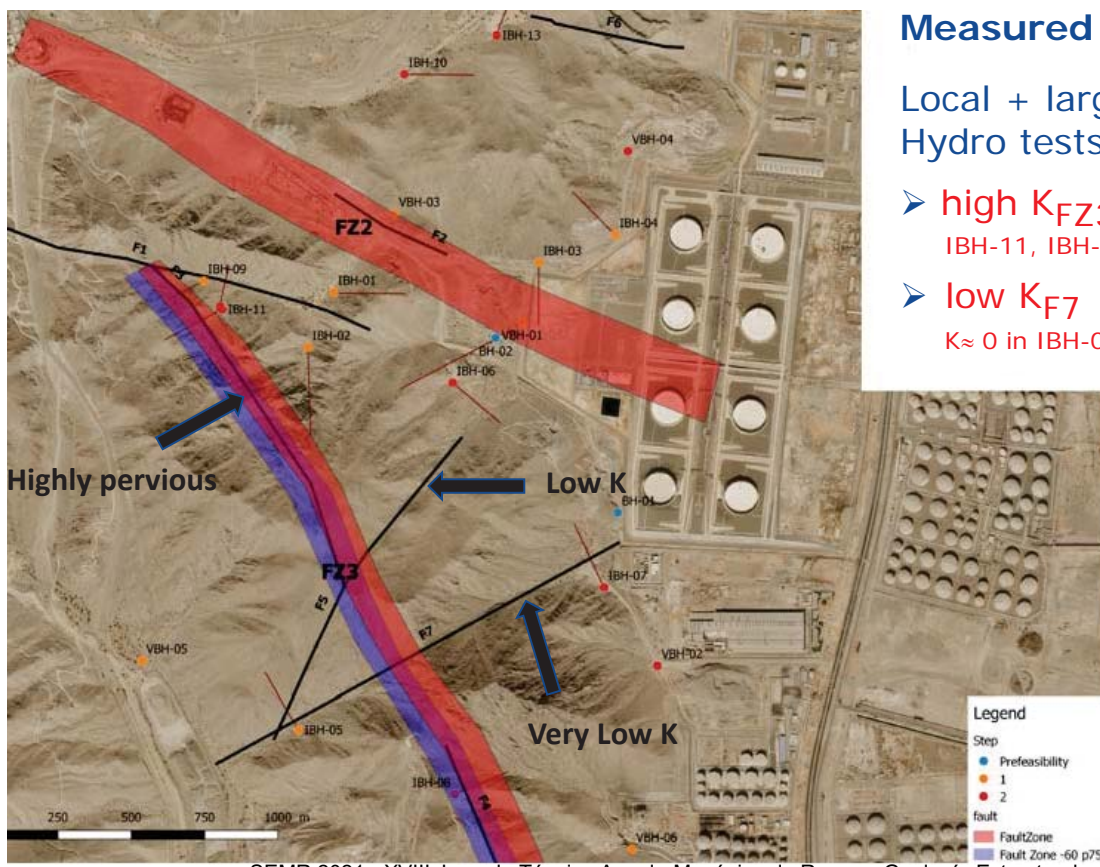
σ_H (azimuth $N157^\circ E$)

σ_h (azimuth $N67^\circ E$)

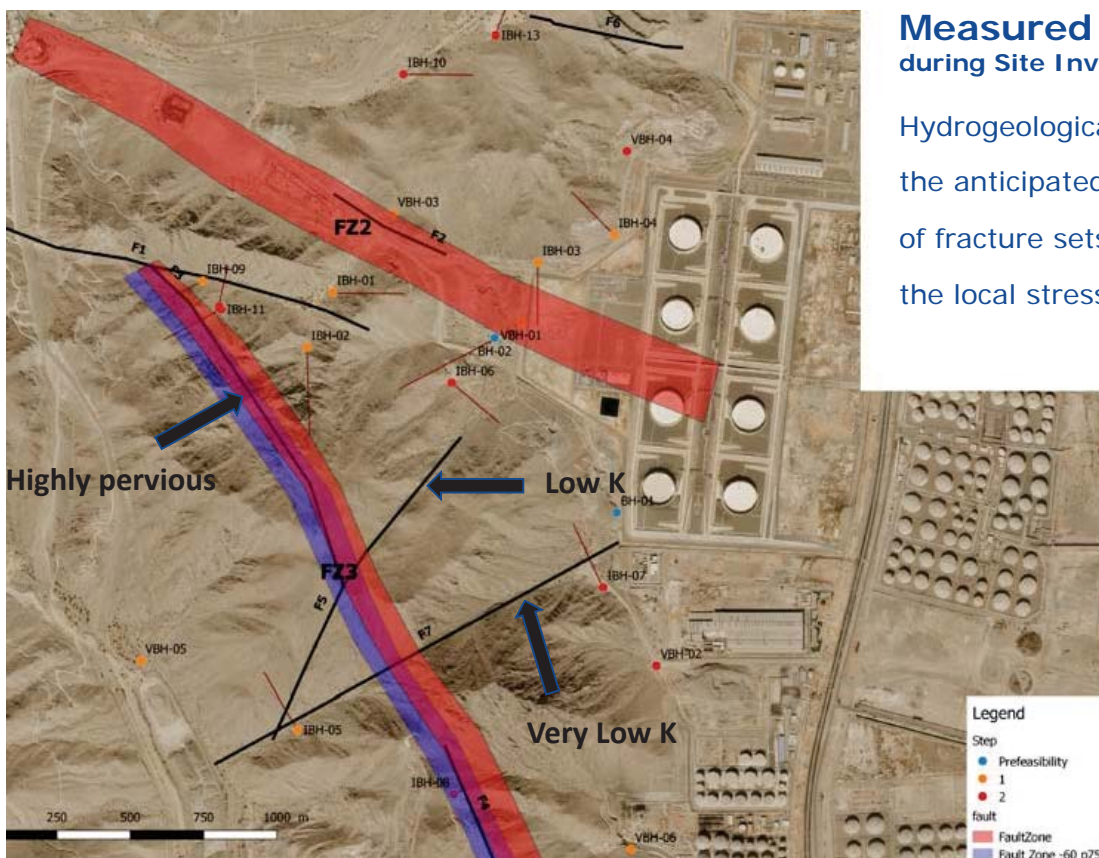
3 – IN SITU STRESS REGIME & FRACTURE PERMEABILITY



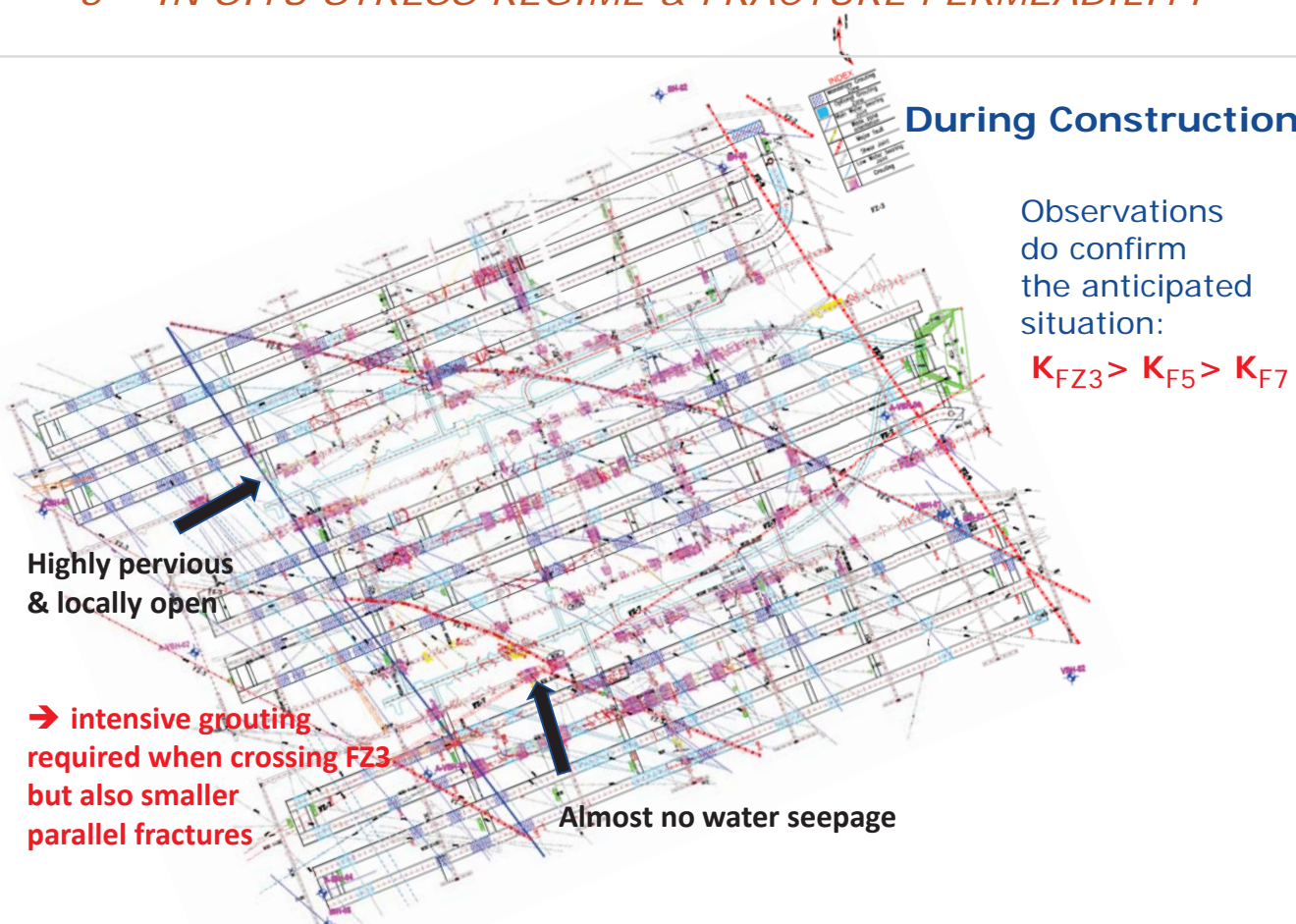
3 – IN SITU STRESS REGIME & FRACTURE PERMEABILITY



3 – IN SITU STRESS REGIME & FRACTURE PERMEABILITY



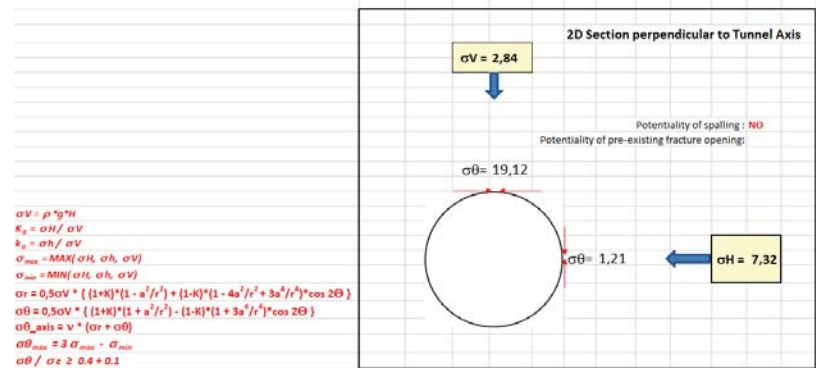
3 – IN SITU STRESS REGIME & FRACTURE PERMEABILITY



3 – IN SITU STRESS REGIME & FRACTURE PERMEABILITY

Even if the approach does not consider parameters as:

- the stress conditions at the periphery of the tunnel



- the stress release due to the effect of biasing
- the connectivity of different fracture sets
- etc.

the geometrical assessment of fracture permeability

as regard to actual stress orientation works well & is recommended!

4 – CONCLUSION

Structural geology helps performing mapping & RMC in tunnels by:

- understanding **the origin of fractures**
- describing **the chronology of fractures**
the geometry of fractures
the termination of joints

➔ ranking the Rock Mass more quickly & more efficiently

4 – CONCLUSION

Finally, adding structural geology to standard geology allows

- to get a comprehensive view of the site
- to perform tunnel mapping better & quicker, in 3D
- to validate the models/design of tunnels

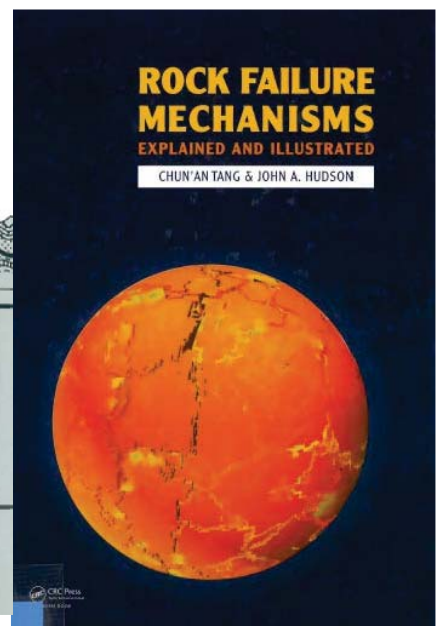
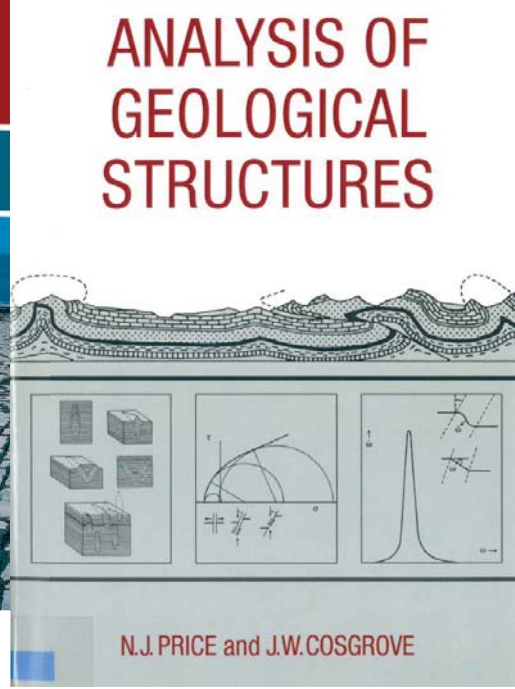
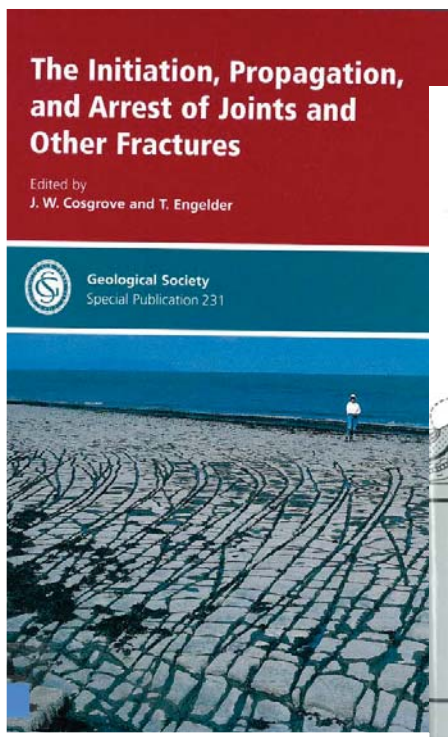
With a structural approach, the action of mapping is much more than reporting observations on paper/computer...

it becomes an **efficient tool to perform rock mass assessment, reinforcement & support** (rock bolting, grouting, etc.)

4 – CONCLUSION

THANK YOU

A few literature on the subject ...





Estructura Interna y Propiedades Mecánicas de la Falla Activa de Alhama de Murcia

Internal Structure and Mechanical Properties of the Active Fault of Alhama de Murcia



Juan Miguel Insua Arévalo
Universidad Complutense de Madrid
Facultad de Ciencias Geológicas



Grupo Geodinámica Planetaria,
Tectónica Activa y Aplicaciones a Riesgos



1/44

XVIII Jornada Técnica Anual
Sociedad Española de Mecánica de Rocas SEMR
MAYO 2021

Internal Structure and Mechanical Properties of the Active Fault of Alhama de Murcia

Estructura Interna y Propiedades Mecánicas de la Falla Activa de Alhama de Murcia

Research Group



Geodinámica Planetaria, Tectónica Activa y Aplicaciones a Riesgos

Planetary Geodynamics, Active Tectonics and Related Risks



UCM MEMBERS

José J. Martínez Díaz
Meaza Tsige
Jorge Alonso Henar
José A. Álvarez Gómez
Carlos Fernández
Paula Herrero Barbero
Juan Miguel Insua Arévalo
David Jiménez Molina
Martín Jesús Rodríguez Peces
José Luis Sánchez Roldán

EXTERNAL MEMBERS

Emilio Rodríguez Escudero
Carolina Canora Catalán
Julián García Mayordomo
Raúl Pérez López
Marta Béjar Pizarro

COLLABORATORS

Ramón Capote del Villar
M.ª José Jurado
Mariano Álvaro
Enrique Aracil
Unai Maruri
Ana Ribera
Fernando Herrera

STUDENTS

Pablo Rodríguez Soto
Sara Álvarez Corral
José M.ª Moratalla
José Javier C.

LABORATORY STAFF

Guillermo Pinto de la Casa
Ana M.ª Sánchez Palomo

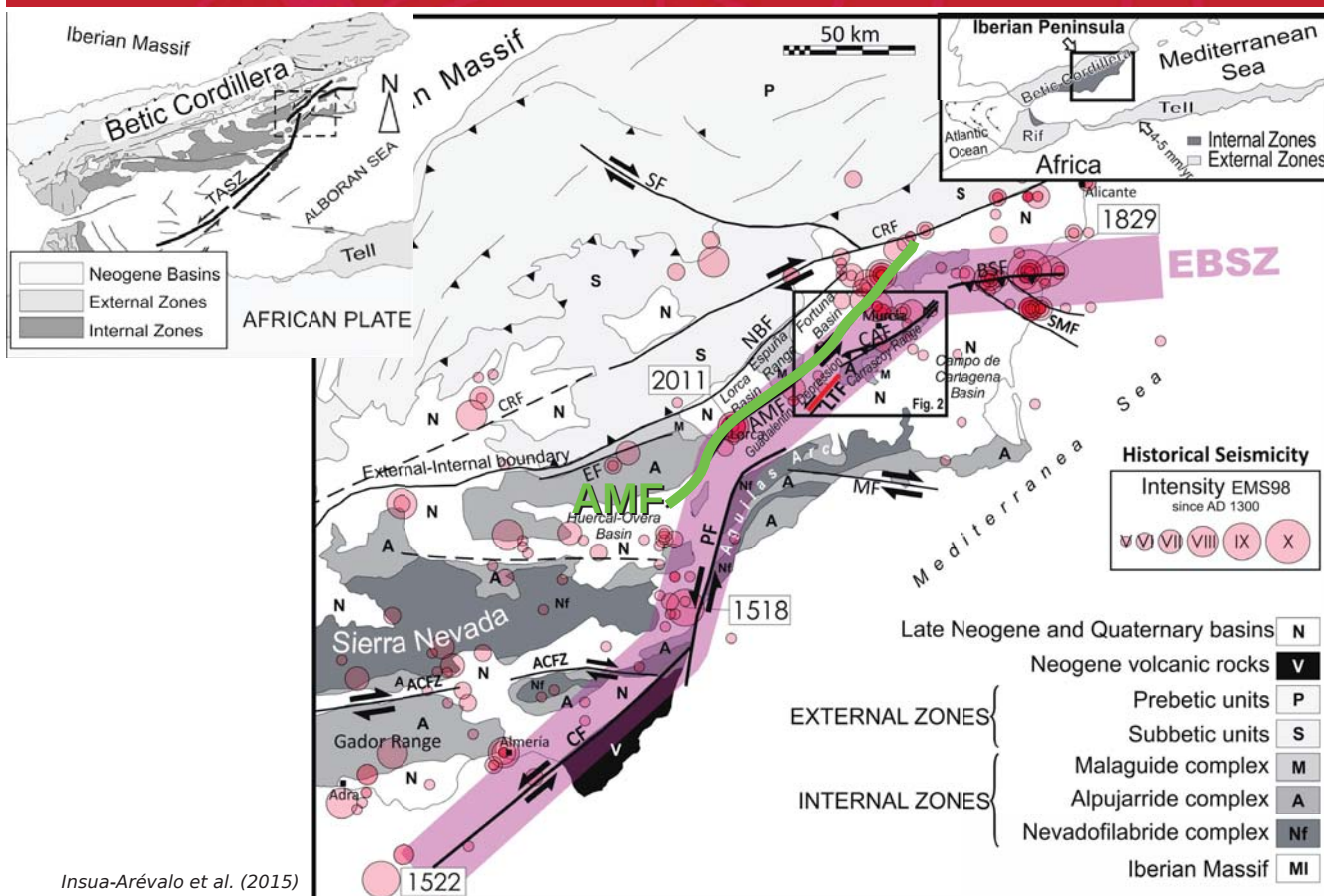
RESEARCH PROJECTS

PROSEIS
GEOTACTICA
INTERGEO
QUAKE STEP

SCIENTIFIC PRODUCTS

> 30 Research papers
1 PhD thesis
3 MSc theses
Congress communications

The Alhama de Murcia Fault (AMF). Tectonic Frame



Insua-Arévalo et al. (2015)

3/44

XVIII Jornada Técnica Anual
Sociedad Española de Mecánica de Rocas

SEMR MAYO 2021

What's a fault?



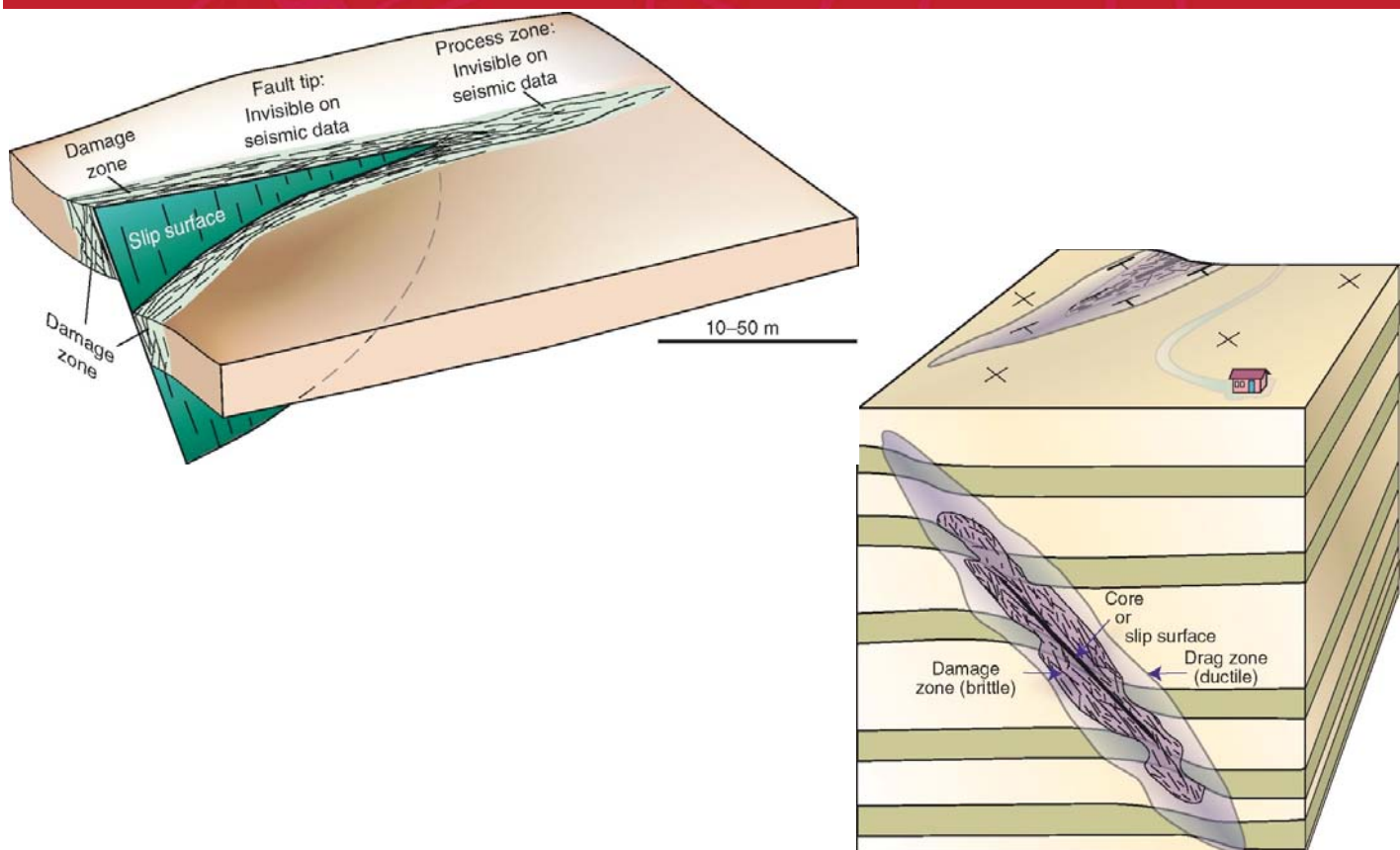
What's a fault?



Fault Damage Zone

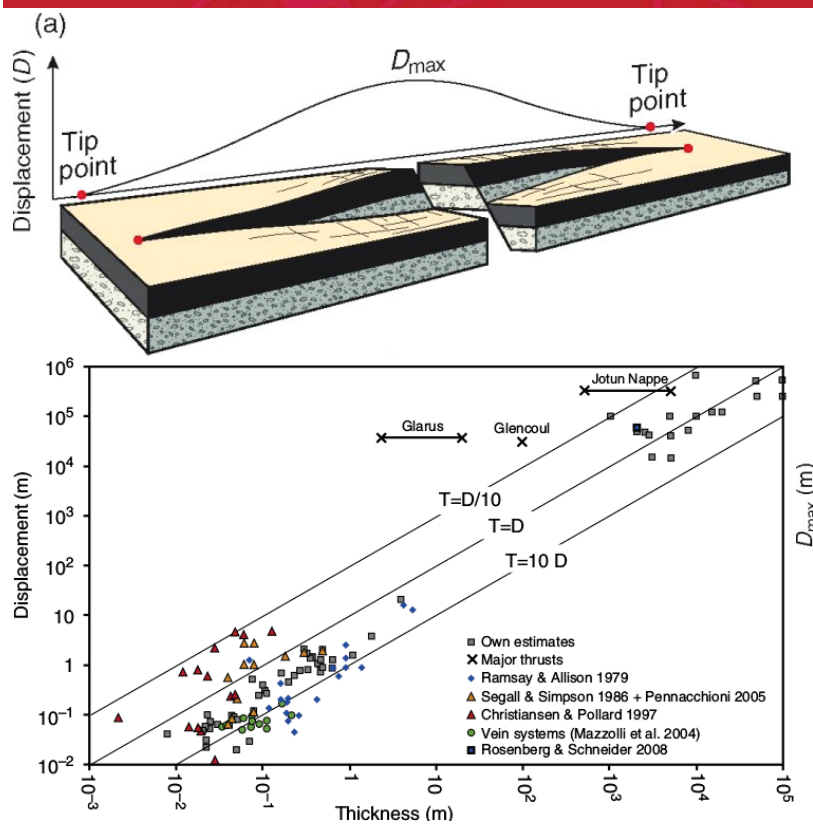


Fault Damage Zone

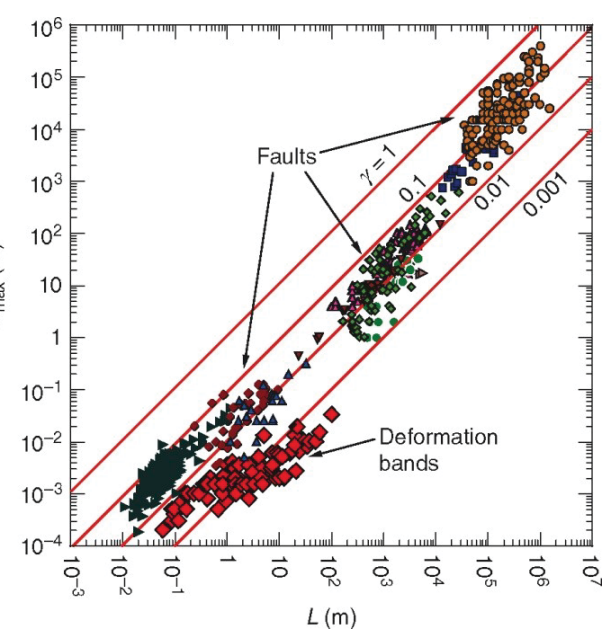


Fossen, 2011 © Cambridge University Press

Displacement, Damage Zone Thickness and Length of Faults

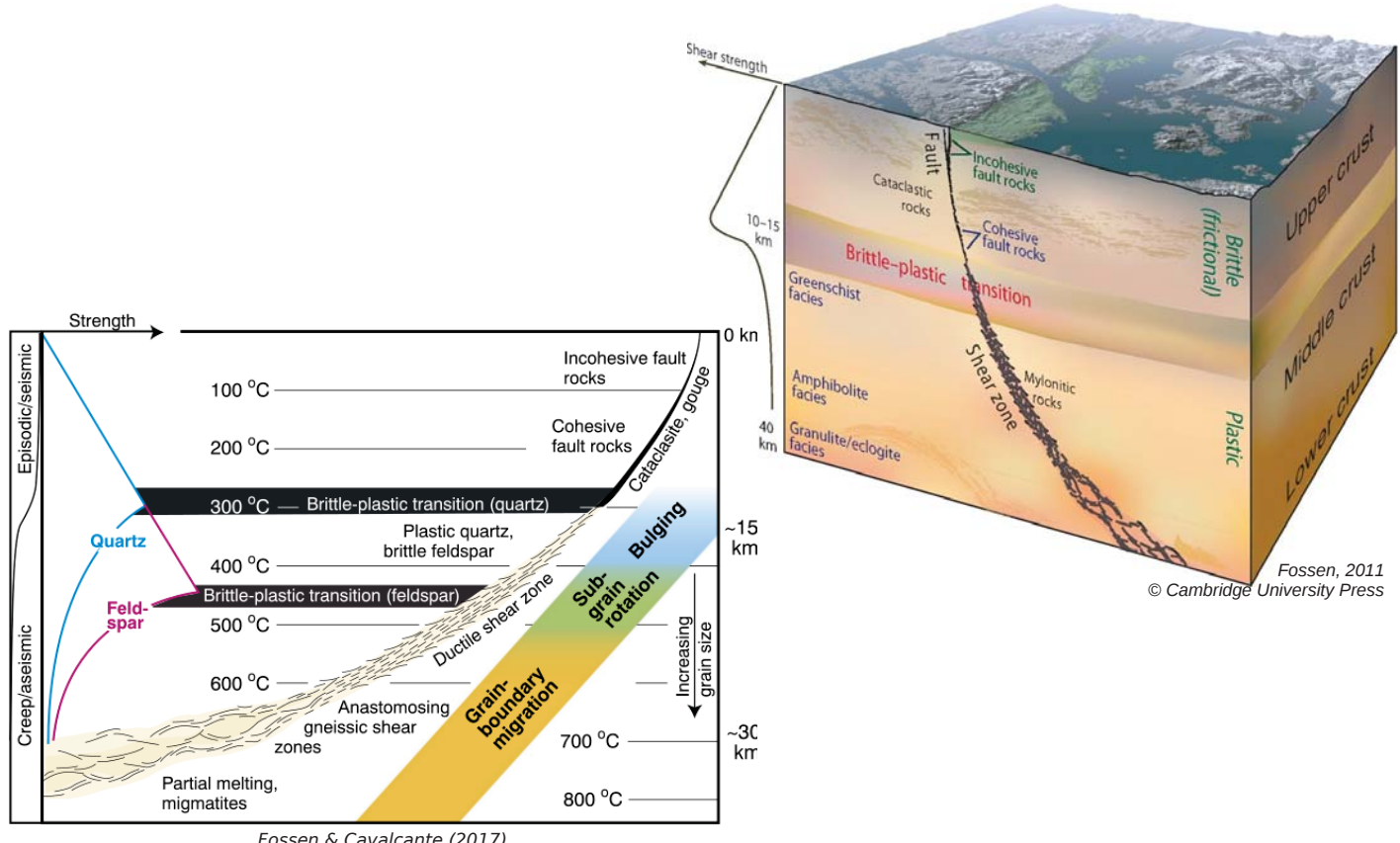


Fossen&Calavante (2017)

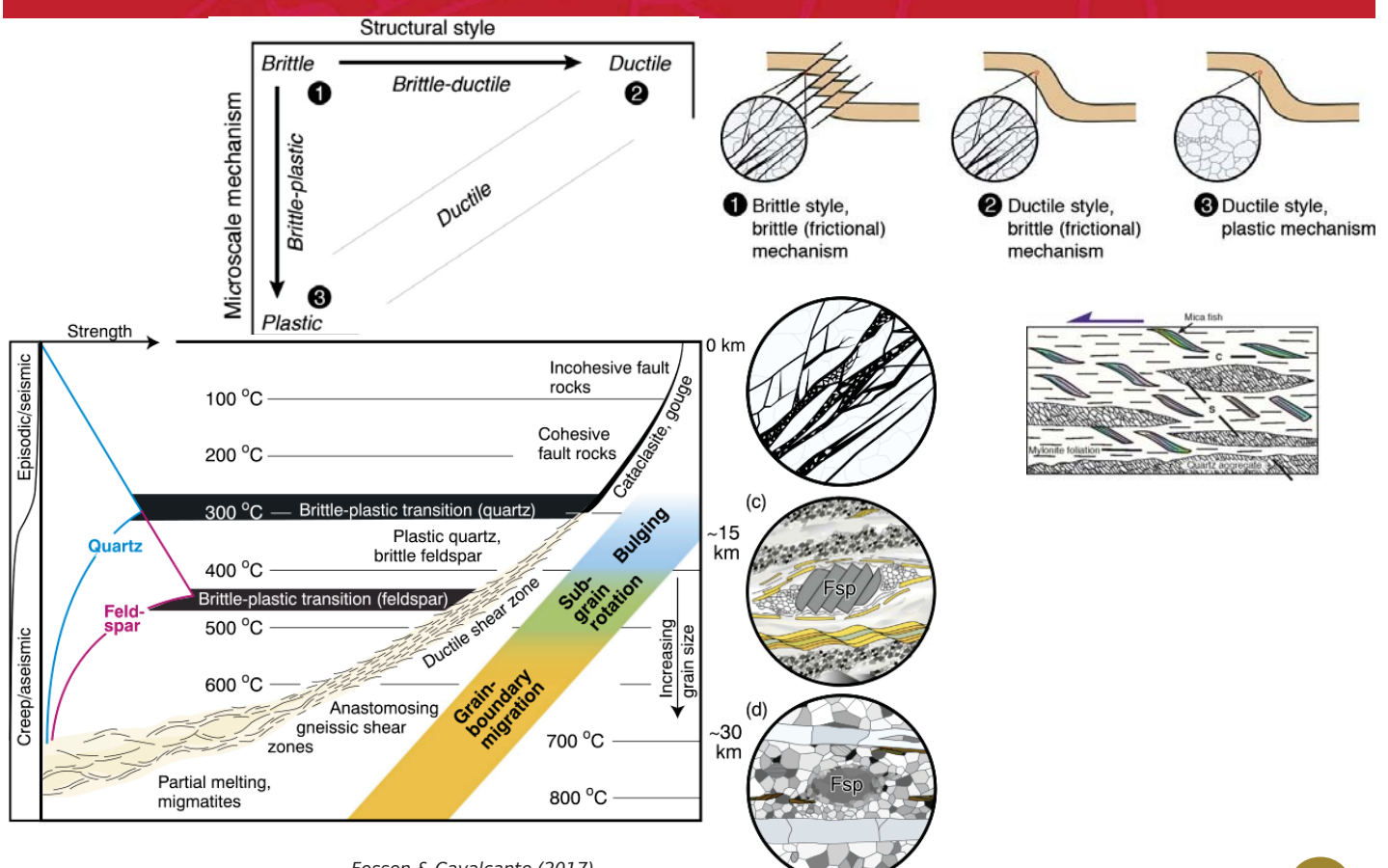


Fossen, 2011 © Cambridge University Press

Cortical Faults



Structural Style vs. Microscale Mechanism

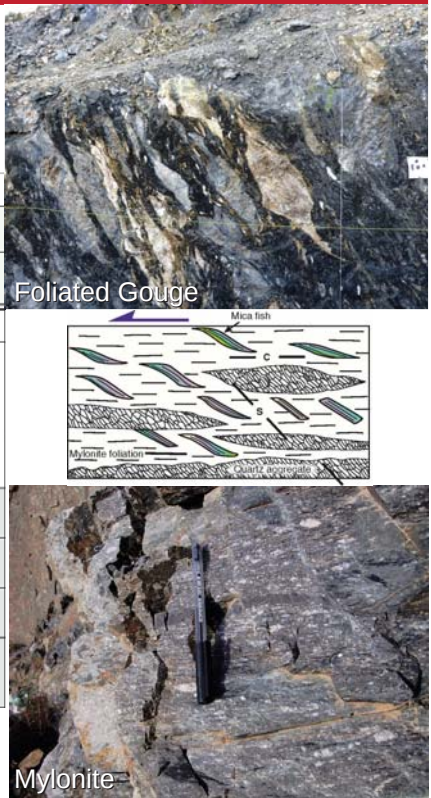


Faults Rocks

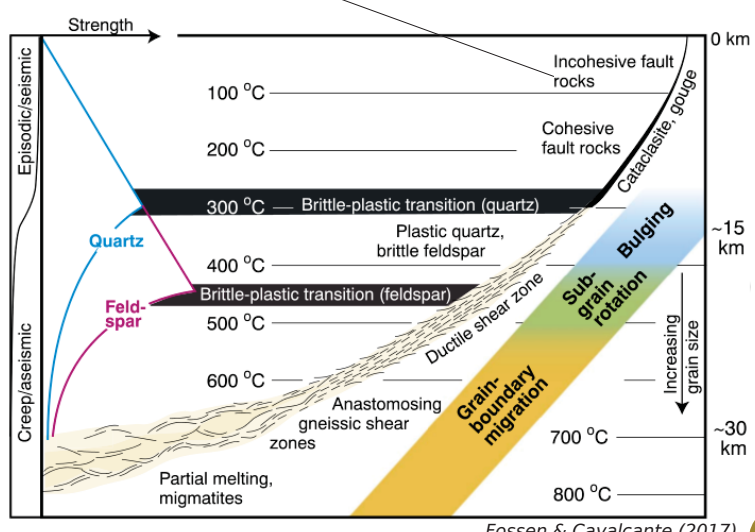
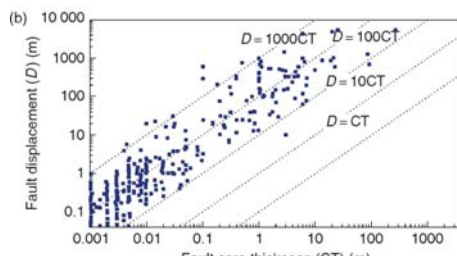
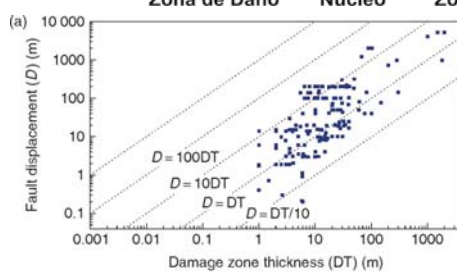
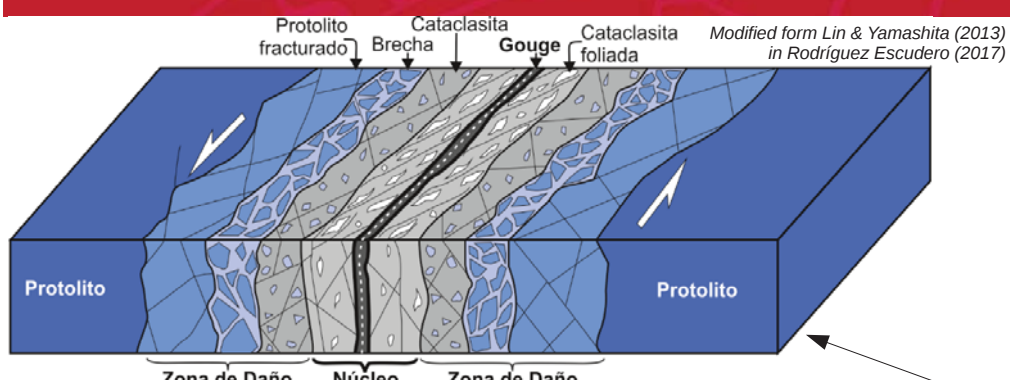


	Non-foliated	Foliated
Incohesive	Fault breccia (>30% visible fragments)	
	Fault gouge (<30% visible fragments)	Foliated gouge
Cohesive	Pseudotachylite	
	Crush breccia (fragments > 5 mm)	
	Fine crush breccia (fragments 1-5 mm)	
	Crush microbreccia (fragments < 1 mm)	
Cataclasites	Protocataclasite	Protomylonite
	Cataclasite	Mylonite
	Ultracataclasite	Ultramylonite
		Blastomylonite
		Mylonite series

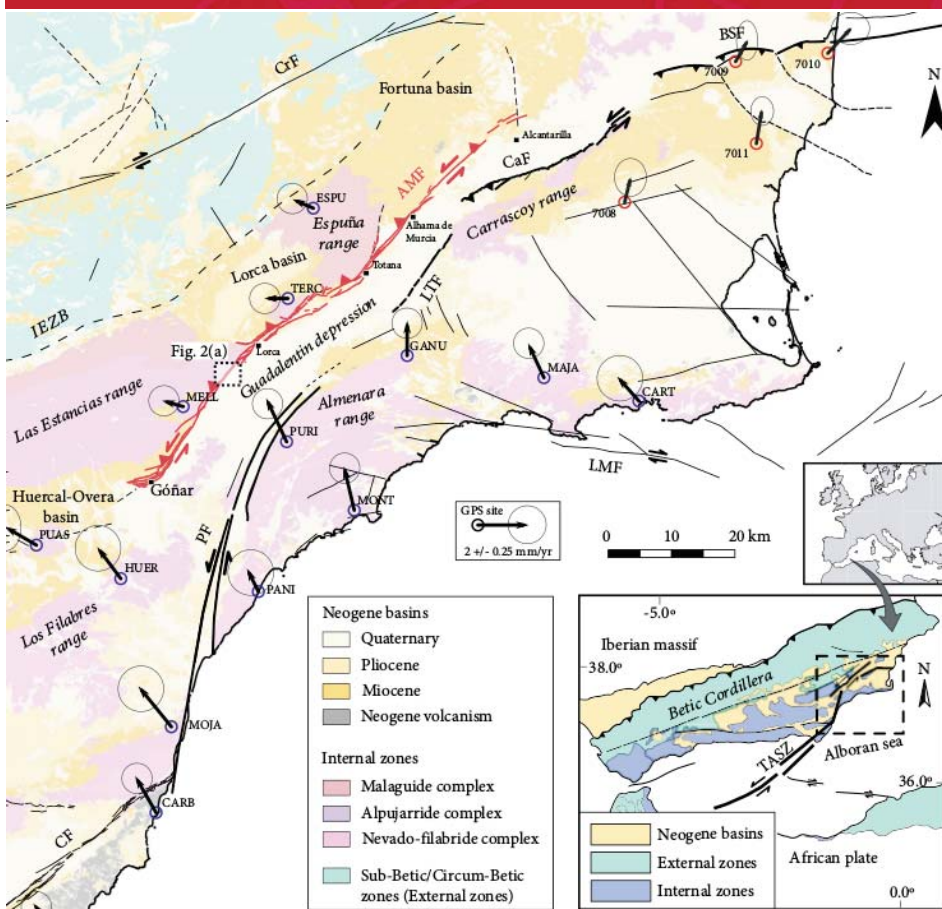
Fossen, 2011 © Cambridge University Press



Fault Rocks Zonation



AMF Geological Frame



AMF is an active cortical fault that controls the relief along the northern border of the Guadalentín Depression.

The Guadalentín Depression is on the downthrown block of the AMF, which is filled up with Quaternary alluvial and fluvial deposits.

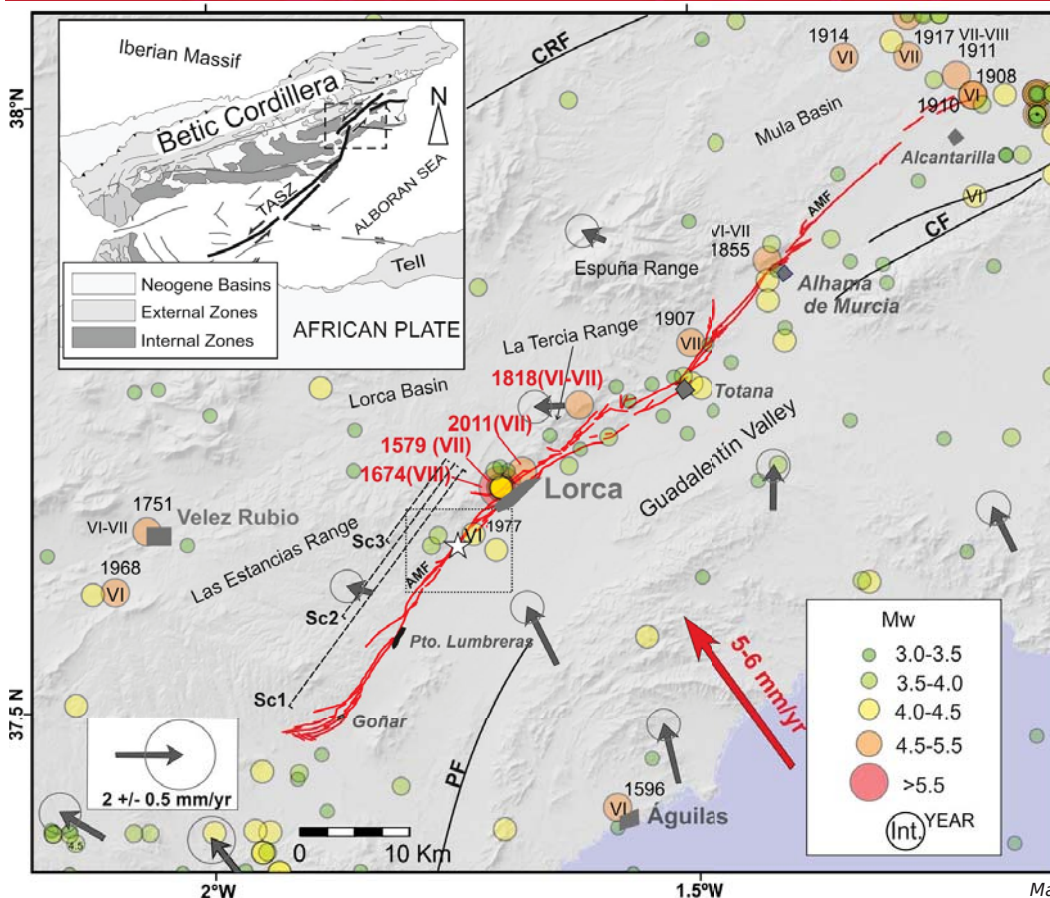
In the upthrown block of the AMF crop out metamorphic and sedimentary materials of the Internal Zones of the Betic Cordillera, as well as Miocene marine deposits.

Alonso-Henar et al. (2021)

XVIII Jornada Técnica Anual
Sociedad Española de Mecánica de Rocas
SEMR MAYO 2021

13/44

AMF Geometry and Kinematics



GEOMETRY

Length: 87 km

Strike: N40E–N65E

Dip: 60°–75° NW

Depth: 12 km

KINEMATICS

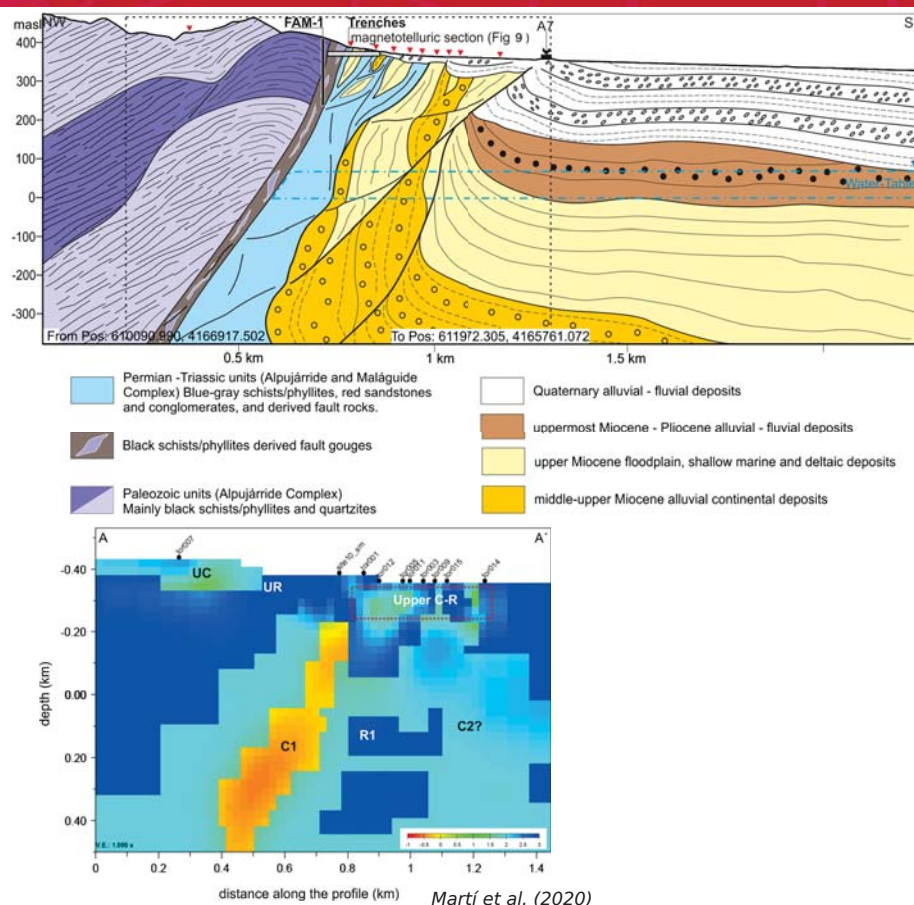
Left-lateral strike-slip with reverse component

Total displacement: 10 km

Slip-rate: up to 1.7 mm/yr

Martínez-Díaz et al. (2018)

AMF Geometry and Kinematics

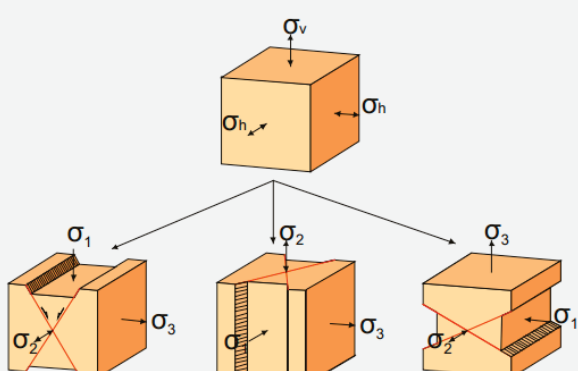


15/44

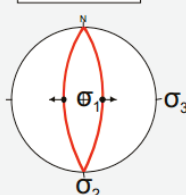
Fault types

Fallas Neoformadas

Esfuerzos y fracturación de una roca homogénea
(Modelo de Anderson)

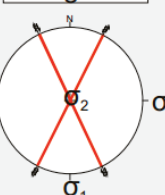


Nomales



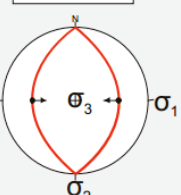
$$\begin{aligned}\sigma_1 &= \sigma_v \\ \sigma_2 &= \sigma_{\text{hmax}} \\ \sigma_3 &= \sigma_{\text{hmin}}\end{aligned}$$

Desgarres



$$\begin{aligned}\sigma_2 &= \sigma_v \\ \sigma_1 &= \sigma_{\text{hmax}} \\ \sigma_3 &= \sigma_{\text{hmin}}\end{aligned}$$

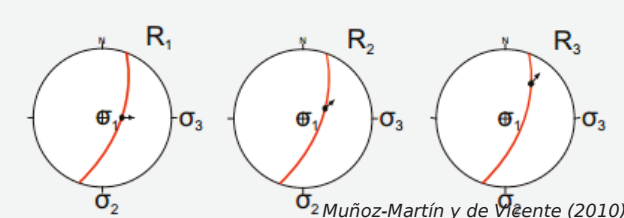
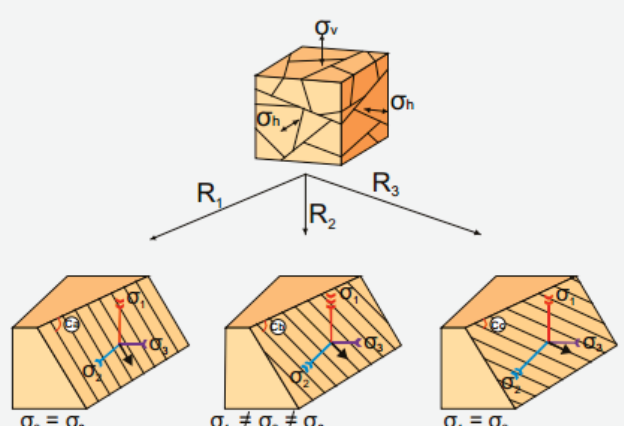
Inversas



$$\begin{aligned}\sigma_3 &= \sigma_v \\ \sigma_1 &= \sigma_{\text{hmax}} \\ \sigma_2 &= \sigma_{\text{hmin}}\end{aligned}$$

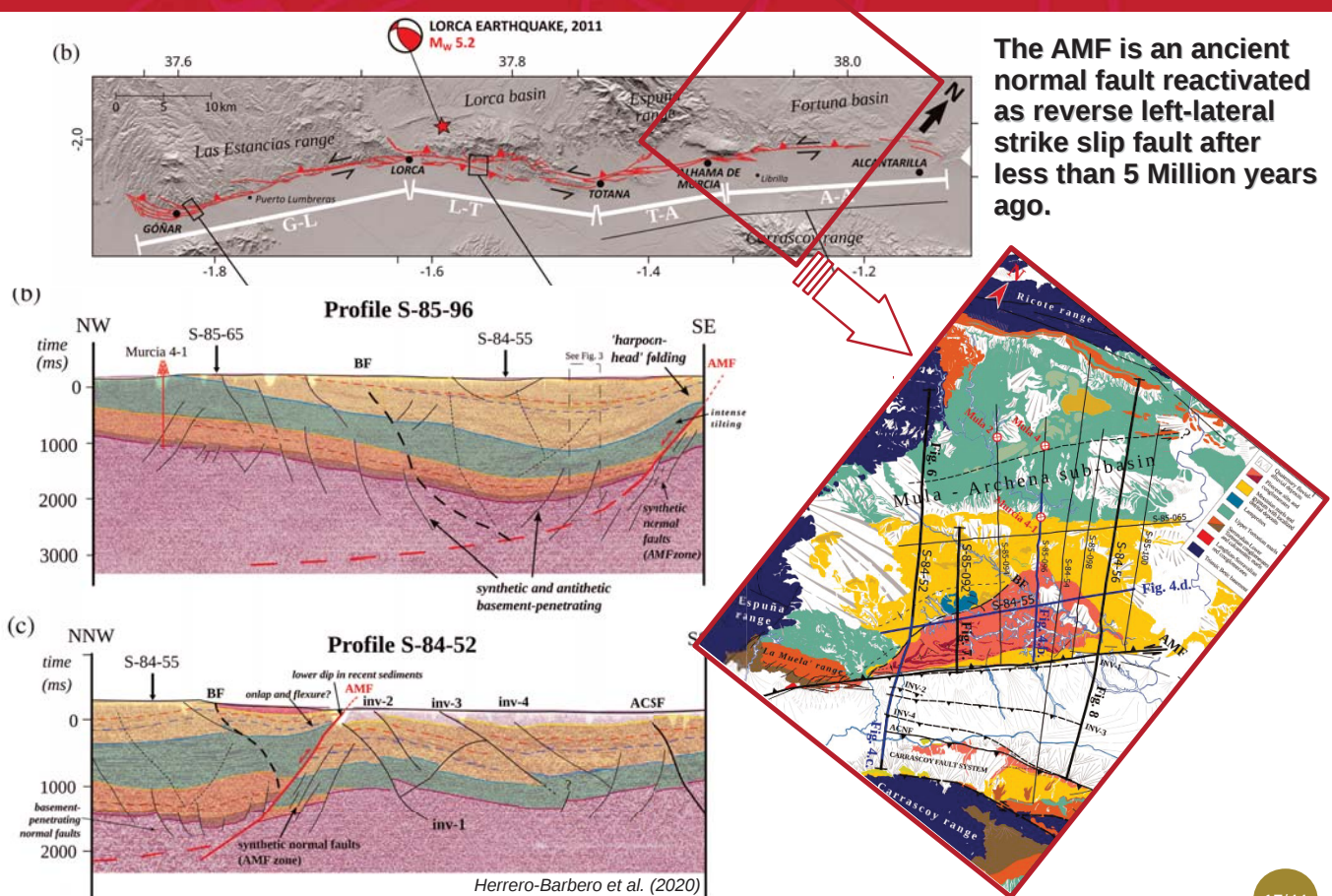
Fallas Reactivadas

Esfuerzos y fracturación de una roca heterogénea
(Ecación de Bott)

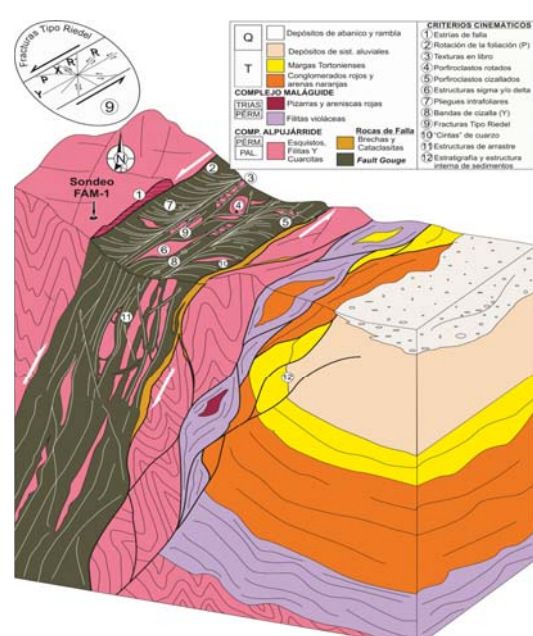
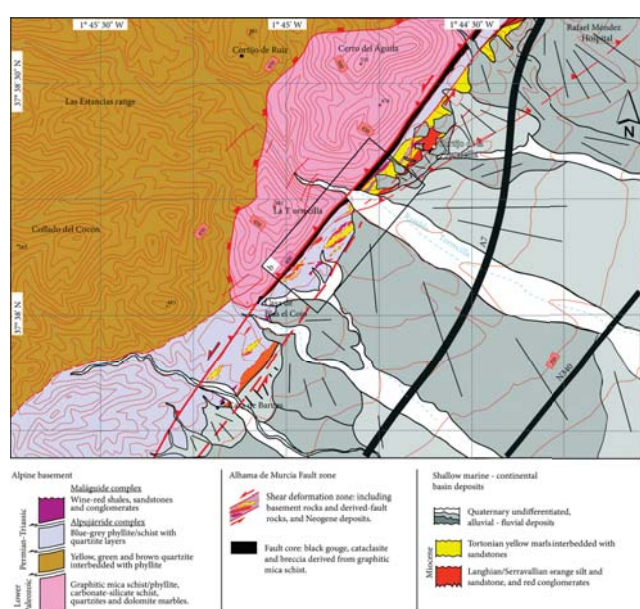
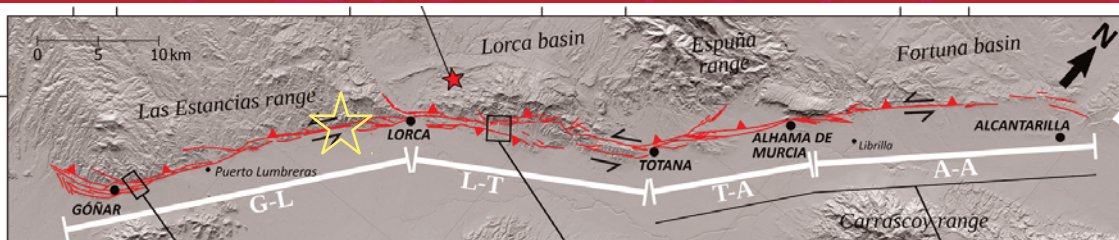


16/44

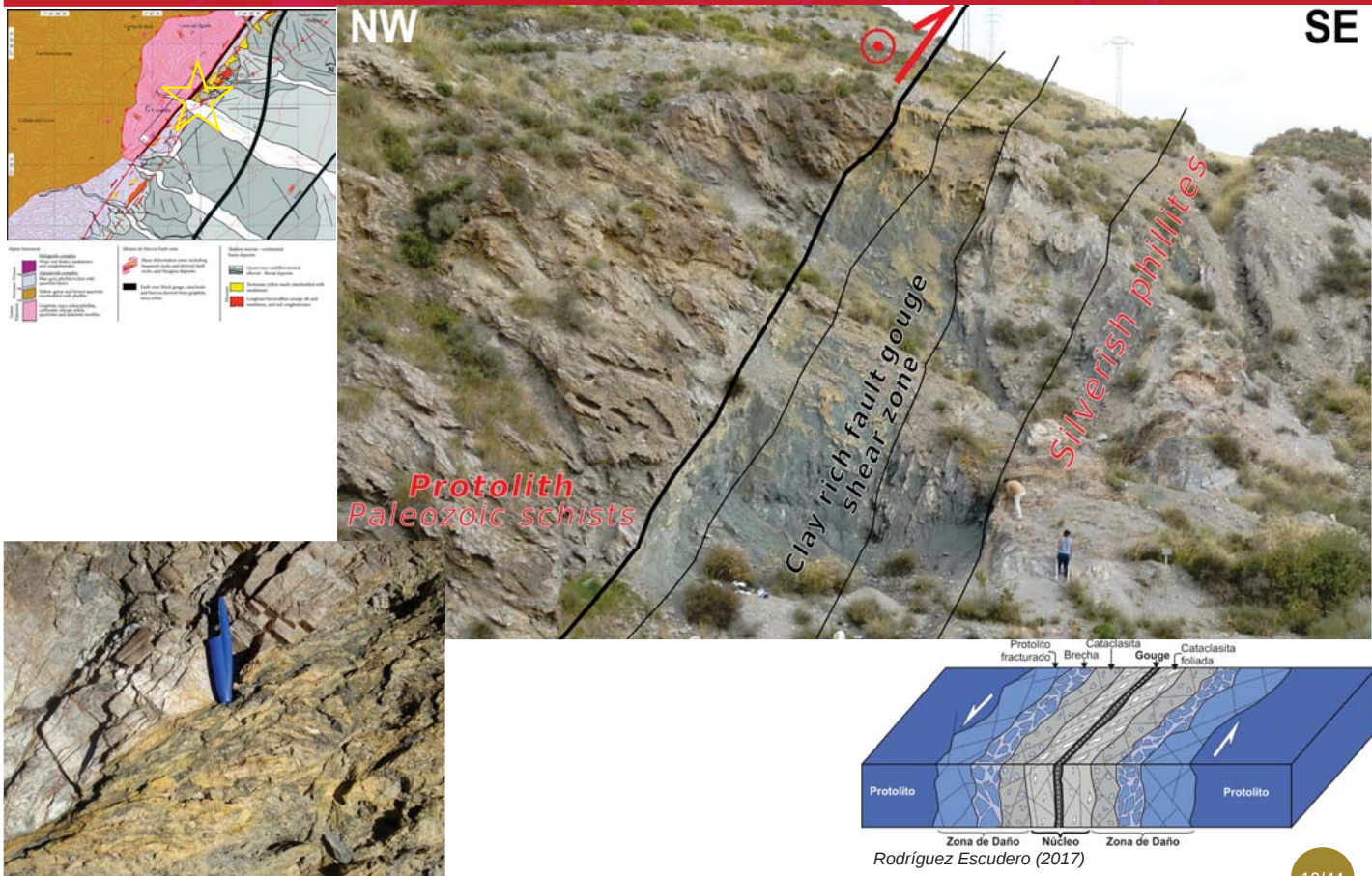
Tectonic Inversion of the AMF



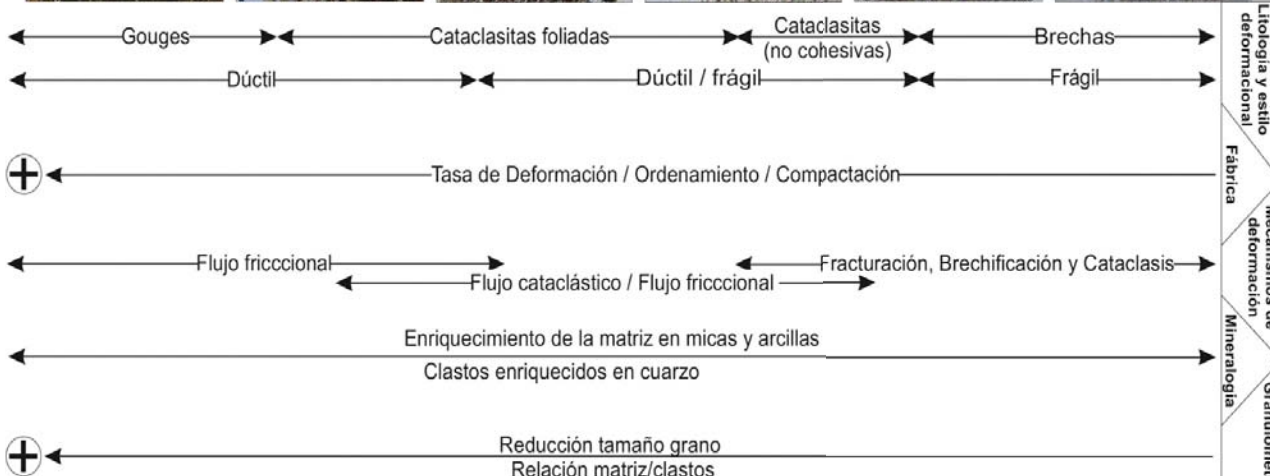
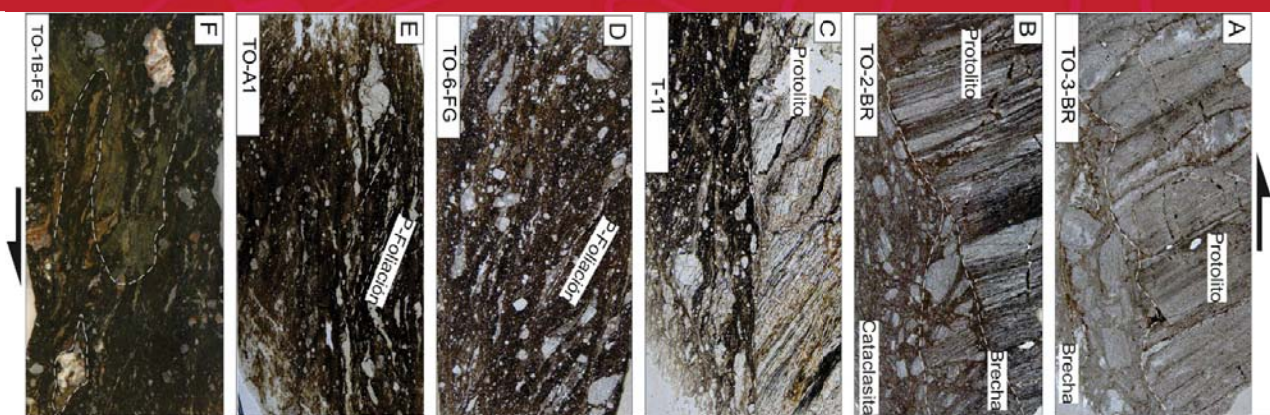
La Torrecilla Site



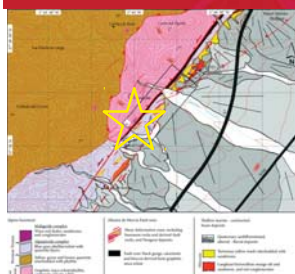
Zonation of the Fault Rocks within the AMF



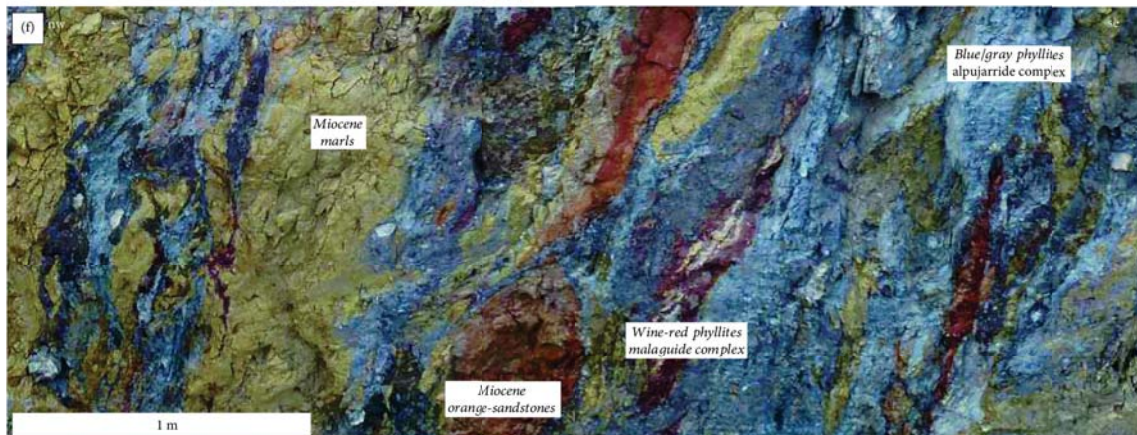
AMF Fault rocks zonation. Thin sections.



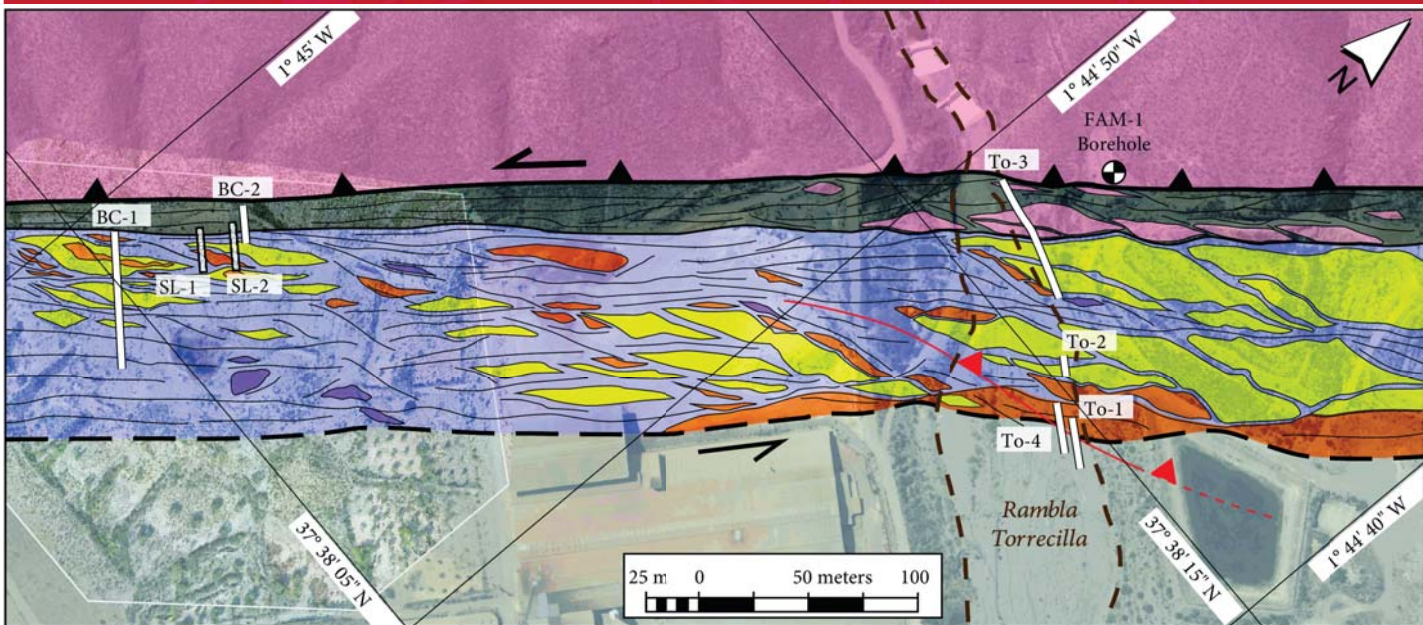
Shear Zone of the AMF (Drone View)



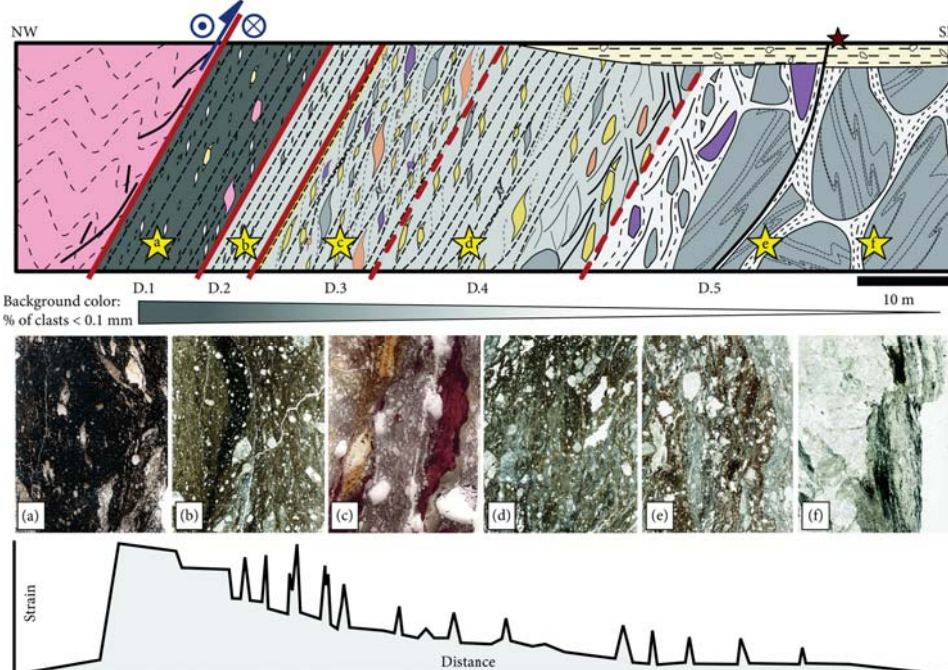
Architecture of the AMF



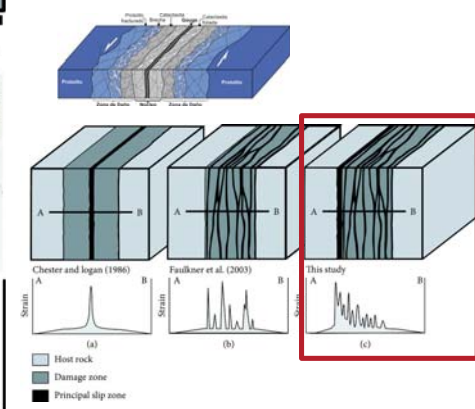
Architecture of the AMF



Architecture of the AMF



Asymmetric Strain Model



Fault rock lithologies

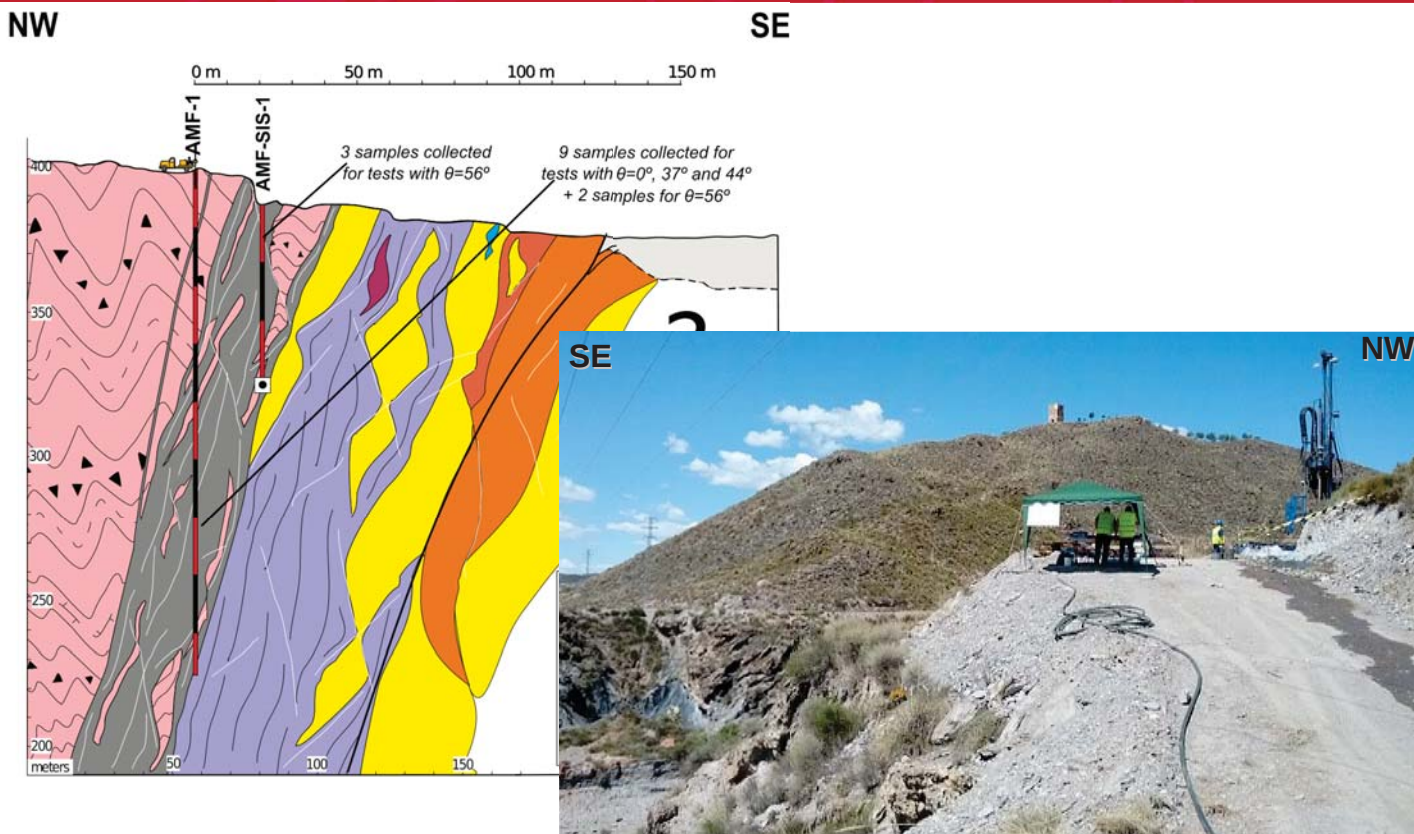
- Alpujarride complex
 - Mica schists
 - Carbonate-silicate schists
 - Blue-grey phyllite
- Maláguide complex
 - Wine-red shales/phyllites

- Miocene deposits
 - Yellow marls
 - Orange silt/sandstones
- Quaternary deposits
 - Quaternary alluvial sediments

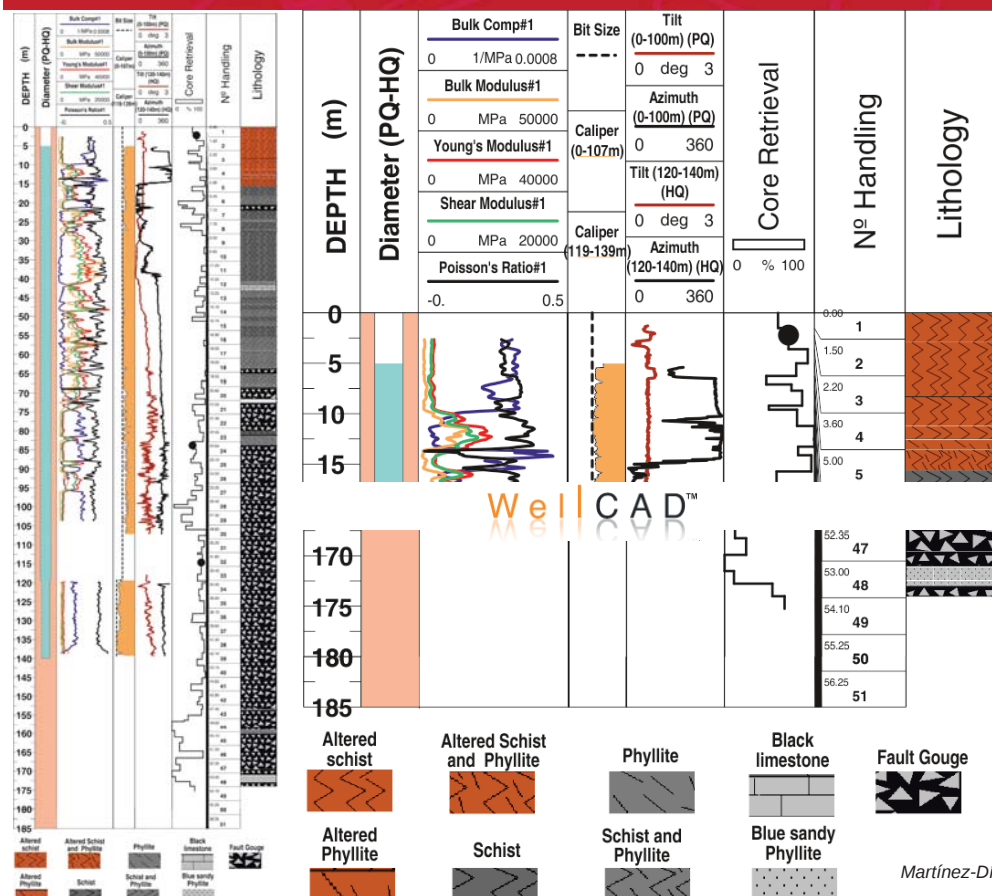
Other features

- ★ Microphotographies location
 - ★ 1674 eq. surface rupture
 - Fracture/fault
 - Foliation/rock fabric
 - Domain boundaries
- Alonso-Henar et al. (2021)

Reseach Boreholes AMF-1 and AMF-SIS-1



Reseach Borehole AMF-1

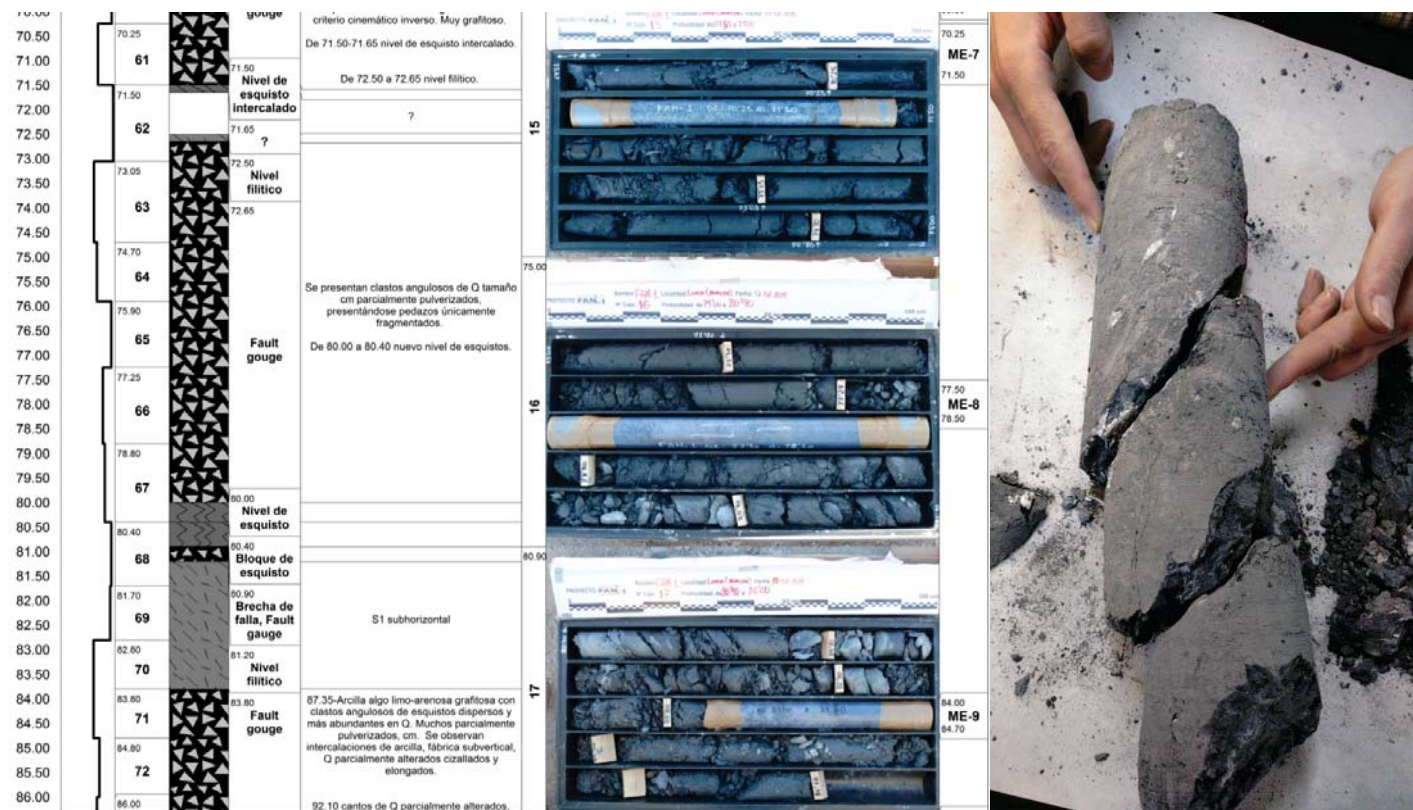


The scientific borehole AMF-1 reaches a depth of 174 m.

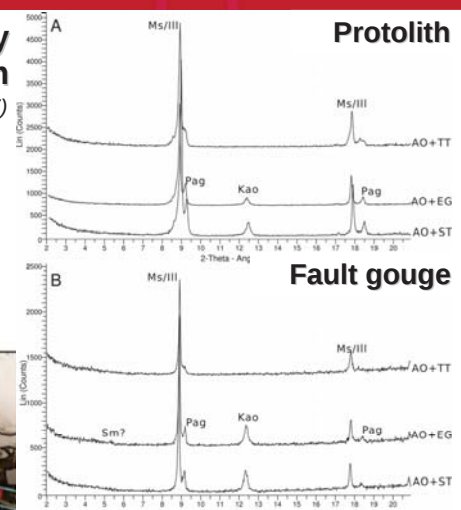
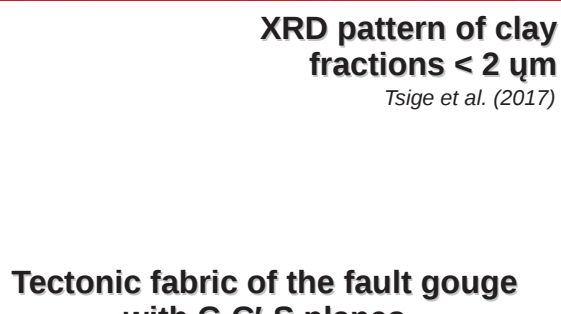
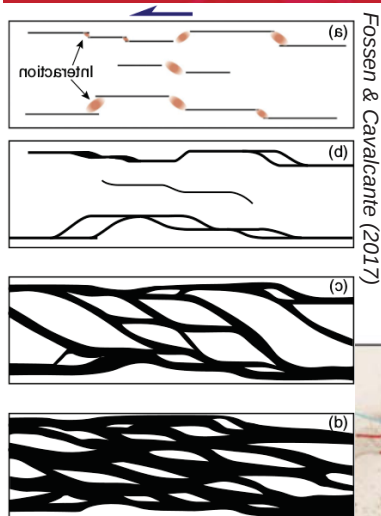
Wireline vertical drilling and coring were chosen to favour the recovery of high-quality fresh rock core.

The fault gouge was encountered at a depth of 64 m and more than 100 m of high-quality fault rock core samples with diameters of 83 mm (PQ-3 size) were obtained.

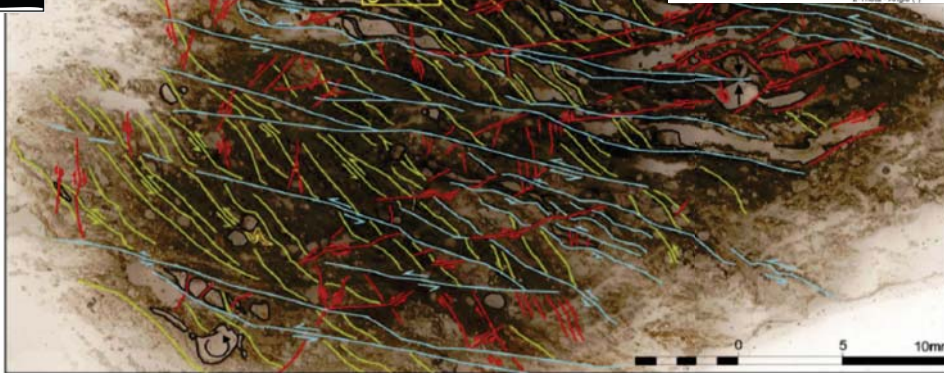
Research Boreholes AMF-1 and AMF-SIS-1



Microstructure and Mineralogy of the Fault Gouge

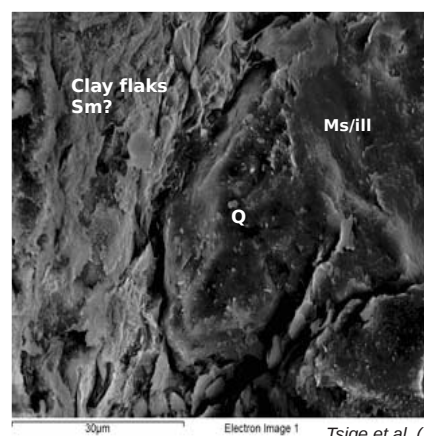
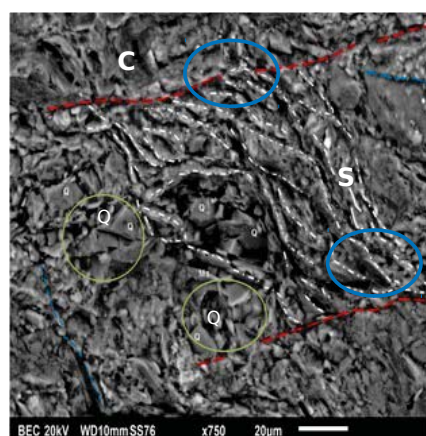
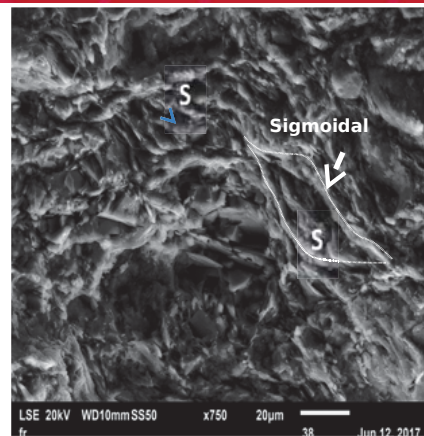


Tectonic fabric of the fault gouge with C-C'-S planes

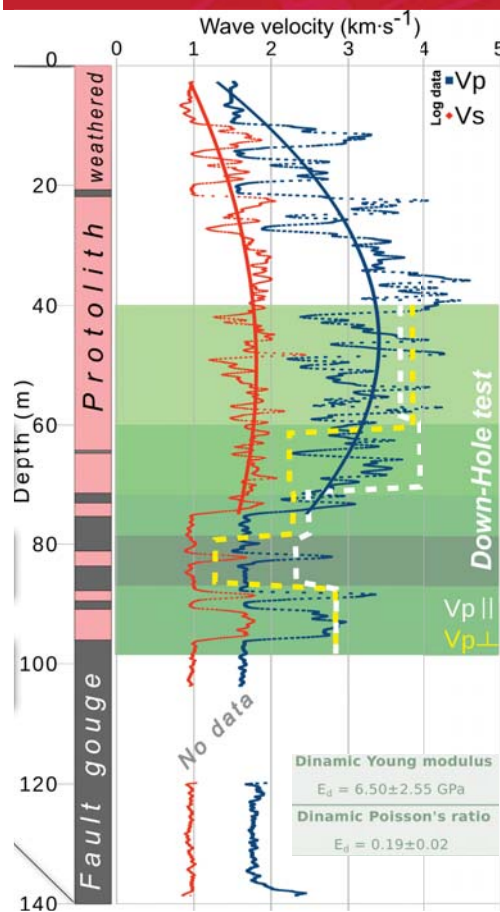


Microstructure of the Fault Gouge

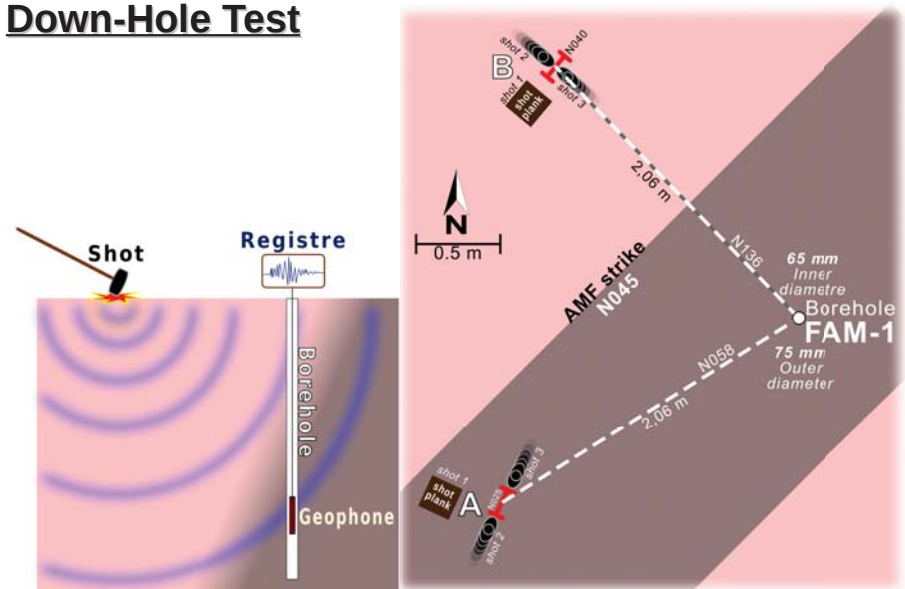
SEM image



Body Waves Velocity along the AMF-1 Borehole



Down-Hole Test

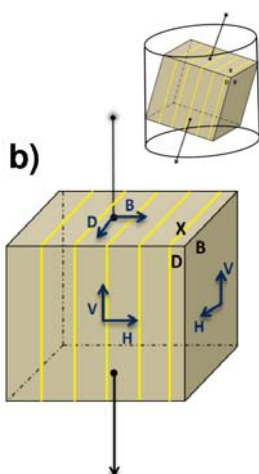
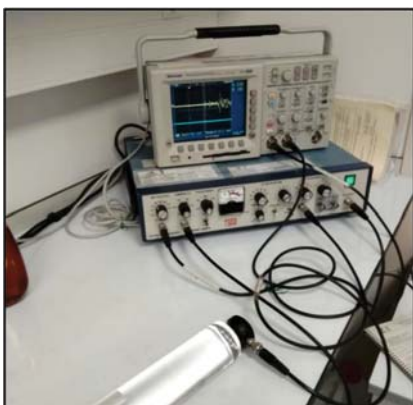


Prof. (m)	Down-hole		Log		$V_s = 1,13 \cdot V_p^{0,913}$
	Shot point A	Shot point B ⊥	Mean ($\pm 1\sigma$)	Mean ($\pm 1\sigma$)	
Protolith	3663	3805	3734 ± 71	3176 ± 492	1717 ± 208 , 1.85 ± 0.51
	3902	2229	3065 ± 836	3082 ± 322	1768 ± 112 , 1.74 ± 0.29
Fault gauge	2474	2265	2370 ± 148	2235 ± 504	1388 ± 336 , 1.61 ± 0.75
	2308	1265	1787 ± 738	1780 ± 302	1040 ± 197 , 1.71 ± 0.61
		2812	2832	2822 ± 14	1331 ± 317 , 1.61 ± 0.81
		Anisotropy 1.82			
→ A: strike velocity ⊥ → B: dip velocity					

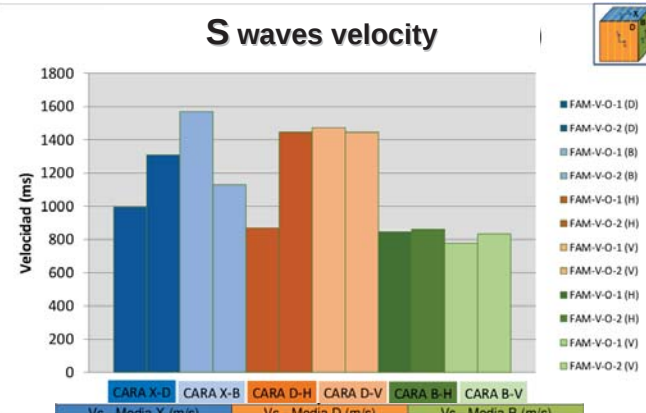
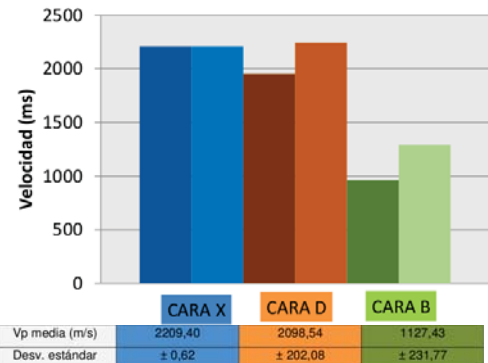
Insua-Arévalo et al. (2018)

Body Waves Velocity through Gouge Specimens

Ultrasonic Velocity



P waves velocity



Laboratorio de Petrofísica del Instituto de Geociencias IGEO (CSIC-UCM)



Álvarez Corral (2018)

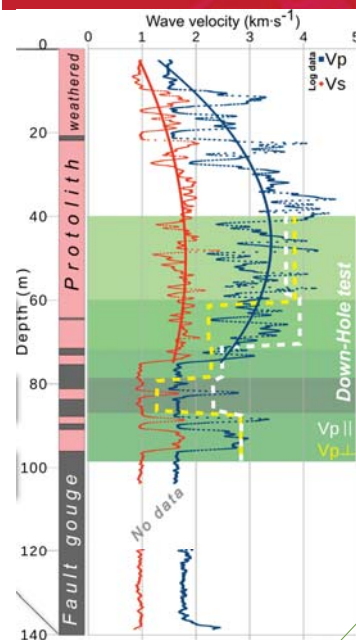


S waves velocity

31/44

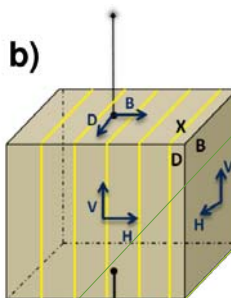
XVIII Jornada Técnica Anual
Sociedad Española de Mecánica de Rocas SEMR
MAYO 2021

Waves Velocity through Gouge Specimens vs. along the AMF-1 Borehole

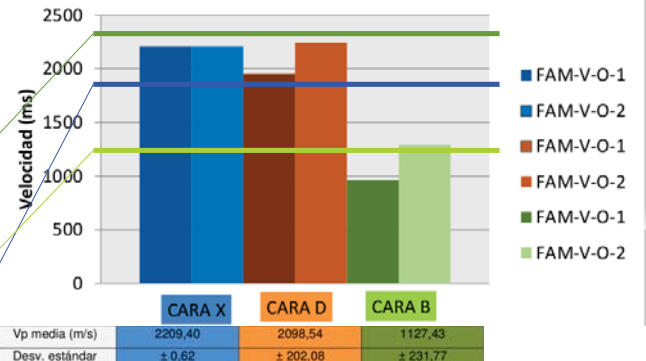


Prof. (m)	Down-hole		Log	
	Shot point A	Shot point B ⊥	Mean (±1σ)	Mean (±1σ)
40 - 60	3663	3805	3734 ±71	3176 ±492
60 - 70	3902	2229	3065 ±836	3082 ±322
70 - 78	2474	2265	2370 ±148	2235 ±504
78 - 86	2308	1265	1787 ±738	1780 ±302
86 - 98	2812	2832	2822 ±14	2229 ±542
Anisotropy 1.82		$V_s = 1,13 \cdot V_p^{0.913}$		

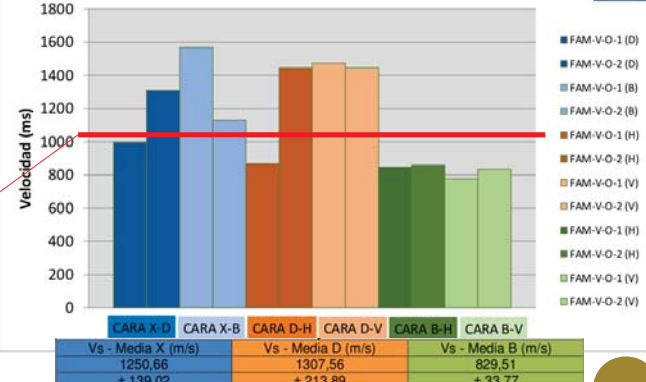
||--A: strike velocity ⊥--B: dip velocity



P waves velocity



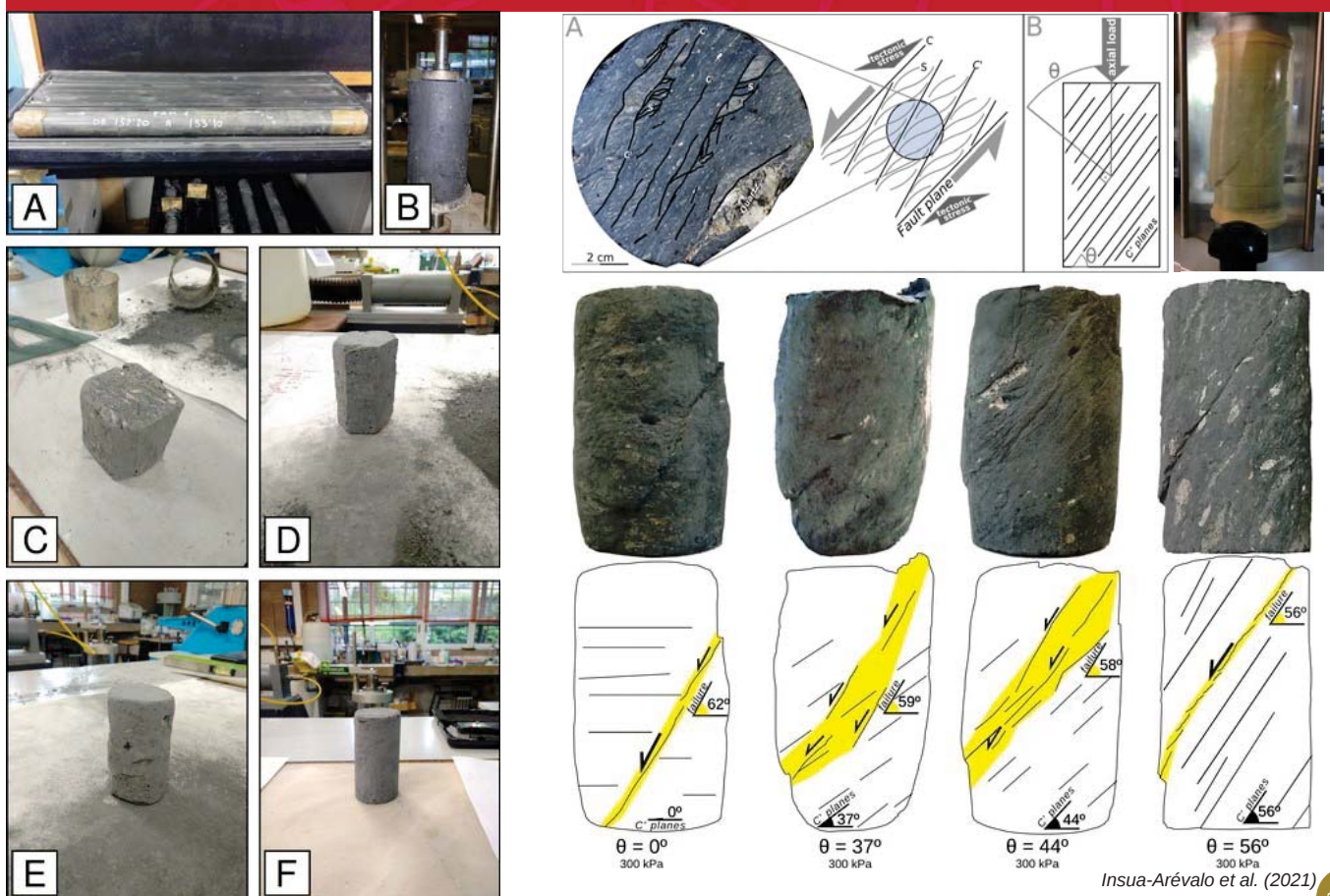
S waves velocity



32/44

MAYO 2021

Fault Gouge Strength: CU Triaxial Tests

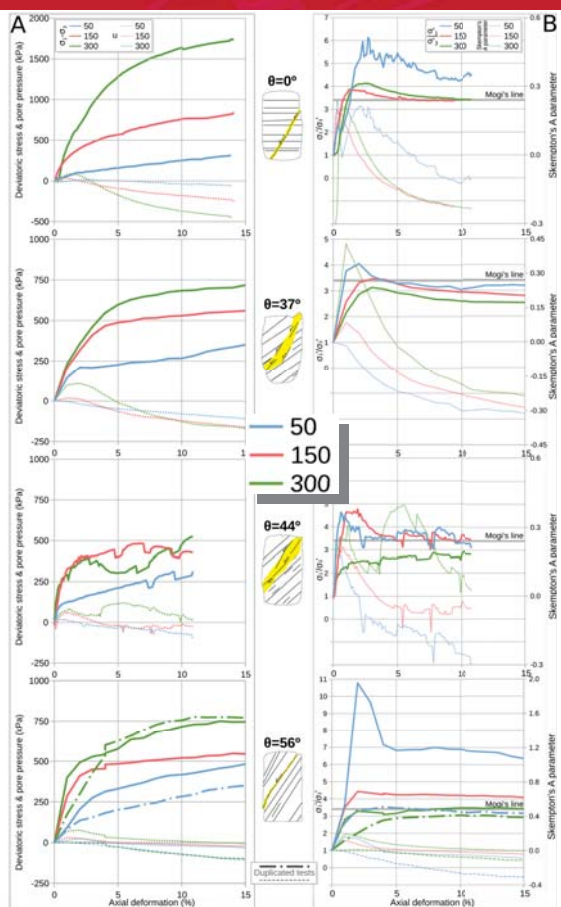


Juan Miguel Insua Arévalo
Universidad Complutense de Madrid
Facultad de Ciencias Geológicas

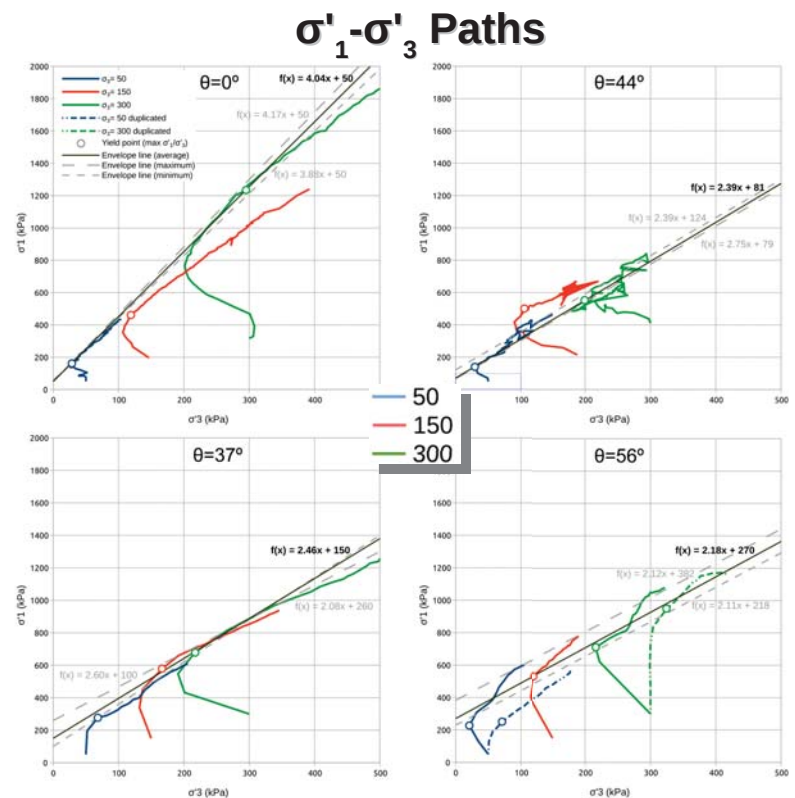
XVIII Jornada Técnica Anual
Sociedad Española de Mecánica de Rocas
SEMR
MAYO 2021

33/44

Fault Gouge Strength



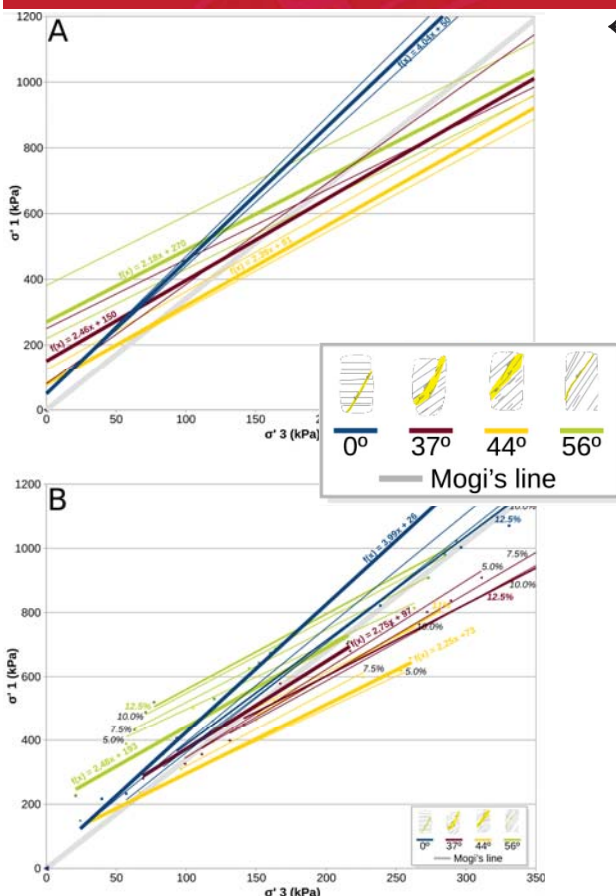
CU Triaxial Tests Results



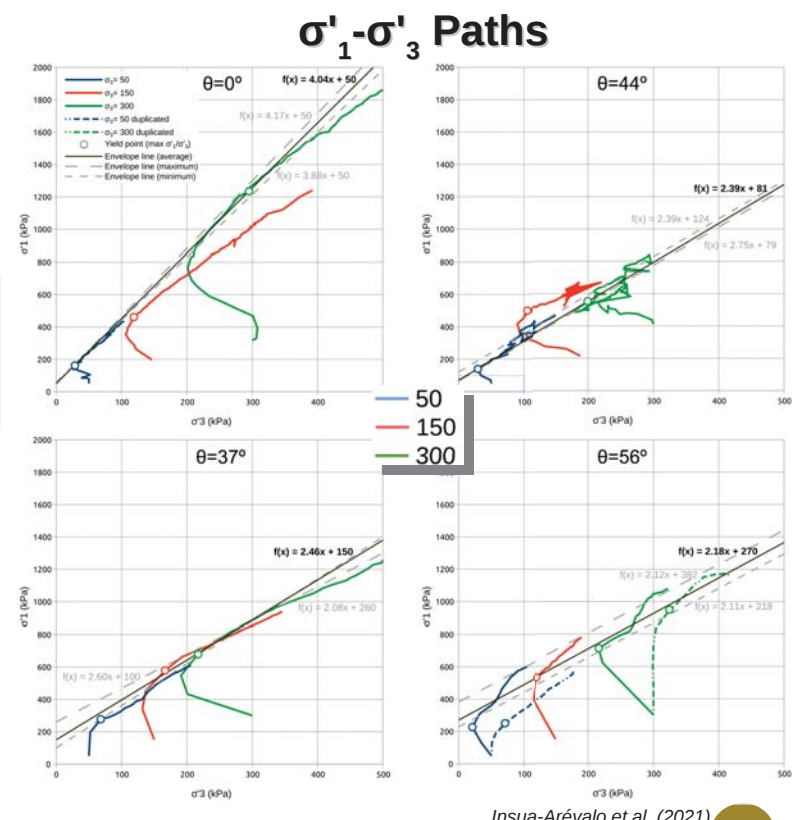
Insua-Arévalo et al. (2021)

34/44

Fault Gouge Strength



← Failure Linear Envelopes



Insua-Arévalo et al. (2021)

XVIII Jornada Técnica Anual
Sociedad Española de Mecánica de Rocas
SEMR MAYO 2021

35/44

Hoek&Brown Non-Linear Strength Criteria

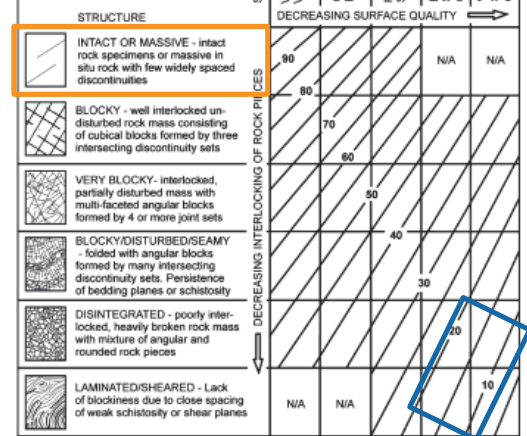
$$\sigma'_1 = \sigma'_3 + \sigma_{ci} \left[m_b \frac{\sigma'_3 + s}{\sigma_{ci}} \right]^a$$

$$m_b = m_i e^{28 - 14 D}$$

$$s = e^{9 - 3 D}$$

$$a = \frac{1}{2} + \frac{1}{6} \left[e^{-\frac{GSI}{15}} - e^{-\frac{20}{3}} \right]$$

GEOLOGICAL STRENGTH INDEX FOR JOINTED ROCKS (Hoek and Marinos, 2000)	
From the lithology, structure and surface conditions of the discontinuities, estimate the average value of GSI. Do not try to be too precise. Quoting a range from 33 to 37 is more realistic than stating that GSI = 35. Note that these tables do not apply to structurally controlled failures. Where weak planar schistosity planes are present in an unfavourable orientation with respect to the excavation face, these will dominate the rock mass behaviour. The shear strength of surfaces in rocks that are prone to deterioration as a result of changes in moisture content will be reduced. In practice, it is better to work with rocks in the fair to very poor categories, a shift to the right may be made for wet conditions. Water pressure is dealt with by effective stress analysis.	
SURFACE CONDITIONS	
VERY GOOD Very rough, fresh unweathered surfaces	
GOOD Rough, slightly weathered, iron stained surfaces	
FAIR Smooth, moderately weathered and altered surfaces	
POR Smooth, highly weathered surfaces with compact coatings or fillings or angular fragments	
POOR Slidescrossed, highly weathered surfaces with soft clay coatings or fillings	
DECREASING SURFACE QUALITY →	



Parameters of the strength criteria considering the fault gouge as INTACT ROCK

Hoek&Brown classification			Hoek&Brown criterion			Intact rock parameters form H&B		
θ	GSI	m_i	m_b	s	a	Tensile strength (-) (kPa)	Unconfined compressive strength (kPa)	
0	100	8	8	8	1	0.50	29	234
37	100	8	8	8	1	0.50	13	107
44	100	8	8	8	1	0.50	9	68
56	100	8	8	8	1	0.50	18	140

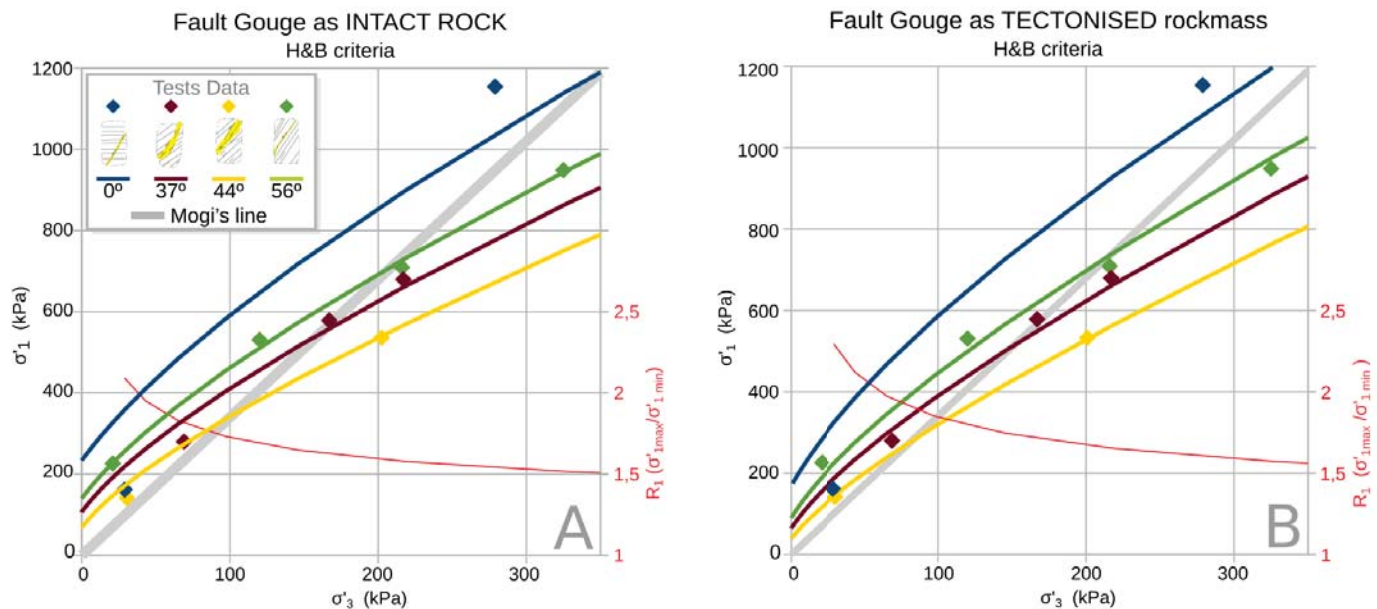
Parameters of the strength criteria considering the fault gouge as TECTONISED ROCKMASS

Hoek&Brown classification			Hoek&Brown criterion			Rockmass parameters from H&B			
θ	Intact unconfined compressive strength (kPa)	GSI	m_i	m_b	s	a	Tensile strength (-) (kPa)	Unconfined compressive strength (kPa)	
0	20,000	20,000	21	3	0.179	0.0002	0.541	17	173
37	20,000	20,000	11	3	0.125	0.0001	0.580	8	65
44	20,000	20,000	7	3	0.108	0.00003	0.604	6	39
56	20,000	20,000	14	3	0.139	0.0001	0.565	10	90

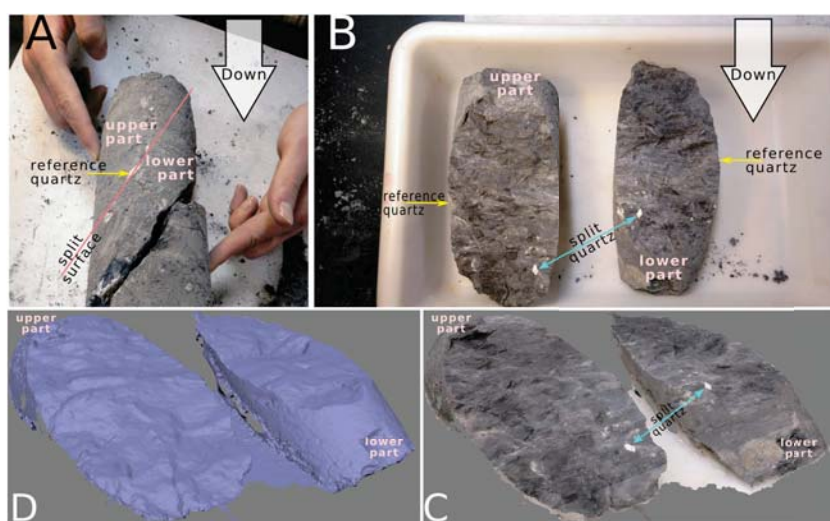
Insua-Arévalo et al. (2021)

36/44

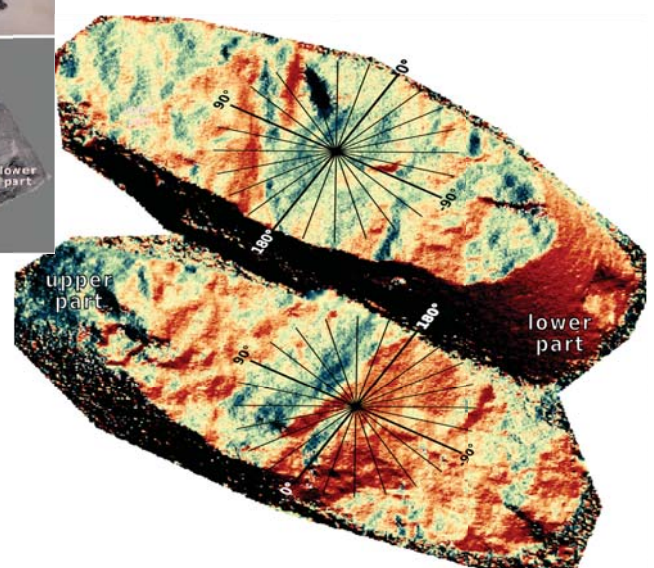
Hoek&Brown Non-Linear Strength Criteria



Influence of the Microstructure and Roughness of Weakness Planes

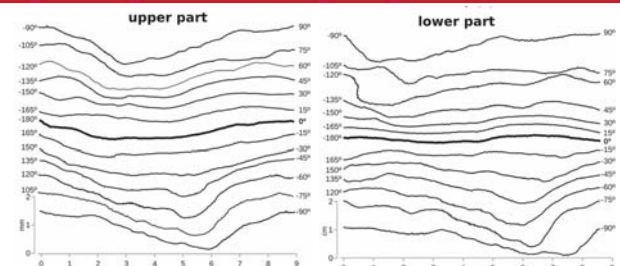
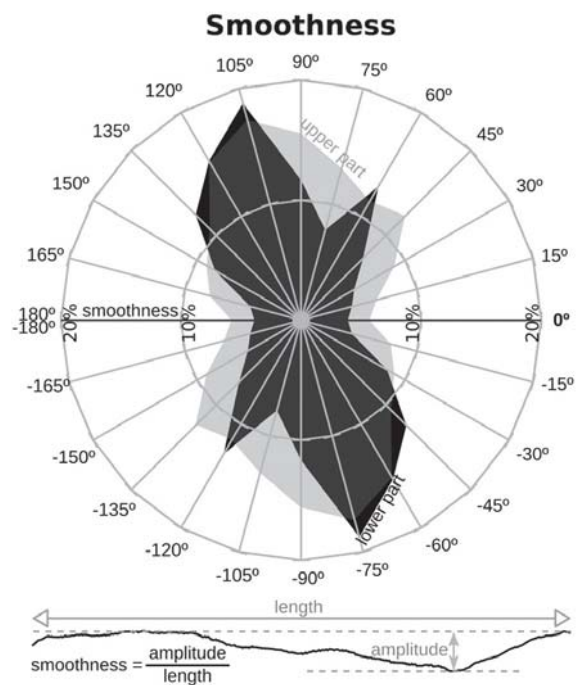


Split c' plane in a core sample

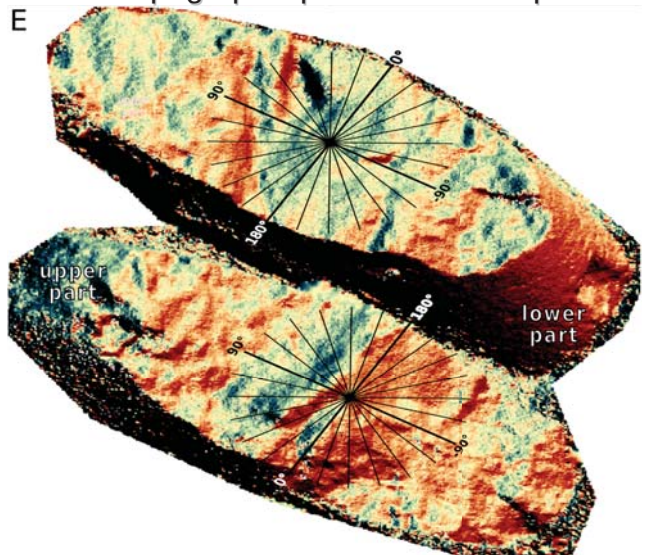


Influence of the Microstructure and Roughness of Weakness Planes

Distribution of the smoothness with the orientation of the profiles



Mesotopographic profiles of the c' plane

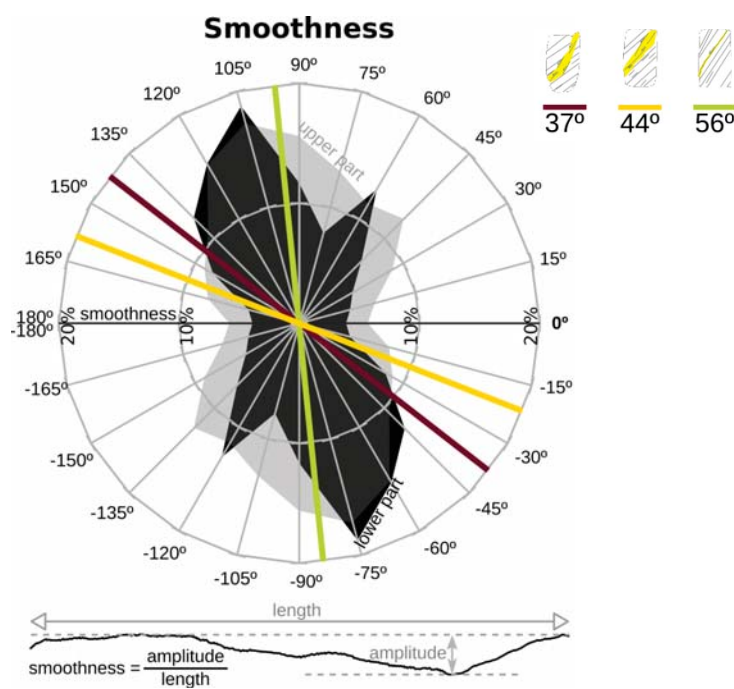


Insua-Arévalo et al. (2021)

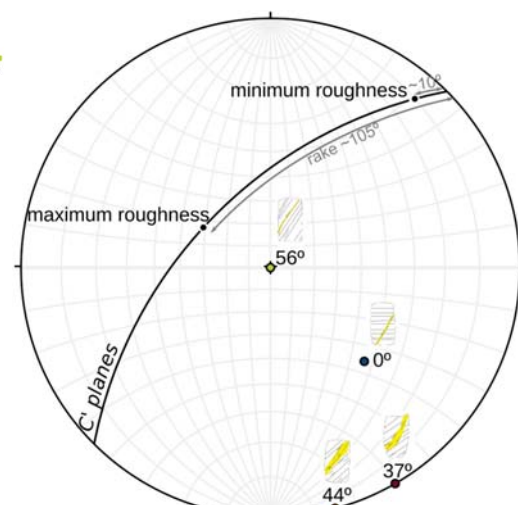
39/44

Influence of the Microstructure and Roughness of Weakness Planes

Distribution of the smoothness with the orientation of the profiles



Stereographic projection (equal angle, lower hemisphere) of the c' planes and the axial load of the tested specimens

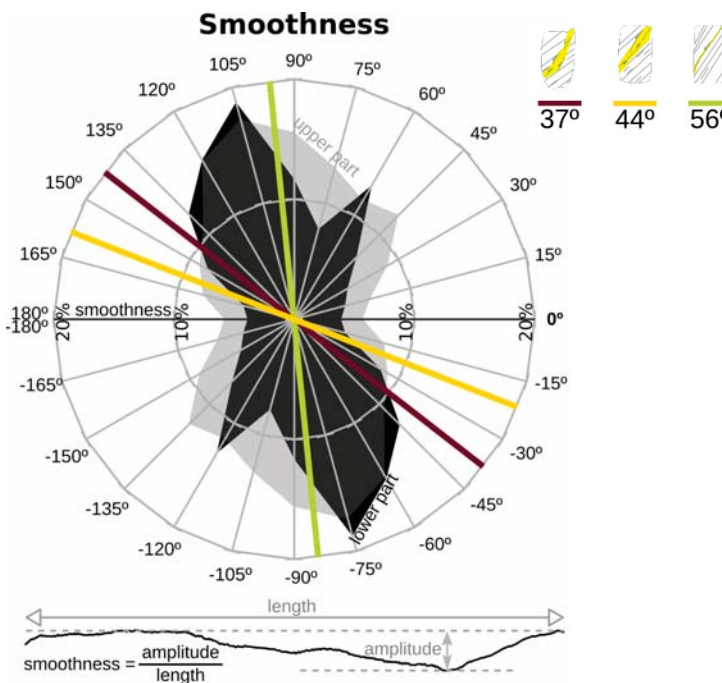


Insua-Arévalo et al. (2021)

40/44

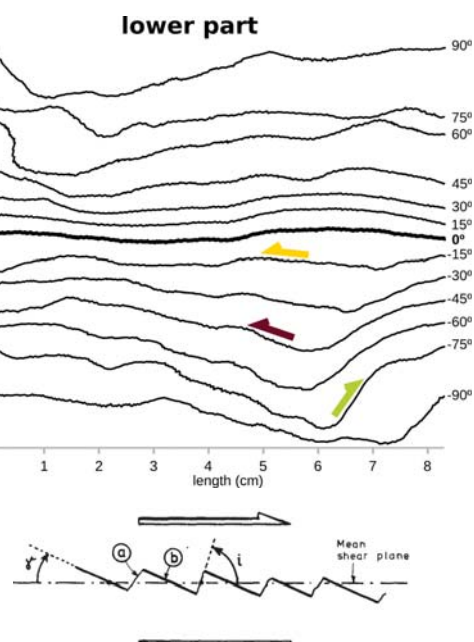
Influence of the Microstructure and Roughness of Weakness Planes

Orientation of the line of maximum dip within the weakness plane



Insua-Arévalo et al. (2021)

Slip direction of failure along the smoothness profiles of the c' plane



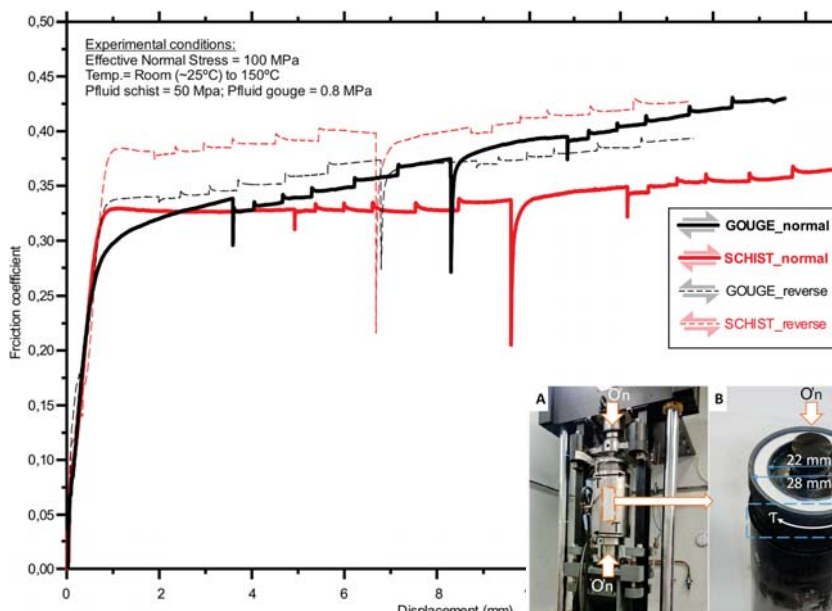
Bock (1979)

41/44

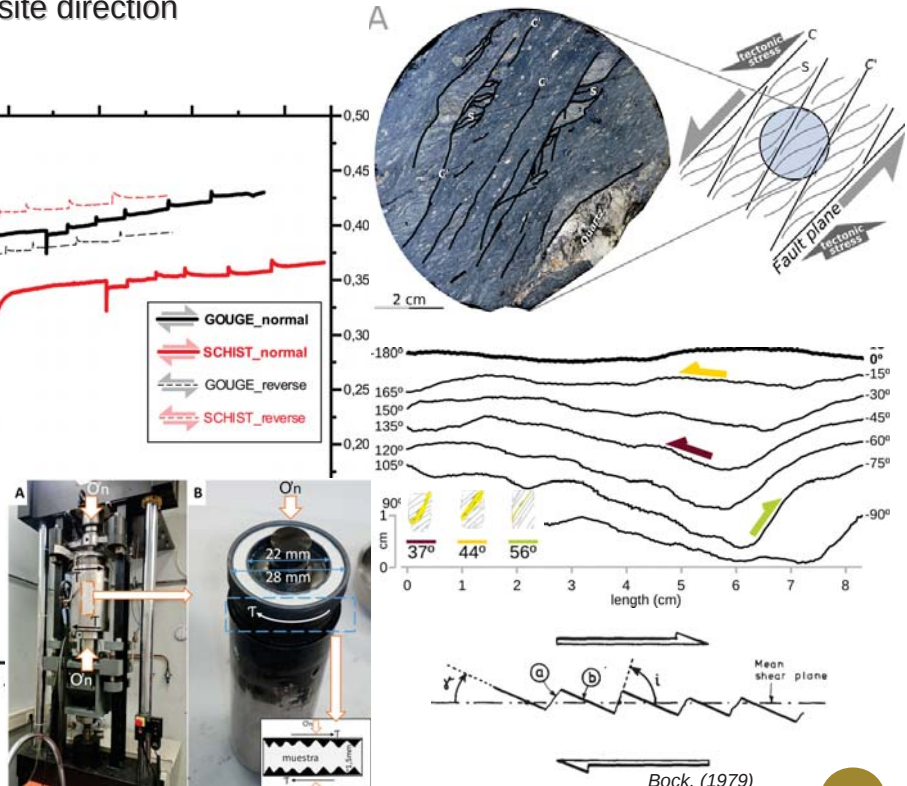
XVIII Jornada Técnica Anual
Sociedad Española de Mecánica de Rocas
SEMR MAYO 2021

Influence of the Microstructure and Roughness of Weakness Planes

Coefficient of friction is higher when microfabric is reactivated in the opposite direction



Rodríguez-Escudero (2017)



42/44

References

Related to the AFM

- Alonso-Henar, J., Rodríguez-Escudero, E., Herrero-Barbero, P., Tsige, M., Martínez-Díaz, J.J., 2021. Complete strain record of a highly asymmetric shear zone. From fault core gouges to surface rupture of historical earthquakes in the Alhama de Murcia Fault (SE Iberian Peninsula). *Lithosphere* (2021) 2021 (1): 8876012. <https://doi.org/10.2113/2021/8876012>
- Álvarez Corrales, S., 2018. Análisis de la anisotropía de la velocidad de propagación de ondas de cuerpo en la "fault gouge" de la Falla de Alhama de Murcia. MSc Thesis. Complutense University of Madrid. 46 pp.
- Herrero-Barbero, P., Álvarez-Gómez, J.A., Martínez-Díaz, J., & Klimowitz, J., 2020. Neogene basin inversion and recent slip rate distribution of the northern termination of the Alhama de Murcia Fault (Eastern Betic Shear Zone, SE Spain). *Tectonics*, 39, e2019TC005750. <https://doi.org/10.1029/2019TC005750>
- Insua-Arévalo, J.M., Tsige, M., Sánchez-Roldán, J.L., Rodríguez-Escudero, E. & Martínez-Díaz, J.J., 2021. Influence of the microstructure and roughness of weakness planes on the strength anisotropy of a foliated clay-rich fault gouge. *Engineering Geology*, 289: 106186. <https://doi.org/10.1016/j.enggeo.2021.106186>
- Marti, A., Queralt, P., Marcuello, A., Ledo, J.J., Rodríguez-Escudero, E., Martínez-Díaz, J.J., Campanyà, J., Meqbel, N., 2020. Magnetotelluric characterization of the Alhama de Murcia Fault (Eastern Betics, Spain) and study of magnetotelluric interstation impedance inversion. *Earth, Planets and Space*, 72:16. <https://doi.org/10.1186/s40623-020-1143-2>
- Martínez Díaz, J.J., Alonso-Henar, J., Insúa Arévalo, J.M., Canora, C., García-Mayordomo, J., Rodríguez Escudero, E., Alvarez Gomez, J.A., Ferrater, M., Ortúñoz, M., Masana, E., 2018. Geological evidences of surface rupture related to a seventeenth century destructive earthquake in Betic Cordillera (SE Spain): constraining the seismic hazard of the Alhama de Murcia fault. *Journal of Iberian Geology*. <https://doi.org/10.1007/s41513-01>
- Martínez-Díaz, J. J., Bejar-Pizarro, M., Álvarez-Gómez, J.A., Mancilla, F. L., Stich, D., Herrera, G., Morales, J., 2012. Tectonic and seismic implications of an intersegment rupture. The damaging May 11th 2011 Mw 5.2 Lorca, Spain, earthquake, Betic Cordillera, Spain. *Tectonophysics* 546-547, 28-37. <https://doi.org/10.1016/j.tecto.2012.04.010>
- Martínez-Díaz, J.J., Insua-Arévalo, J.M., Tsige, M., Rodríguez-Escudero, E., Alonso-Henar, J., Crespo, J., Jiménez-Molina, D., Moratalla, J.M., Rodríguez-Peces, M.J., Álvarez-Gómez, J. A., Pérez-López, R., Jurado, M.J., Alvaro M., Capote, R., 2016. FAM-1 Borehole: first results from the scientific drilling of the Alhama de Murcia Fault, Betic Cordillera, Spain. *GeoTemas*, 16 (2), 579-582.
- Rodríguez-Escudero, E., 2017. Implicaciones de la estructura interna de una zona de falla activa en la génesis de terremotos. PhD Thesis. Universidad Autónoma de Madrid, 304pp.
- Rodríguez-Escudero, E., A. Niemeijer, J.J. Martínez-Díaz, J.L. Giner-Robles, M. Tsige, J.M. Insua-Arévalo, J. Cuevas-Rodríguez, J., 2018. Propiedades mineralógicas y friccionales de la gouge de la Falla de Alhama de Murcia (SE España): implicaciones sismogénicas. In Canora, C., F. Martín, E. Masana, R. Pérez y M. Ortúñoz, (Eds.), pp. 191-194. Tercera reunión ibérica sobre fallas activas y paleoseismología, Alicante (España).
- Rodríguez-Escudero, E., Martínez-Díaz, J. J., Giner-Robles, J.L., Tsige, M., Cuevas-Rodríguez, J., 2020. Pulverized quartz clasts in gouge of the Alhama de Murcia fault (Spain): Evidence for coseismic clast pulverization in a matrix deformed by frictional sliding. *Geology* 48, 283-287. <https://doi.org/10.1130/G47007.1>
- Rodríguez-Soto, P., Tsige, M., Insua-Arévalo, J.M., Martínez-Díaz, J.J., Rodríguez-Escudero, E., Jiménez Molina, D. 2017. Caracterización geotécnica y geomecánica de la roca de falla de la falla activa de Alhama de Murcia. *Geogaceta*, 62, 7-10.
- Tsige, M., Insua-Arévalo, J.M., Martínez-Díaz, J.J., Rodríguez-Escudero, E., Rodríguez-Soto, P., Crespo, E., Mata, P., 2017. Microfabric, Mineralogical And Geomechanical Characterization Of Clay Rich Fault Gouge From AMF (Murcia, Southeast Spain). Scientific research Abstract, VII International Clay Conference, Granada, Spain.

General

- Bock, H., 1979. A simple failure criterion for rough joints and compound shear surfaces. *Eng. Geol.* 14, 241–254. [https://doi.org/10.1016/0013-7952\(79\)90066-8](https://doi.org/10.1016/0013-7952(79)90066-8)
- Fossen, H., 2011. Structural Geology. Cambridge University Press. <https://doi.org/10.1017/CBO9780511777806>
- Fossen, H., Calavante, G.C., 2017. Shear zones – A review. *Earth Science Reviews*, 171, pp. 434-455. <https://doi.org/10.1016/j.earscirev.2017.05.002>
- Hoek, E., Brown, E.T., 2019. The Hoek-Brown failure criterion and GSI – 2018 edition. *J. Rock Mech. Geotech. Eng.* 11, 445-463. <https://doi.org/10.1016/j.jrmge.2018.08.001>
- Hoek, E., Carranza Torres, C., Corkum, B., 2002. Hoek-Brown criterion – 2002 edition. R. Hammah, W. Bawden, J. Curran, M. Telesnicki (Eds.), Mining and tunnelling innovation and opportunity, proceedings of the 5th North American rock mechanics symposium and 17th tunnelling association of Canada conference, University of Toronto, Toronto, Canada. Toronto: 267-273.



XVIII Jornada Técnica Anual
Sociedad Española de Mecánica de Rocas SEMR
MAYO 2021

43/44

Estructura Interna y Propiedades Mecánicas de la Falla Activa de Alhama de Murcia

Internal Structure and Mechanical Properties of the Active Fault of Alhama de Murcia

Gracias
Thank you



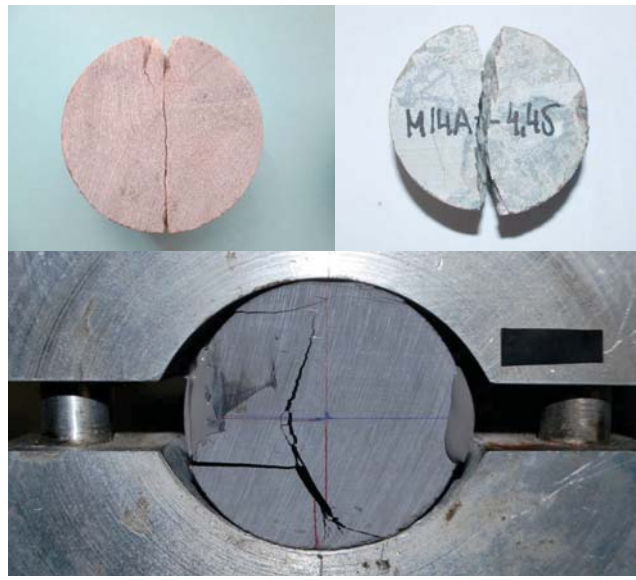
Juan Miguel Insua Arévalo
Universidad Complutense de Madrid
Facultad de Ciencias Geológicas



**Grupo Geodinámica Planetaria,
Tectónica Activa y Aplicaciones a Riesgos**



44/44



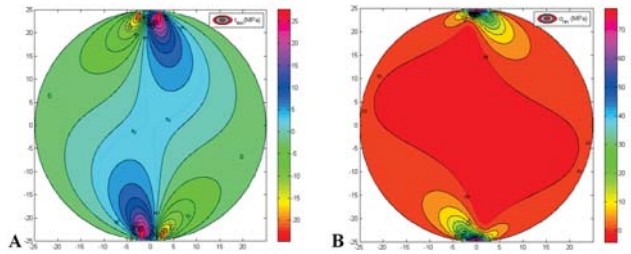
SOCIEDAD ESPAÑOLA DE
MECÁNICA DE ROCAS

XVIII JORNADA TÉCNICA ANUAL
13 de mayo 2021

VIII Premio SEMR al mejor trabajo de investigación en
Mecánica de Rocas para Jóvenes Investigadores

**MECANISMO DE INICIO DE LA ROTURA EN MATERIAL
DE COMPORTAMIENTO FRÁGIL BAJO CONDICIONES
TRACCIONALES**

Carmen Covadonga García Fernández
Dpto. Explotación y Prospección de Minas



Universidad de Oviedo
Universidá d'Uviéu
University of Oviedo



Esquema de la presentación

1. INTRODUCCIÓN
2. ANTECEDENTES
3. OBJETIVOS
4. ESTRUCTURA DEL TRABAJO DE INVESTIGACIÓN
5. DETERMINACIÓN DE LA RESISTENCIA A TRACCIÓN EN EL ENSAYO BRASILEÑO. PARÁMETROS DE INFLUENCIA
6. NUEVAS APLICACIONES DEL ENSAYO BRASILEÑO
7. NUEVO ENSAYO DE CARACTERIZACIÓN DE LA RESISTENCIA A TRACCIÓN
8. CONCLUSIONES



¿Cómo determinamos la resistencia a tracción?



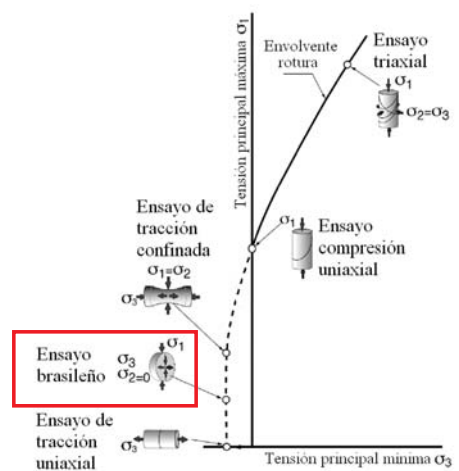
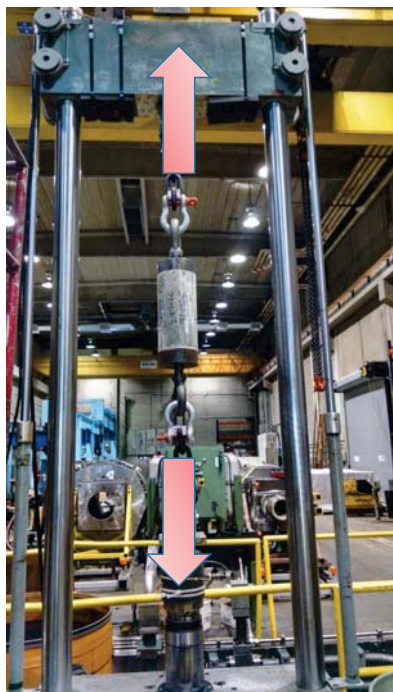
F. Azpiri, D. Guerrero, and V. Ormaetxea

E. Hoek and C. D. Martin (2014)

J. W. Cho, S. Jeon, S. H. Yu, and S. H. Chang (2010)

www.pizarras-gallegas.com

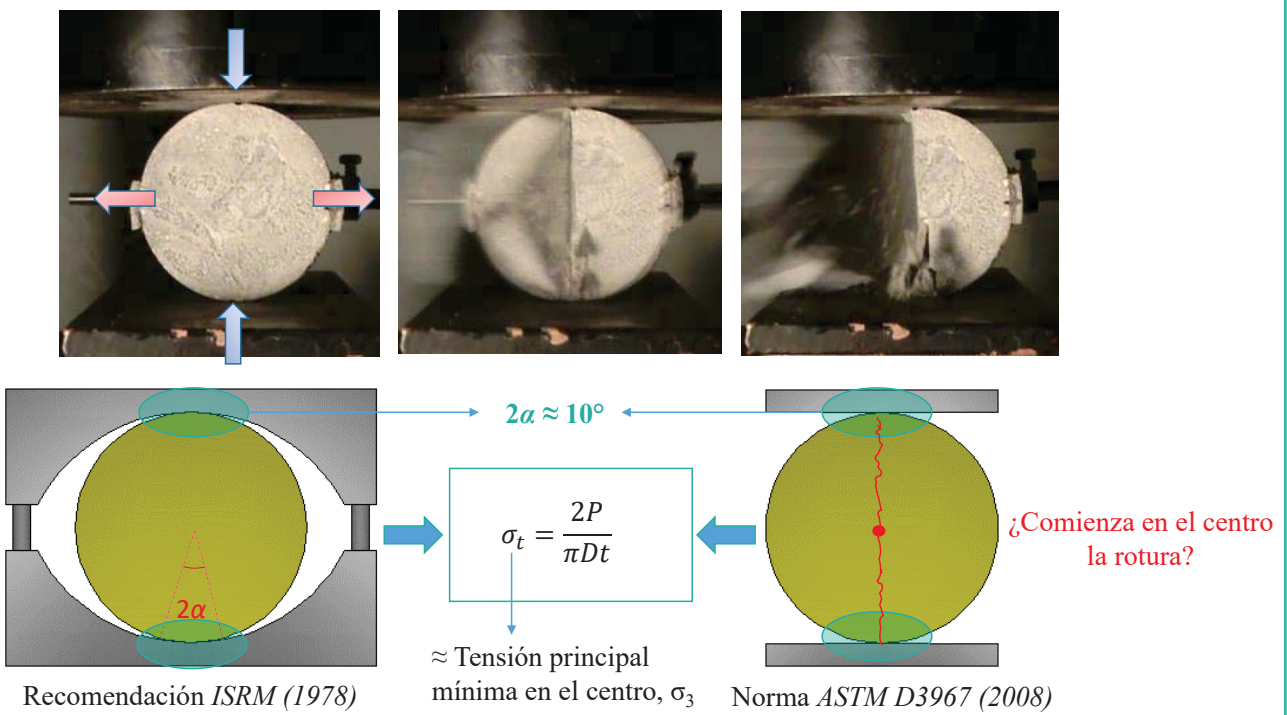
Ensayo de tracción directa



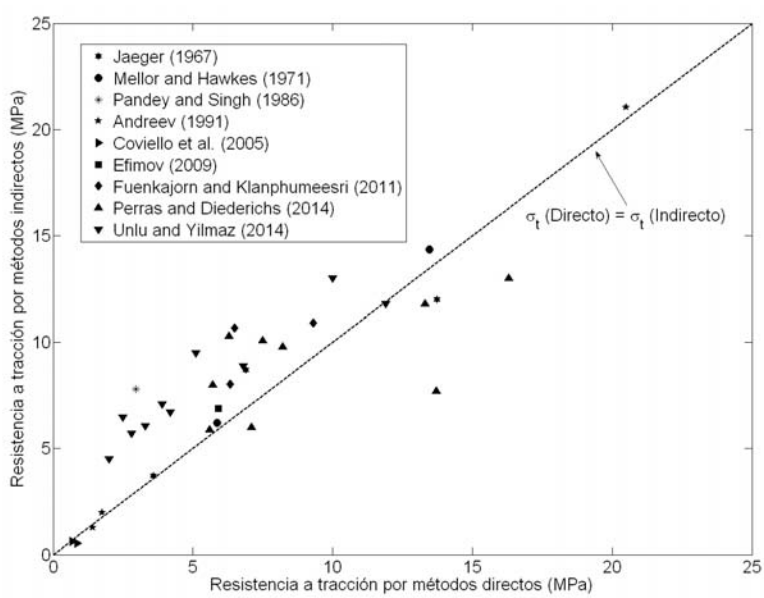
A. Covillejo, R. Lagioia, and R. Nova (2005)

S. Patel and C. D. Martin (2018)

Ensayo Brasileño o compresión diametral

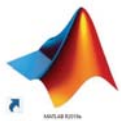


Ensayo Brasileño o compresión diametral



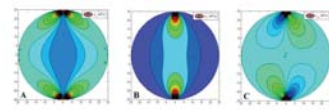
K. Tufekci, S. Demirdag, N. Sengun, R. Altindag, and D. Akbay (2016)

Soluciones analíticas para el cálculo del estado tensional



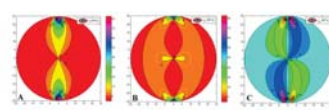
Distribución de carga puntual

S. Timoshenko and J. N. Goodier (1951)



Distribución de carga uniforme

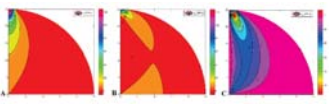
C. C. Ma and K. M. Hung (2008)



Distribución de carga sinusoidal

C. F. Markides and S. K. Kourkoulis (2012)

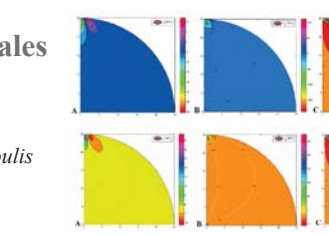
C. F. Markides, D. N. Pazis, and S. K. Kourkoulis (2012)



Influencia de las tensiones friccionales

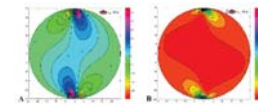
C.F. Markides, and S. K. Kourkoulis (2013)

C. F. Markides, D. N. Pazis, and S. K. Kourkoulis (2011, 2012)



Disco constituido por múltiples planos de discontinuidad

S. D. Priest (1963)



“Estudio detallado del mecanismo que controla el inicio de la rotura en materiales frágiles bajo condiciones traccionales”

“Estudio detallado del mecanismo que controla el inicio de la rotura en materiales frágiles bajo condiciones traccionales”

Determinación de la Resistencia a Tracción en el Ensayo Brasileño. Parámetros de Influencia

- Estudio experimental y analítico del inicio de la rotura en el ensayo Brasileño
- Verificación computacional de las condiciones de contorno óptimas en el ensayo Brasileño
- Influencia del ángulo de contacto en el patrón de rotura en pizarra bajo el ensayo Brasileño
- Efecto de la humedad relativa ambiental en la resistencia a tracción de la foliación en pizarra

Nuevas Aplicaciones del Ensayo Brasileño

- Determinación de diferentes estados tensionales límite en la región de tracción usando el ensayo Brasileño
- Nueva metodología de estimación de los parámetros resistentes de la foliación en pizarra usando el ensayo Brasileño

Nuevo Ensayo de Caracterización de la Resistencia a Tracción

Nuevo ensayo de caracterización de la resistencia a tracción de materiales rocosos

Estudio experimental y analítico del inicio de la rotura en el ensayo Brasileño

C.C. Garcia-Fernandez, C. Gonzalez-Nicieza, M.I. Alvarez-Fernandez, R.A. Gutierrez-Moizant, “Analytical and experimental study of failure onset during a Brazilian test”, *Int J of Rock Mech Min Sci.*, vol. 13, pp. 254-265, 2018



Analytical and experimental study of failure onset during a Brazilian test

C.C. Garcia-Fernandez^a, C. Gonzalez-Nicieza^{a*}, M.I. Alvarez-Fernandez^b, R.A. Gutierrez-Moizant^b

^aDpto. of Exploration and Prospecting Mines, Mining Engineering School, University of Oviedo, Aviles, Spain

^bDpto. of Mechanical Engineering, University Carlos III, Madrid, Spain

ARTICLE INFO

Keywords:
Brazilian test
Contact angle
Stress distribution
Failure initiation point

ABSTRACT

The location of the failure initiation in the Brazilian test is strongly influenced by the contact angle created in the loaded area. As this angle increases, the position of the initial failure point is closer to the center of the disc, which is a result of both: uniform radial pressure and sinusoidal radial pressure; as well as adopting different failure criteria and materials. Moreover, the frictional stresses throughout the contact between the jaw (or platens) and the disc cannot be considered as a critical failure parameter for failures initiated from the origin to a radial distance of about 10% of the disc radius.

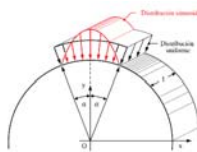
In this paper, firstly, the influence of the above mentioned parameters in the location of the initial failure point was analytically studied. Secondly, the analytical results have been proven through experimental tests. Finally, once the importance of the contact angle in the location of the initiation point was checked, a procedure is suggested in order to increase the contact angle with same load applied to one specific sample, by using various jaw curvatures.

The variation of failure initiation does not cause great disturbances in the determination of the indirect tensile strength. However, the position is important in order to adjust the failure criteria in the tension region. According to the location of the initial failure, the stress field in terms of principal stresses (σ_1 and σ_3) will be different. So by knowing this position, the precise failure criteria could be established in $\sigma_1 - \sigma_3$, specifically in the tension region. Meaning that as well as the triaxial test is mostly used to calculate the failure criteria in the compression region, the Brazilian test could be used to obtain the limiting stress states in the tension region.

Consideraciones preliminares

1) Distribución de presión:

- Uniforme (Ma and Hung , 2008)
- Sinusoidal (Markides and Kourkoulis, 2012)



2) Materiales:

- Pizarra
- Calcarenita
- PMMA

3) Criterios de rotura:

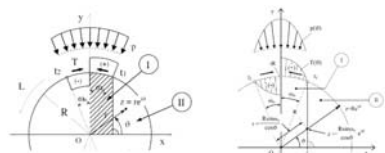
- Mohr-Coulomb (truncado)
- Hoek-Brown

Propiedades	Pizarra	Calcarenita	PMMA
Módulo de elasticidad (GPa)	47.55	73.75	3.20
Coeficiente de Poisson	0.24	0.18	0.40
Coeficiente de fricción mandíbula-disco	0.55	0.62	0.38
Resistencia a compresión uniaxial (MPa)	179.52	113.99	124.40
Resistencia a tracción (MPa)	24.04	8.89	65.26
Cohesión (MPa)	26.18	18.16	40.69
Ángulo de fricción interna ($^{\circ}$)	47.99	54.52	22.68
m_b	7.46	12.81	1.90

4) Influencia de las tensiones friccionales:

- Distribución uniforme (Markides, Pazis , Kourkoulis, 2011)
- Distribución sinusoidal (Markides, Pazis , Kourkoulis, 2012)

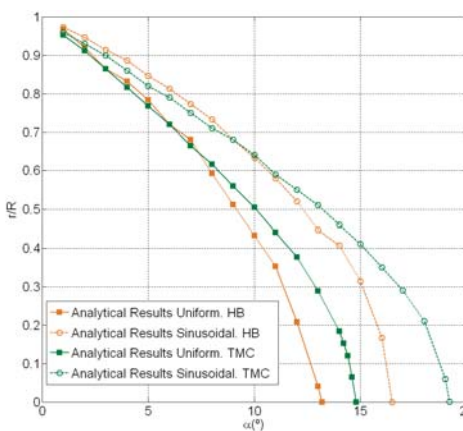
Determinación analítica del primer punto en alcanzar el criterio de rotura, según varía el ángulo de contacto



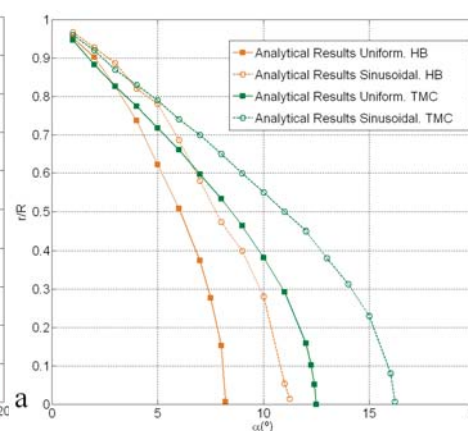
C.C. Garcia-Fernandez, C. Gonzalez-Nicieza, M.I. Alvarez-Fernandez, R.A. Gutierrez-Moizant (2018)

Estudio analítico

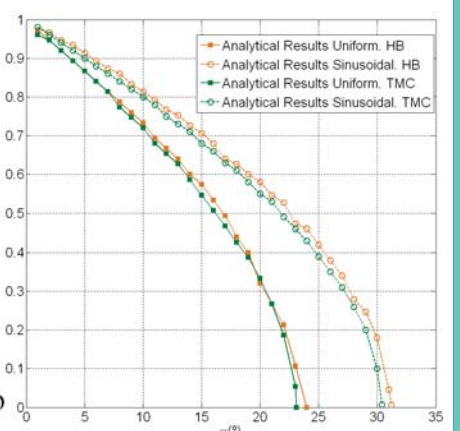
Pizarra



Calcarenita



PMMA



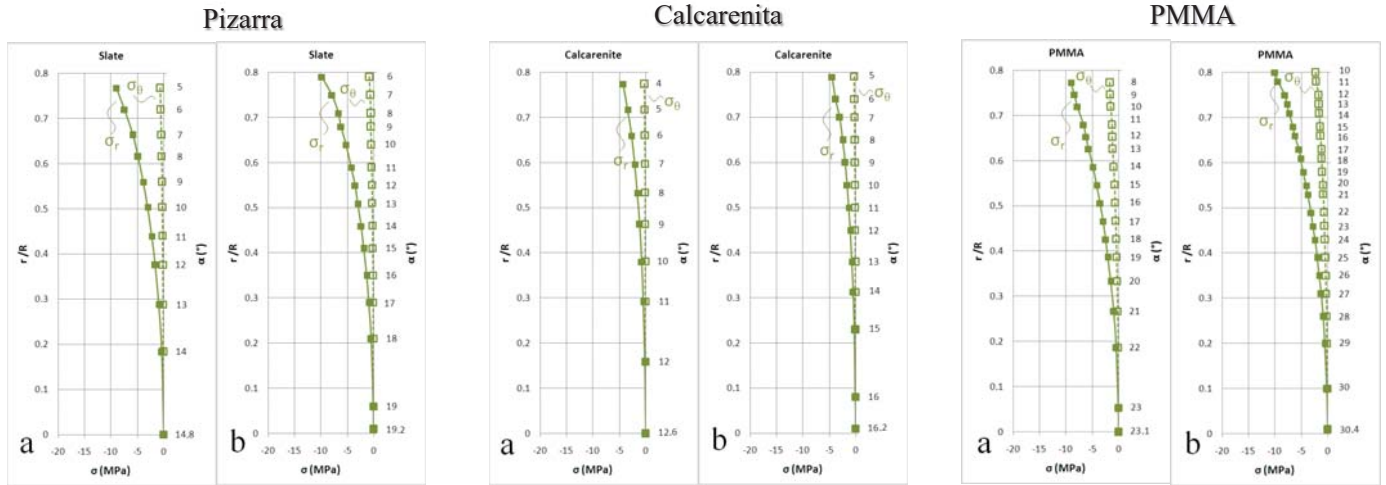
- Variación del punto de rotura inicial (r/R) según el semiángulo de contacto (α)

C.C. Garcia-Fernandez, C. Gonzalez-Nicieza, M.I. Alvarez-Fernandez, R.A. Gutierrez-Moizant (2018)

Estudio experimental y analítico del inicio de la rotura en el ensayo Brasileño

5. Parámetros de influencia

Estudio analítico



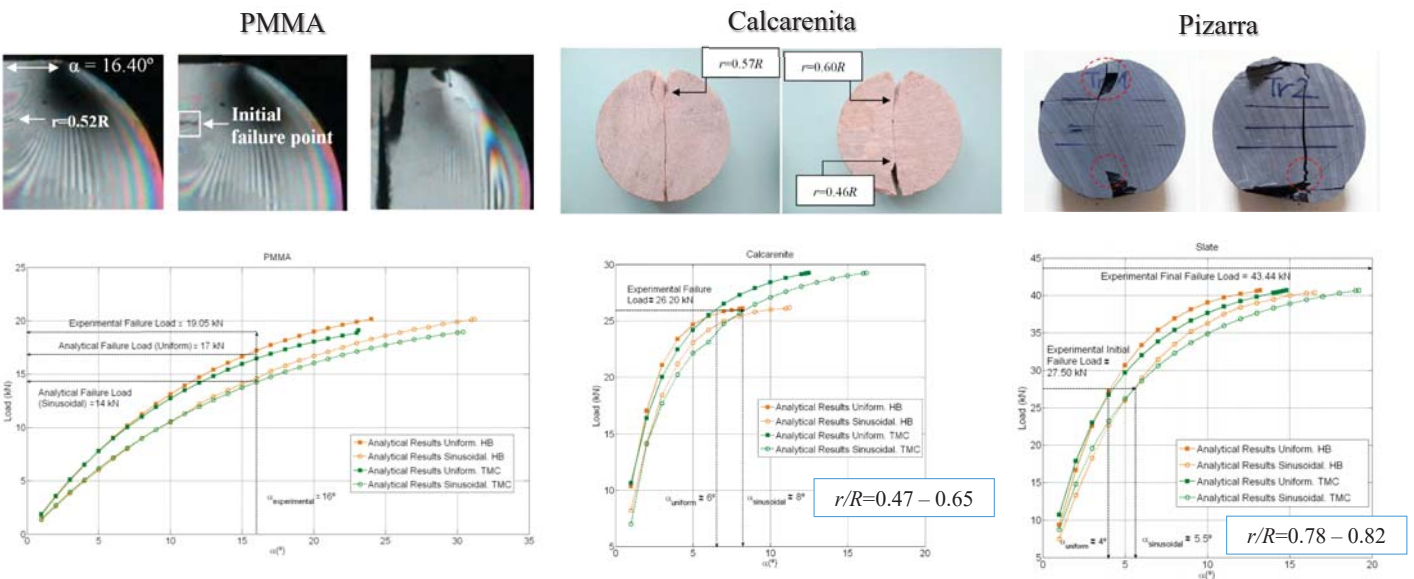
- Variación del punto de rotura inicial (r/R) según el semiángulo de contacto (α)
- Tensiones friccionales: podría cambiar ligeramente el punto en que se inicia la rotura, pero no tanto como para empezar en el centro.

C.C. Garcia-Fernandez, C. Gonzalez-Nicieza, M.I. Alvarez-Fernandez, R.A. Gutierrez-Moizant (2018)

Estudio experimental y analítico del inicio de la rotura en el ensayo Brasileño

5. Parámetros de influencia

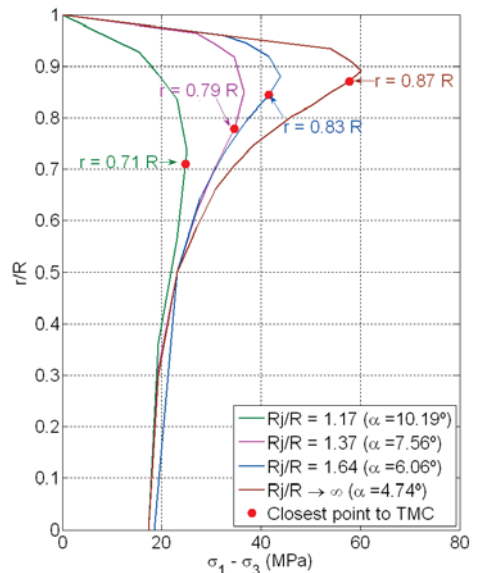
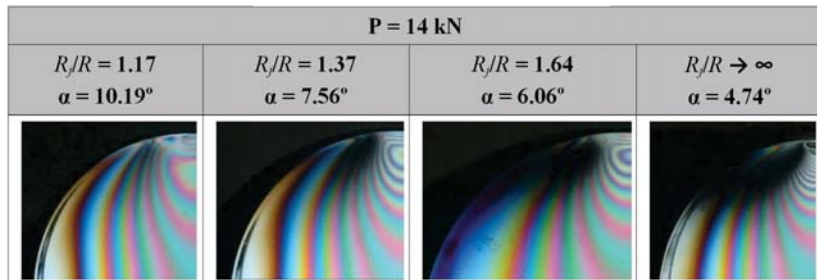
Resultados experimentales



C.C. Garcia-Fernandez, C. Gonzalez-Nicieza, M.I. Alvarez-Fernandez, R.A. Gutierrez-Moizant (2018)

Modificación experimental del ángulo de contacto

Modificando la relación de curvaturas entre mandíbulas de carga (R_j) y radio del disco (R) → Variación del ángulo de contacto → Cambio del estado tensional



C.C. Garcia-Fernandez, C. Gonzalez-Nicieza, M.I. Alvarez-Fernandez, R.A. Gutierrez-Moizant (2018)

Verificación computacional de las condiciones de contorno óptimas en el ensayo de tracción Brasileño

R. Gutierrez-Moizant, M. Ramirez-Berasategui, S. Santos-Cuadros, C.C. Garcia-Fernandez, “Computational verification of the optimum boundary condition of the Brazilian Tensile Test”, *Rock Mech Rock Eng*, vol. 51, pp. 3505-3519, 2018.

Rock Mechanics and Rock Engineering
<https://doi.org/10.1007/s00603-018-1553-7>

ORIGINAL PAPER

Computational Verification of the Optimum Boundary Condition of the Brazilian Tensile Test

R. Gutiérrez-Moizant¹ · M. Ramírez-Berastegui² · S. Santos-Cuadros³ · C. García-Fernández²

Received: 6 March 2018 / Accepted: 10 July 2018
© Springer-Verlag GmbH Austria, part of Springer Nature 2018

Abstract

The present research analyses the configuration of jaws to avoid the premature failure of the disc in the Brazilian test. The objective is to depict the loading device configuration that most likely produces results comparable to the Hondros' analytical stress solution. To this end, several numerical analyses have been carried out for different contact angles with the finite element method. It was deduced that the final contact angle plays an important part in the success of the Brazilian test and that the Griffith criterion can be fulfilled if the equivalent stress is calculated. Additionally, the orientation of the forces in the contact between the loading device and the disc has been studied for different friction conditions. According to the numerical results, it was found that a loading arc configuration of 20° shows the best agreement with the probable values given by the analytical stress model when the uncertainty of its magnitudes is taken into account. The study also demonstrates that the friction in the contact between the optimal loading configuration and the disc does not seem to significantly affect the theoretical predictions in the centre of the disc.

Keywords: Brazilian test · Crack initiation point · Equivalent stress · Comparison index

List of Symbols

P	Applied load
P_V	Vertical load
a	Width of the loaded section of the disc
D	Diameter of the disc
R	Radius of the disc

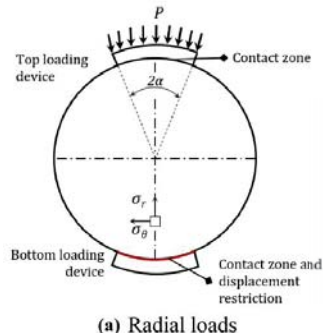
k_p Coverage factor for a confidence level of 95%
 r Radii ratio between the distance from the centre of the disc and the radius of the disc

1 Introduction

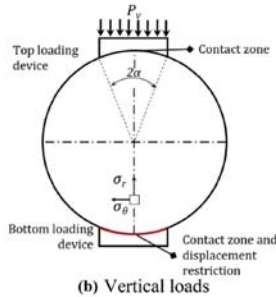
Verificación computacional de las condiciones de contorno óptimas

5. Parámetros de influencia

Material y metodología



(a) Radial loads



(b) Vertical loads

Modelo numérico con dos configuraciones de carga, A. radial y B. vertical

Influencia de la fricción (μ)

Variación del ángulo de carga (2α)

$$\sigma_r = -\frac{P}{\pi R t \alpha} \left\{ \frac{\left[1 - \left(\frac{r}{R}\right)^2\right] \sin 2\alpha}{1 - 2\left(\frac{r}{R}\right)^2 \cos 2\alpha + \left(\frac{r}{R}\right)^4} + \tan^{-1} \left[\frac{1 + \left(\frac{r}{R}\right)^2}{1 - \left(\frac{r}{R}\right)^2} \tan \alpha \right] \right\},$$

$$\sigma_\theta = \frac{P}{\pi R t \alpha} \left\{ \frac{\left[1 - \left(\frac{r}{R}\right)^2\right] \sin 2\alpha}{1 - 2\left(\frac{r}{R}\right)^2 \cos 2\alpha + \left(\frac{r}{R}\right)^4} - \tan^{-1} \left[\frac{1 + \left(\frac{r}{R}\right)^2}{1 - \left(\frac{r}{R}\right)^2} \tan \alpha \right] \right\},$$

$$\tau_{r\theta} = 0, \quad (1)$$

Comparación con la solución de Hondros (1959) para el cálculo del estado tensional en el diámetro vertical

Parámetros	Mortero
Diámetro (mm)	53.60
Espesor (mm)	27.00
Módulo de elasticidad (GPa)	30.00
Coeficiente de Poisson	0.31

R. Gutierrez-Moizant, M. Ramirez-Berasategui, S. Santos-Cuadros, C.C. Garcia-Fernandez (2018)

Verificación computacional de las condiciones de contorno óptimas

5. Parámetros de influencia

Resultados numéricos

Inicio probable de la rotura → máxima tensión equivalente, Griffith (1921):

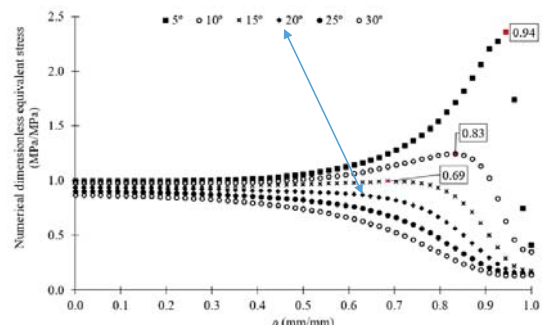
Determinación del ángulo de contacto óptimo

Cuando $3\sigma_\theta + \sigma_r \geq 0$

$$\sigma_G = \sigma_\theta$$

Cuando $3\sigma_\theta + \sigma_r < 0$

$$\sigma_G = -\frac{(\sigma_\theta - \sigma_r)^2}{8(\sigma_\theta - \sigma_r)}$$



Influencia del ángulo de contacto en la posición relativa del punto probable de inicio de la rotura, utilizando el modelo numérico

Límite de aplicabilidad y error

μ	$\sigma_{G,FEM}$ (MPa)	σ_G (MPa)	Ic
0	4.25	4.31	0.93
0.25	4.17		1.11
0.50	4.14		1.53
0.75	4.13		1.67

Factor de corrección propuesto por Satoh (1986):

$$\sigma_{GC} = \sigma_G \frac{\sin \alpha \cos^2 \alpha}{\alpha}$$

μ	$\sigma_{G,FEM}$ (MPa)	σ_G (MPa)	Ic
0	4.25	4.12	1.74
0.25	4.17		0.75
0.50	4.14		0.33
0.75	4.13		0.18

R. Gutierrez-Moizant, M. Ramirez-Berasategui, S. Santos-Cuadros, C.C. Garcia-Fernandez (2018)



Efecto del ángulo de contacto en el patrón de rotura en pizarra en el ensayo Brasileño

M.I. Alvarez-Fernandez, C.C. Garcia-Fernandez, C. Gonzalez-Nicieza, D.J. Guerrero-Miguel, "Effect of the contact angle in the failure pattern in slate under Brazilian tests", *Rock Mech Rock Eng*, vol. 53, pp. 2123-2139, 2020.

Effect of the Contact Angle in the Failure Pattern in Slate Under Diametral Compression

M. I. Alvarez-Fernandez¹ · C. C. Garcia-Fernandez¹ · C. Gonzalez-Nicieza¹ · D. J. Guerrero-Miguel¹

Received: 3 April 2019 / Accepted: 3 January 2020 / Published online: 19 January 2020
© Springer-Verlag GmbH Austria, part of Springer Nature 2020

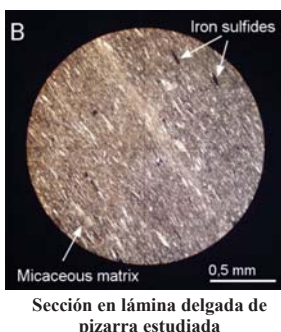
Abstract

The failure pattern in slate tested under diametral compression is strongly influenced by the contact angle created in the loaded area. A small angle is created throughout the contact between the jaws (or platens) and the disc by adopting flat platens (ASTM standard) or curved jaws (suggested method by ISRM) load configurations, inducing failures due to shear stresses in the limit of the load rim. This causes failure patterns that do not exactly match the central diameter when the material is tested with the load direction parallel and perpendicular to foliation, which contradicts the failure by pure tensile typically assumed in the test for these orientations. In the present work, a new interpretation of the failure pattern in slate samples tested with the Brazilian method is established, playing the contact angle a significant role. Brazilian tests with the loading direction along and across foliation were carried out in the laboratory, by using the load configurations of ASTM standard and the ISRM recommendation. Furthermore, an analytical study allowed the estimation of the point in the whole of the disc in which a critical stress state is firstly reached by taking into account both the foliation and the intact rock failure criteria, hence justifying the experimental failure patterns. Finally, regarding the initial failure the influence of the strength properties in order to satisfy the classic hypothesis of the Brazilian test in rocks with multiple weak planes was analysed. An appropriate interpretation of the failure pattern can be an important indicator in order to reveal the true failure mechanism of rocks; this may help to improve the characterization and prediction of the initial failure of this material, which is widely used as an industrial rock or in dam foundations, underground excavations and slope engineering.

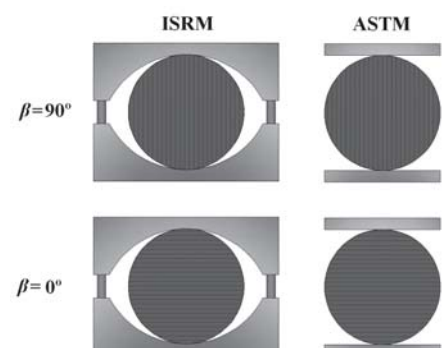
Keywords Brazilian test · Slate · Initial failure point · Contact angle · Failure pattern

Efecto del ángulo de contacto en el patrón de rotura en pizarra bajo compresión diametral 5. Parámetros de influencia

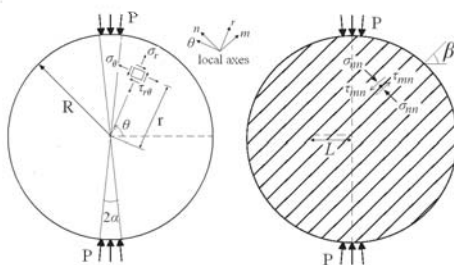
Material y métodos



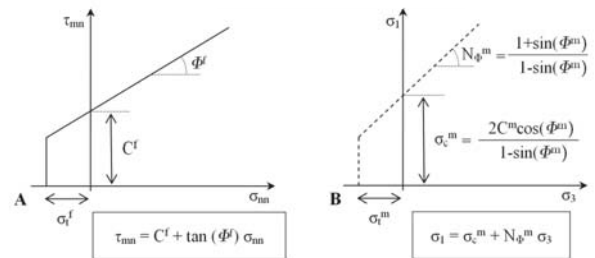
Propiedades	Roca intacta	Foliación
Resistencia a compresión uniaxial, σ_c (MPa)	179.52	115.60
Resistencia a tracción, σ_t (MPa)	24.04	7.90
Cohesión (MPa)	36.18	11.90
Ángulo de fricción interna, Φ (°)	47.99	30.37



Modelo analítico

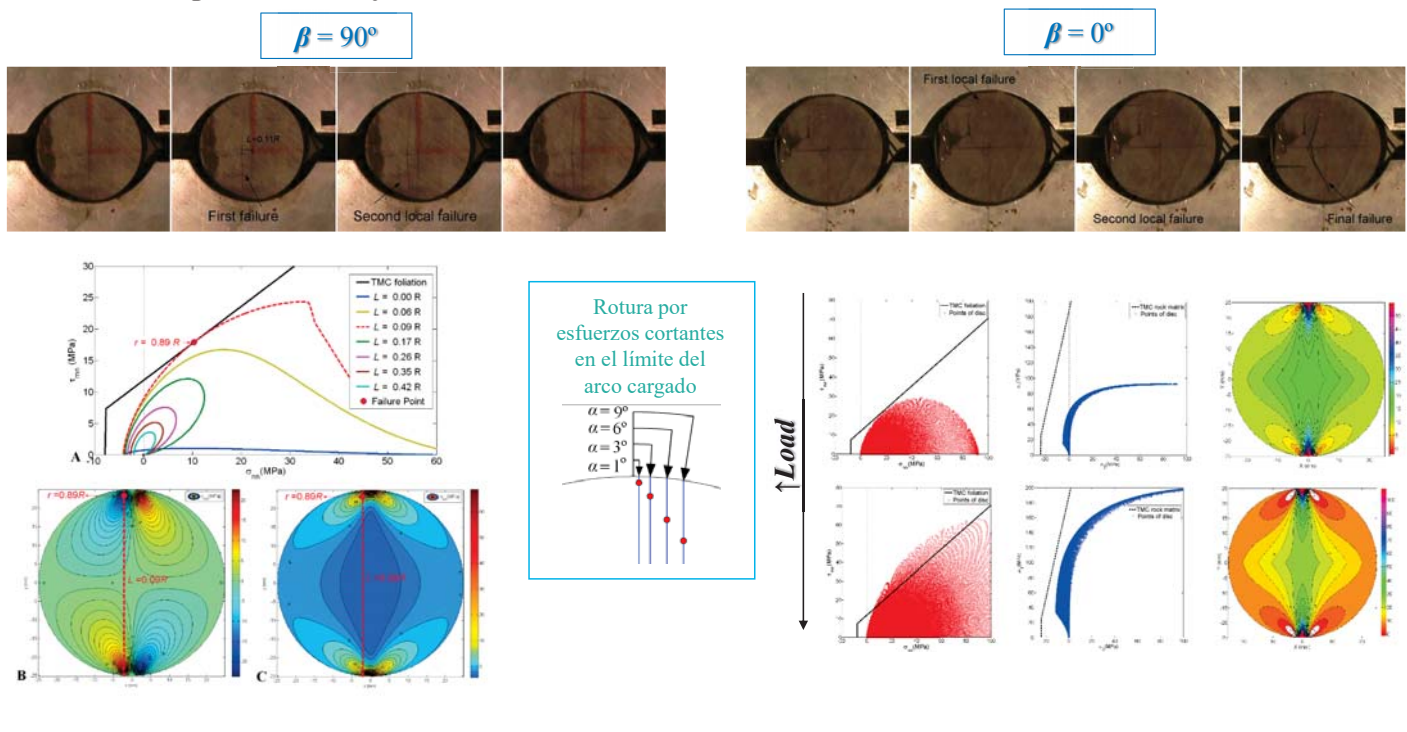


Criterio de rotura



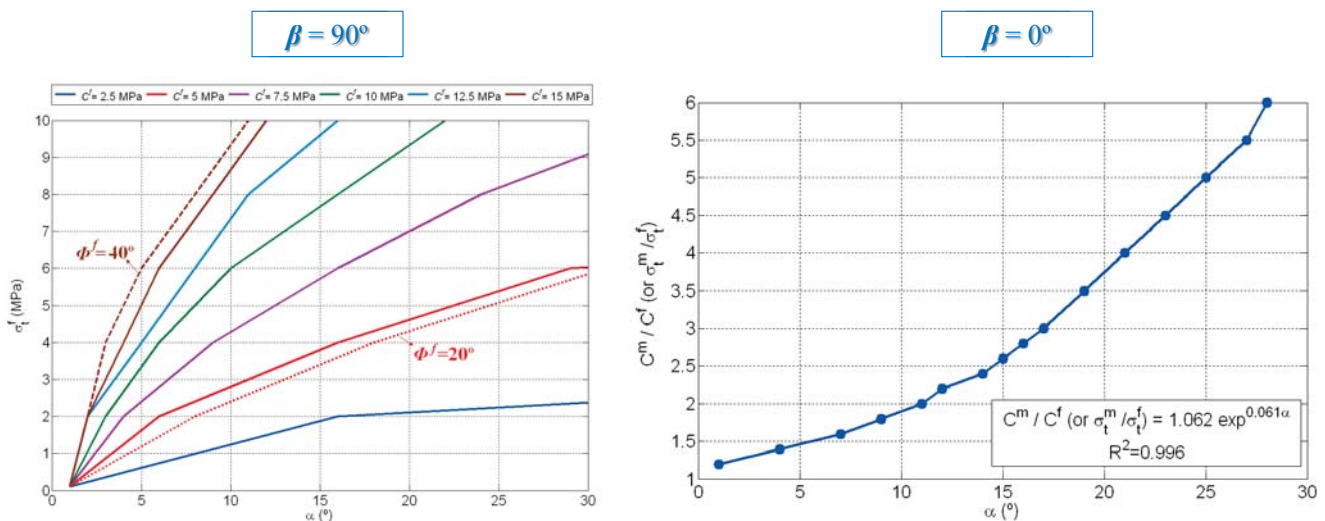
Efecto del ángulo de contacto en el patrón de rotura en pizarra bajo compresión diametral 5. Parámetros de influencia

Resultados experimentales y analíticos



Efecto del ángulo de contacto en el patrón de rotura en pizarra bajo compresión diametral 5. Parámetros de influencia

Influencia de parámetros resistentes de roca intacta y foliación



Semiángulos de contactos necesarios para inducir la rotura inicial en el centro del disco, dependiendo de parámetros resistentes de la foliación y de la roca matriz

M.I. Alvarez-Fernandez, C.C.Garcia-Fernandez,
C. Gonzalez-Nicieza, D.J.Guerrero-Miguel (2020)

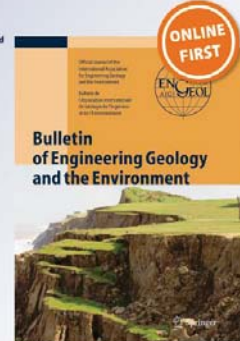
Efecto de la humedad relativa en la resistencia a tracción de la foliación en pizarra

C.C. Garcia-Fernandez, M.I. Alvarez-Fernandez, R. Cardoso, C. Gonzalez-Nicieza, "Effect of environmental relative humidity in the tensile strength of layering in slate stone", *Bull Eng Geol Environ*, vol. 79, pp. 1399-1411, 2020.

Effect of environmental relative humidity in the tensile strength of layering in slate stone

C. C. Garcia-Fernandez, M. I. Alvarez-Fernandez, R. Cardoso & C. Gonzalez-Nicieza

Bulletin of Engineering Geology and the Environment
The official journal of the International Association for Engineering Geology
ISSN 1435-9529
Bull Eng Geol Environ
DOI 10.1007/s10064-019-01619-7

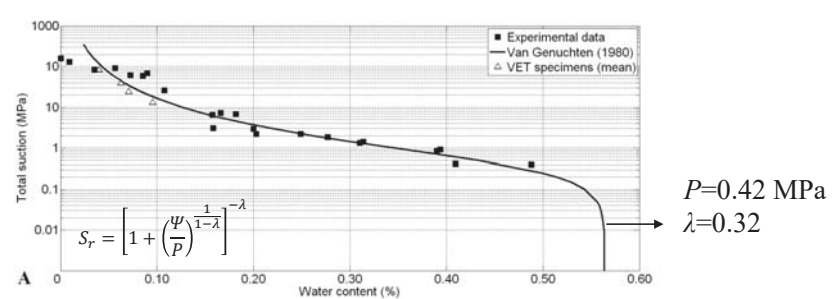
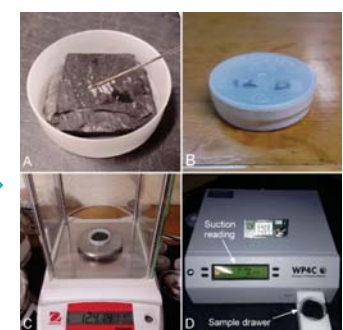


Springer

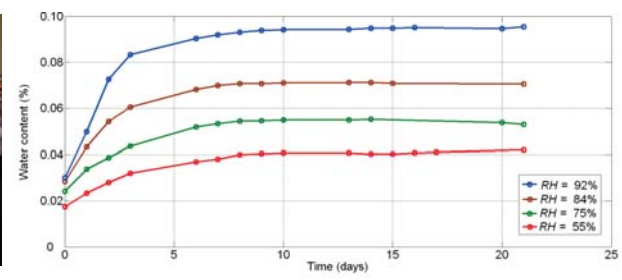
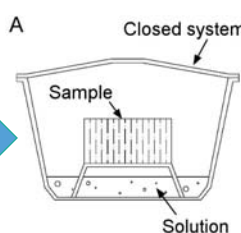
Efecto de la humedad relativa en la resistencia a tracción de la foliación

Método: Técnica de equilibrio de vapor (VET)

Curva de retención de agua

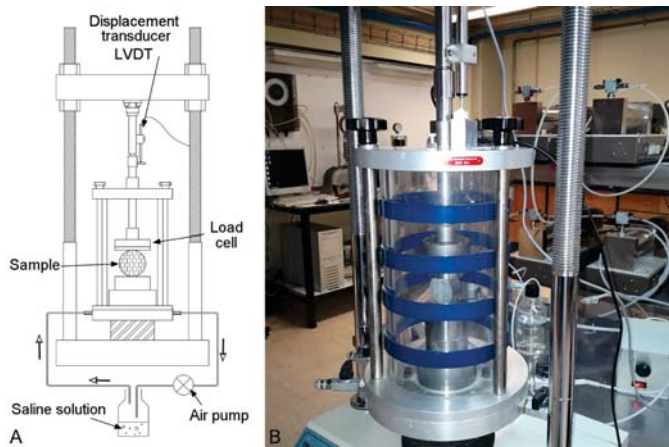


Técnica de equilibrio de vapor (VET)

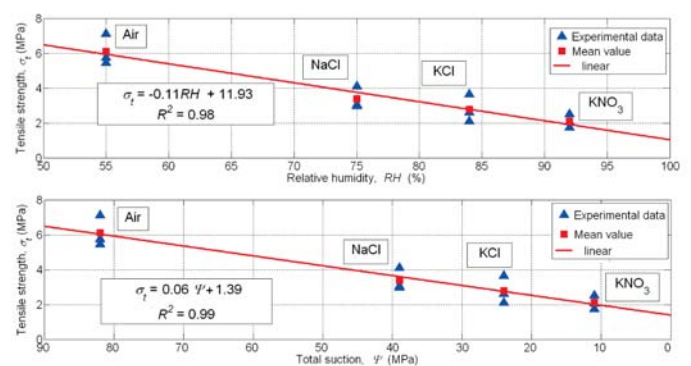


C. C. Garcia-Fernandez, M. I. Alvarez-Fernandez, R. Cardoso and C. Gonzalez-Nicieza (2019)

Resultados experimentales



Esquema de ensayo brasileño en pizarras con control de humedad relativa (o succión total) y equipo empleado en laboratorio



Relación de la resistencia a tracción de los planos de foliación con A. la humedad relativa ambiente y B. Succión total.

C. C. Garcia-Fernandez, M. I. Alvarez-Fernandez,
R. Cardoso and C. Gonzalez-Nicieza (2019)

Determinación de diferentes estados tensionales límite en la región de tracción utilizando el ensayo Brasileño

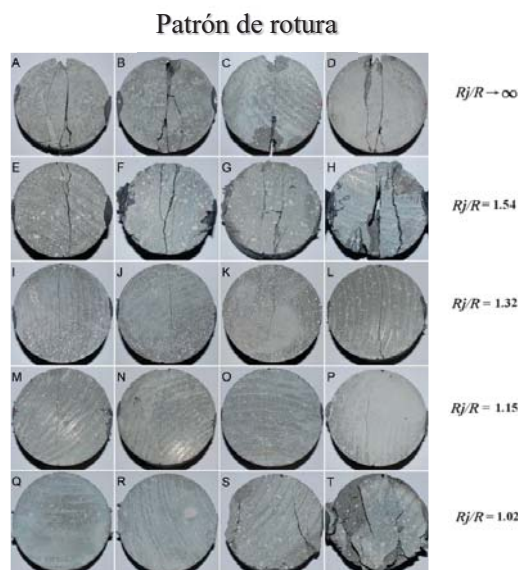
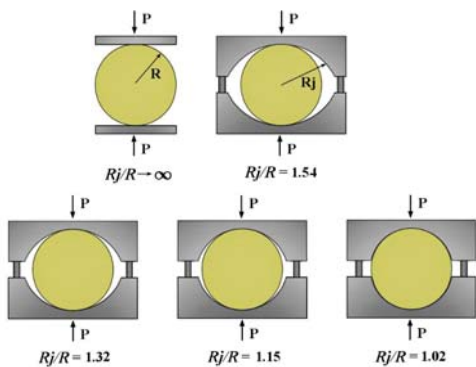
C.C. Garcia-Fernandez, R.A. Gutierrez-Moizant, M.I. Alvarez-Fernandez, M. Ramírez-Berasategui, C. Gonzalez-Nicieza, “Determination of different stress state limits in the tension region by using the Brazilian test”

Determinación de diferentes estados tensionales límite en la región de tracción

6. Nuevas aplicaciones

Estudio experimental

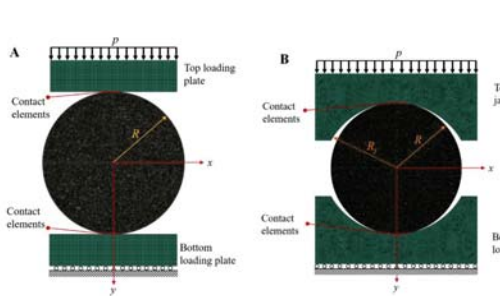
Propiedades	Mortero
Densidad, ρ (kg/m ³)	1990
Módulo de elasticidad, E (GPa)	24.20
Coeficiente de Poisson, ν	0.17
Coeficiente de fricción Mandíbula-Disco, μ	0.50



Determinación de diferentes estados tensionales límite en la región de tracción

6. Nuevas aplicaciones

Estudio numérico



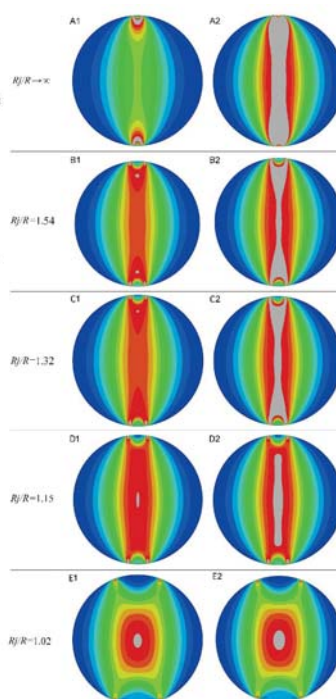
Inicio probable de la rotura → máxima tensión equivalente, Griffith (1921):

$$\text{Cuando } 3\sigma_\theta + \sigma_r \geq 0$$

$$\sigma_G = \sigma_\theta$$

$$\text{Cuando } 3\sigma_\theta + \sigma_r < 0$$

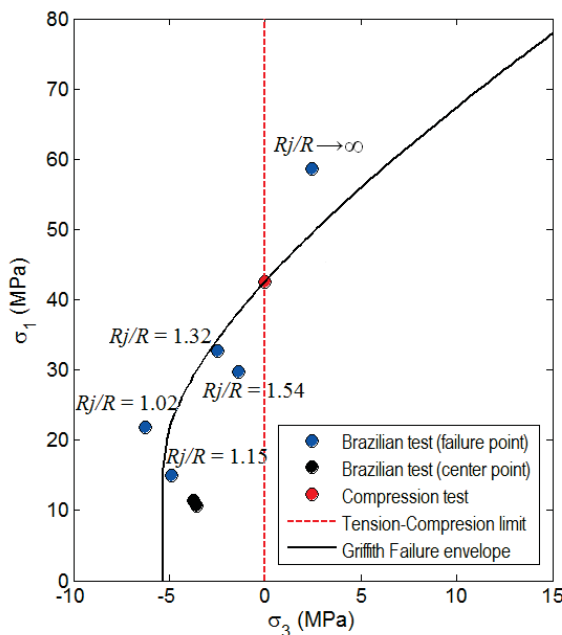
$$\sigma_G = -\frac{(\sigma_\theta - \sigma_r)^2}{8(\sigma_\theta - \sigma_r)}$$



Mapa de distribución de tensiones equivalentes de Griffith para cada relación simulada según dos etapas sucesivas de la modelización

Rj/R	r/R	$2\alpha(^{\circ})$
∞	0.91	6.70
1.54	0.79	12.90
1.32	0.75	13.30
1.15	0.00	16.60
1.02	0.00	39.44

Estados tensionales límite



Representación del estado tensional de las zonas probables de inicio de la rotura

Rj/R	$\sigma_\theta = -\sigma_3$ (MPa)	$\sigma_r = -\sigma_1$ (MPa)
∞	2.43 (-3.56)	58.68 (10.70)
1.54	-1.40 (-3.75)	29.77 (11.39)
1.32	-2.49	32.66
1.15	-4.91	15.04
1.02	-6.29	21.84

Nueva metodología para estimar los parámetros resistentes de la foliación en pizarra utilizando el ensayo Brasileño

C.C. Garcia-Fernandez, C. Gonzalez-Nicieza, M.I. Alvarez-Fernandez, R.A. Gutierrez-Moizant, "New methodology for estimating the shear strength of layering in slate by using the Brazilian test", *Bull Eng Geol Environ*, vol. 78, pp. 2283 – 97, 2019.

Bulletin of Engineering Geology and the Environment (2019) 78:2283–2297
<https://doi.org/10.1007/s10064-018-1297-3>

ORIGINAL PAPER



New methodology for estimating the shear strength of layering in slate by using the Brazilian test

C. C. Garcia-Fernandez¹ • C. Gonzalez-Nicieza¹ • M. I. Alvarez-Fernandez² • R. A. Gutierrez-Moizant²

Received: 19 December 2017 / Accepted: 26 April 2018 / Published online: 11 May 2018
 © Springer-Verlag GmbH Germany, part of Springer Nature 2018

Abstract

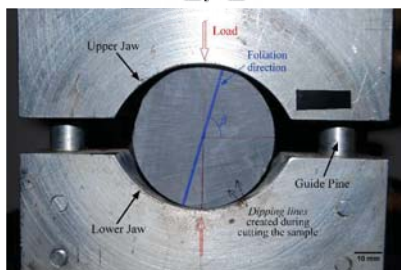
A new method is proposed in order to estimate the shear strength of schistosity planes in slate in terms of Mohr-Coulomb cohesion and internal friction angle. The procedure consists in carrying out the Brazilian method under different loading-foliation angles, for which experimental tests were achieved in slates from the northwest of the Iberian Peninsula (Spain). The experimental fracture patterns were analytically studied and justified by simulating the stress field in the discontinuity planes contained in the whole sample, taking into account the first failure registered in the tests. By combining experimental and analytical studies and a procedure based on the representation of the threshold state of stresses—in the elastic regime—in the failure plane, it is possible to estimate the foliation's strength envelope through a linear adjustment according to the Mohr-Coulomb criterion and, thus, to characterize the layering. Finally, the proposed procedure was validated by the direct shear test. The cohesion and the internal friction angle obtained with this conventional test were very close to that calculated by the proposed method, verifying the methodology developed by the authors. This procedure may be interesting in various engineering applications, either in the study of the properties of cleavage in slate, which is commonly used as an industrial rock, or in dam foundations, underground excavations and slope engineering, since one of the main failures in civil engineering is due to sliding along weak planes.

Keywords Brazilian test · Slate · Foliation · Internal friction angle · Cohesion · Strength parameters

Nueva metodología de estimación de los parámetros resistentes de la foliación

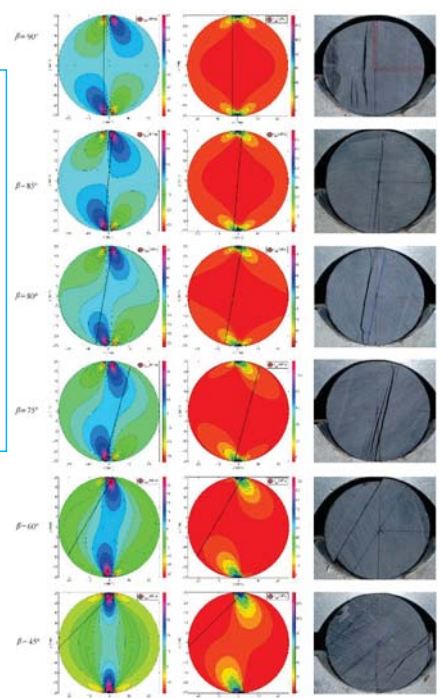
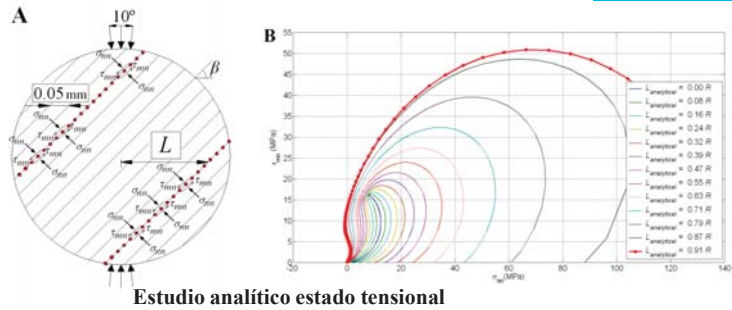
Estudio experimental y analítico

$$90^\circ \geq \beta \geq 45^\circ$$



Configuración de ensayo

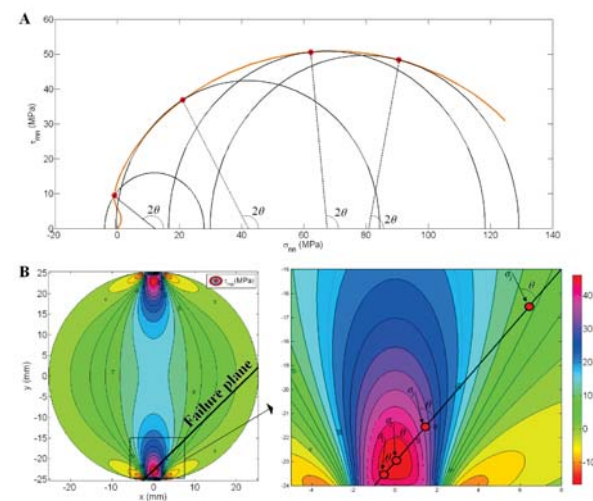
β (°)	$L_{\text{experimental}}$	$L_{\text{analítico}}$
90	0.11 R	0.10 R
85	0.05 R	0.00 R
80	0.14 R	0.10 R
75	0.17 R	0.18 R
60	0.48 R	0.49 R
45	0.84 R	0.91 R



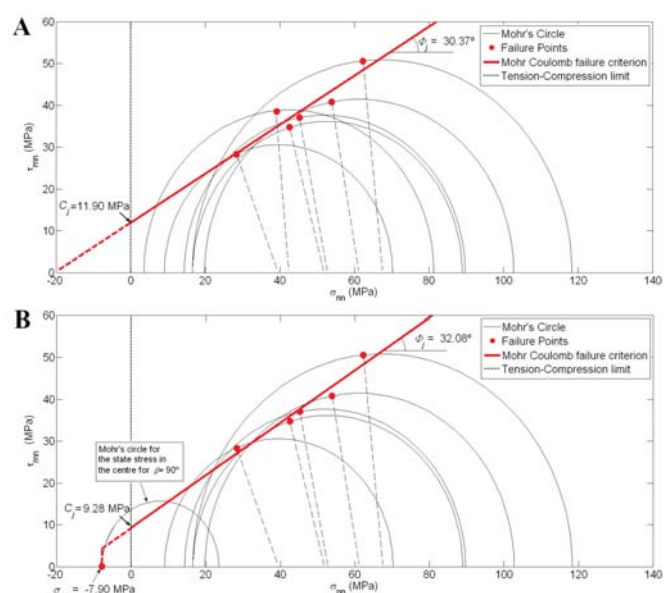
C.C.Garcia-Fernandez, C. Gonzalez-Nicieza, M.I. Alvarez-Fernandez, A. Gutierrez-Moizant (2019)

Nueva metodología de estimación de los parámetros resistentes de la foliación

Determinación de cohesión y ángulo de fricción de la foliación



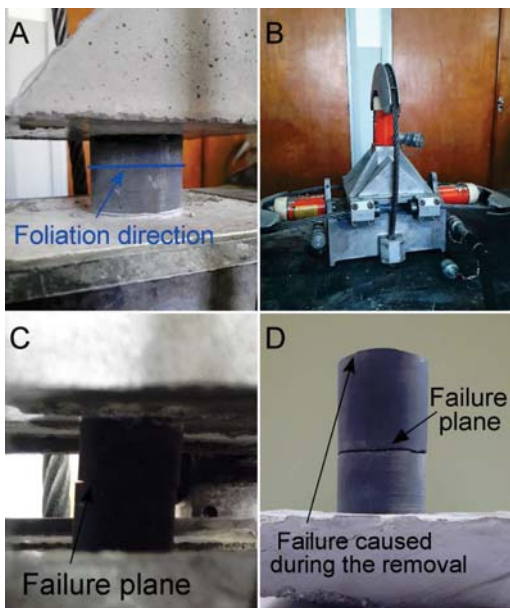
Curva tensional en el plano de rotura cuando $\beta = 45^\circ$ y correspondiente círculo de Mohr en cuatro puntos contenidos en el plano. B. Ángulo θ representado en el disco



Criterio de Mohr-Coulomb obtenido con el método propuesto

C.C.Garcia-Fernandez, C. Gonzalez-Nicieza, M.I. Alvarez-Fernandez, A. Gutierrez-Moizant (2019)

Validación del método propuesto



Método	Ángulo de fricción interna (°)	Cohesión (MPa)
Propuesto ($\beta = 90^\circ$, rotura por cortante)	30.37	11.90
Propuesto ($\beta = 90^\circ$, rotura por tracción)	32.08	9.28
Ensayo corte	29.50	7.20

Ensayo de corte directo. A: muestra de pizarra embebida en cemento. B. Caja de corte directo. C. Primera rotura. D. Patrón de rotura final

C.C.Garcia-Fernandez, C. Gonzalez-Nicieza, M.I. Alvarez-Fernandez, A. Gutierrez-Moizant (2019)

Nuevo ensayo de caracterización de la resistencia a tracción de materiales rocosos

C.C García Fernández, M.I. Álvarez Fernández, J.R. García Menéndez, A. González Fuentes, et al., “Nuevo ensayo de caracterización de la resistencia a tracción de materiales rocosos”, *10º Simposio Nacional de Ingeniería Geotécnica; Reconocimiento, Tratamiento y Mejora del Terreno*. Sociedad Española de Mecánica del Suelo, A Coruña, 2016. pp. 157-164. ISBN 978-84-945284-2-2.

10º Simposio Nacional
de Ingeniería Geotécnica
**Reconocimiento, tratamiento
y mejora del terreno**

5º JORNADAS LUSO-ESPAÑOLAS DE GEOTECNIA
**Desafíos para la Geotecnia
en España y Portugal**

TOMO I

A CORUÑA
19, 20 y 21 de octubre de 2016



Sociedad Portuguesa
de Geotecnia



Sociedad Española
de Mecánica del Suelo
a Ingeniería de Construcciones



Sociedad Española
de Mecánica de Rocas

Nuevo ensayo de caracterización de la resistencia a tracción

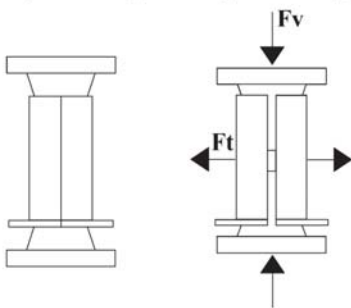
7. Nuevo ensayo de caracterización

Procedimiento de ensayo



Configuración del ensayo

Etapa sin carga Etapa con carga



Mecanismo de funcionamiento del ensayo



Probeta de ensayo

Determinación de la resistencia a tracción (σ_t):

$$\sigma_t = \frac{F_v \cos \alpha - \mu \sin \alpha}{A}$$

$$\sin \alpha + \mu \cos \alpha$$

α ángulo de inclinación
 μ coeficiente de fricción
 F_v fuerza vertical de rotura
 A Área de rotura

C.C. García Fernández, M.I. Álvarez Fernández, J.R. García Menéndez, A. González Fuentes, et al. (2016)

Nuevo ensayo de caracterización de la resistencia a tracción

7. Nuevo ensayo de caracterización

Resultados experimentales

PMMA



Modo de rotura en muestras de PMMA

Pizarra



Modo de rotura en muestras de pizarra paralelamente a la foliación (tipo I) y en dirección perpendicular (tipo II)

Muestra	Fuerza de rotura (kN)	Resistencia a tracción (MPa)
Mt 1	48.99	59.69
Mt 2	51.63	63.36
Mt 3	51.83	63.15
Mt 4	52.44	63.89
Mt 5	49.80	60.68
Valor medio		62.15 (\pm 1.85)

$$\sigma_t = 62.67 \text{ MPa}$$

Muestra	Fuerza de rotura (kN)	Resistencia a tracción (MPa)
Pz 1 (I)	4.17	3.32
Pz 2 (I)	3.71	2.89
Pz 3 (I)	4.52	3.65
Valor medio		3.29 (\pm 0.37)
Pz 4 (II)	20.13	13.25
Pz 5 (II)	19.69	13.41
Pz 6 (III)	22.06	15.01
Valor medio		13.89 (\pm 0.97)

C.C. García Fernández, M.I. Álvarez Fernández, J.R. García Menéndez, A. González Fuentes, et al. (2016)

- ANÁLISIS**
- ↓
- PROPIUESTA**
- Análisis detallado del inicio de la rotura en material frágil sometido a compresión diametal (o ensayo Brasileño), controlando las variables que influyen en el mecanismo de inicio del fallo, tanto a nivel de propiedades del material como la propia configuración del ensayo. Se ha verificado la importancia que tiene el ángulo de contacto creado en la zona de aplicación de la carga en el punto de inicio de la rotura.
 - Se han encontrado nuevas vías de aplicación del ensayo Brasileño. Es posible la utilización del ensayo como un método para establecer diferentes estados tensionales límite de los materiales rocosos.
 - Se ha propuesto un nuevo método de determinación precisa de la resistencia a tracción que podría complementar a los ensayos ya existentes.

Aportación científica del trabajo de investigación

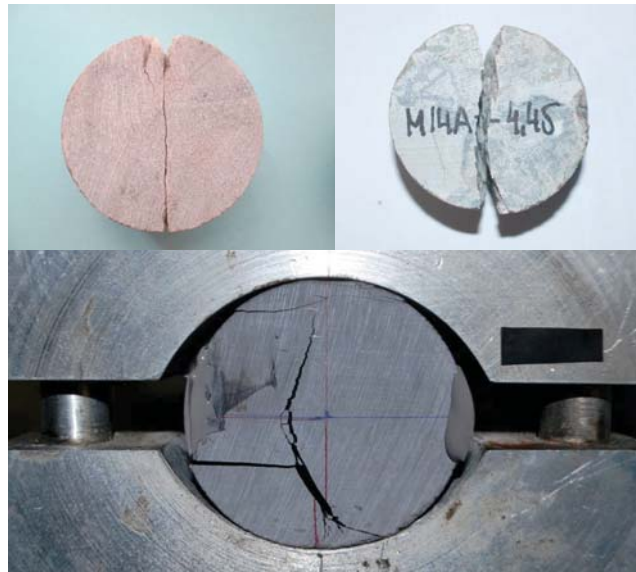
Artículos publicados en revistas con JCR

- ✓ C.C. Garcia-Fernandez, C. Gonzalez-Nicieza, M.I. Alvarez-Fernandez, R.A. Gutierrez-Moizant, “**Analytical and experimental study of failure onset during a Brazilian test**”, *Int J of Rock Mech Min Sci.*, vol.13, pp. 254-265, 2018.
- ✓ R. Gutierrez-Moizant, M. Ramirez-Berasategui, S. Santos-Cuadros, C. Garcia-Fernandez, “**Computational verification of the optimum boundary condition of the Brazilian Tensile Test**”, *Rock Mech Rock Eng.*, vol.51, pp. 3505-3519, 2018.
- ✓ C.C. Garcia-Fernandez, C. Gonzalez-Nicieza, M.I. Alvarez-Fernandez, R.A. Gutierrez-Moizant, “**New methodology for estimating the shear strength of layering in slate by using the Brazilian test**”, *Bull Eng Geol Environ*, vol. 78, pp. 2283 – 97, 2019.
- ✓ C.C. Garcia-Fernandez, M.I. Alvarez-Fernandez, R. Cardoso, C. Gonzalez-Nicieza, “**Effect of environmental relative humidity in the tensile strength of layering in slate stone**”, *Bull Eng Geol Environ*, vol. 79, pp. 1399-1411, 2020.
- ✓ M.I. Alvarez-Fernandez, C.C. Garcia-Fernandez, C. Gonzalez-Nicieza, D.J. Guerrero-Miguel, “**Effect of the contact angle in the failure pattern in slate under Diametral Compression**”, *Rock Mech Rock Eng*, vol. 53, pp. 2123-2139, 2020.
- ✓ R. Gutierrez-Moizant, M. Ramirez-Berasategui, S. Santos-Cuadros, C. Garcia-Fernandez, “**A Novel Analytical Solution for the Brazilian Test with Loading Arcs**”, *Mathematical Problems in Engineering*, pp. 1-19, 2020.

Aportación científica del trabajo de investigación

Comunicaciones en Congresos

- ✓ C.C García Fernández, M.I. Álvarez Fernández, J.R. García Menéndez, A. González Fuentes, et al., “Nuevo ensayo de caracterización de la resistencia a tracción de materiales rocosos”, *Ingiería Geotécnica Reconocimiento y tratamiento de Materiales del Terreno*. Sociedad Española de Mecánica del Suelo, La Coruña, 2014 pp. 157-144. ISBN 978-84-945284-2-2.
- ✓ C. González Nicieza, M.I. Álvarez Fernández, C.C. García Fernández, R. Fernández Rodríguez, J.R. García Menéndez, “New failure criterion for rocks by using compression tests”, *EUROCK 2018*, San Petersburgo, 2018. pp. 325-332. ISBN 978-1-138-61645-5.
- ✓ C. González Nicieza, M.I. Álvarez Fernández, C.C. García Fernández, J.R. García Menéndez, “The GIT tensile test: new characterization of the tensile strength in rock materials”, paper presented at the ISRM International Symposium - *EUROCK 2020*, physical event not held, June 2020. ISBN: 978-82-8208-072-9.
- ✓ C.C. García Fernández, R. Cardoso, M.I. Álvarez Fernández, C. González Nicieza, "Changes on diametral compression behaviour of compacted marls due to drying", E-UNSAT 2020, Lisbon, 195(3):03008. DOI:10.1051/e3sconf/202019503008.



SOCIEDAD ESPAÑOLA DE
MECÁNICA DE ROCAS

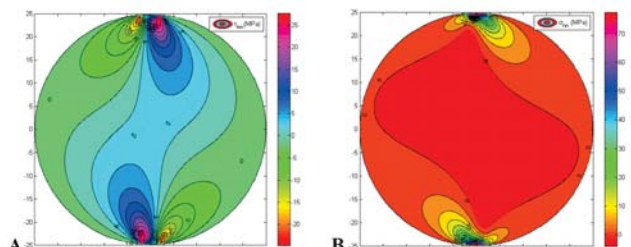
XVIII JORNADA TÉCNICA ANUAL
13 de mayo 2021

VIII Premio SEMR al mejor trabajo de investigación en
Mecánica de Rocas para Jóvenes Investigadores

MUCHAS GRACIAS

Carmen Covadonga García Fernández
Dpto. Explotación y Prospección de Minas

✉ garciafercarmen@uniovi.es
carmencovagarciafer@gmail.com



Universidad de Oviedo
Universidá d'Uviéu
University of Oviedo

